Supporting Information

Methods

Screening small molecules that alter circadian rhythms

CCA1:LUC and *TOC1:LUC* transgenic plant seeds generated in the *Arabidopsis thaliana* Col-0 background (1) were sterilized with 2.5% hypochlorous acid and sown on full-strength Mirashige-Skoog (MS) plates (392-00591, Wako) without sucrose, and kept at 4˚C for two days. Four-day-old *CCA1:LUC* seedlings held under 12 h white light at 70 to 100 μmol s^{-1} m^{-2} / 12 h dark conditions (LD) were transferred to 96-well plates (136101 Nunc MicroWell White plate, ThermoFisher Scientific) with a 6 mm dia dropper. Seedlings were treated with one of the 90 molecules from the LOPAC compounds library at 50 μM (LO5100-1ea; Sigma-Aldrich) at a final concentration of 5% (v/v) DMSO in 20 μL of MS liquid containing 2% (w/v) sucrose, and 500 μM luciferin. Adding MS liquid containing 5% (v/v) DMSO did not significantly change the circadian period compared to DMSO-free MS (Fig. S17). Bioluminescence of *CCA1:LUC* was analyzed starting the next day using a CL96 automated bioluminometer (Churitsu, Toyoake, Japan) under constant light conditions (LL). Period and amplitude parameters of circadian rhythms were automatically calculated by the CL96 instrument, as described previously (2). Data with high error value (larger than 0.05) showing fault to period- and amplitude-determination, were excluded. Alterations in the circadian period were analyzed after the initial screening using *CCA1:LUC* with 40, 80, 160, 320, or 640 μM PHA767491 (2-pyridin-4-yl-1,5,6,7-tetrahydropyrrolo[3,2-c]pyridin-4- one;hydrochloride) (Fig. 1b). Circadian period changes were also determined using *TOC1:LUC* with 10, 20, 40, 80, 160, 320, and 640 μM PHA767491 (Fig. 1c). Commercially -available PF-670462 (Sigma-Aldrich) (5, 10, 25, 50, 100, 250, 500 μM, Fig. 3d) and synthesized analogues of PHA767491 (250 μM for analogues **1** to **4**, 25, 50, 100, 300, and 500 μM for analogues **5** and **6**, Fig. 2a) were used to treat *CCA1:LUC* seedlings, and circadian periods were determined as described above. One-way ANOVA (GraphPad Prism) was used to determine the statistical significance of treated samples compared to untreated controls.

Synthesis of PHA767491 analogues and molecular probe

www.pnas.org/cgi/doi/10.1073/pnas.1903357116

General

Unless otherwise noted, all materials including dry solvents were obtained from commercial suppliers and used without further purification. $Pd(OAc)_2$ and $[Pd(allyl)Cl]_2$, 2-bromo-1-(pyridin-4-yl)ethan-1-one hydrobromide, ammonium acetate, 1,5,6,7-tetrahydro-4*H*-indol-4-one, 4-bromopyridine hydrochloride, potassium acetate, and 1-bromopropane were obtained from Wako chemicals. Hydrogen chloride solution (4.0 M in dioxane) was obtained from Sigma-Aldrich. 2-Bromo-1-phenylethan-1-one and 4,5,6,7-tetrahydrothieno[3,2-*c*]pyridine were obtained from Tokyo Chemical Industry. *tert*-Butyl 2,4-dioxopiperidine-1-carboxylate (**1**) (3), *tert*-butyl 2,4-dioxo-5-propylpiperidine-1-carboxylate (**2**) (4), 6,7-dihydrothieno [3,2-*c*]pyridine-4(5*H*)-thione (**3**) (5), 6,7-dihydrothieno[3,2-*c*]pyridin-4(5*H*)-one (**4**) (6), 11-azidoundecyl 4-methylbenzenesulfonate (**5**) (7), and 1,5,6,7-tetrahydro-4*H*-pyrrolo[3,2-*c*]pyridin-4-one (**6**) (8) were synthesized according to procedures reported in the literature. Unless otherwise noted, all reactions were performed with dry solvents under an atmosphere of argon or nitrogen in flame-dried glassware, using standard vacuum-line techniques. All work-up and purification procedures were carried out with reagent-grade solvents in air.

Analytical thin-layer chromatography (TLC) was performed using E. Merck silica gel 60 F_{254} precoated plates (0.25 mm). The developed chromatogram was visualized using a UV lamp (254 nm). Flash column chromatography was performed with E. Merck silica gel 60 (230–400 mesh) and Kanto Chemical Co. Inc. silica gel 60N, spherical neutral (40–100 mm). Preparative thin-layer chromatography (PTLC) was performed using Wako-gel® B5-F silica coated plates (0.75 mm) prepared in our laboratory. High-resolution mass spectra (HRMS) were obtained from a JEOL JMS-T100TD (direct analysis in real time mass spectrometry, DART). Nuclear magnetic resonance (NMR) spectra were recorded on a JEOL JNM-ECA-600 (^{1}H 600 MHz, ^{13}C 150 MHz) spectrometer. Chemical shifts for ^{1}H NMR are expressed in parts per million (ppm) relative to tetramethylsilane (δ 0.00 ppm), CD_3OD (δ 3.31 ppm), or DMSO-d_6 (δ 2.50 ppm). Chemical shifts for ^{13}C NMR are expressed in ppm relative to $CDCl_3$ (δ 77.0 ppm), CD_3OD (49.0 ppm), or DMSO-d_6 (δ 39.5 ppm). Data are reported as follows: chemical shift, multiplicity (s = singlet, d = doublet, dd = doublet of doublets, dt = doublet of triplets, t = triplet, td, triplet of doublets, quin = quintet, sext = sextet, m = multiplet, brs = broad signal), coupling constant (Hz), and integration.

Preparation of PHA derivatives

***tert*-Butyl**

4-oxo-2-(pyridin-4-yl)-1,4,6,7-tetrahydro-5*H*-pyrrolo[3,2-*c*]pyridine-5-carboxylate (S0)[1]

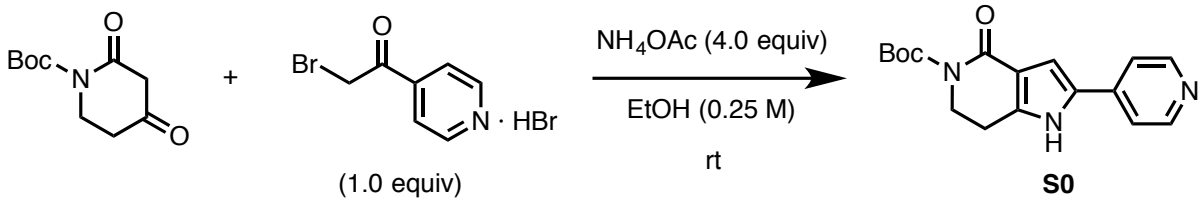

S0

To a solution of *tert*-butyl 2,4-dioxopiperidine-1-carboxylate (53.3 mg, 0.25 mmol, 1.0 equiv) and 2-bromo-1-(pyridin-4-yl)ethan-1-one hydrobromide (70.2 mg, 0.25 mmol, 1.0 equiv) in EtOH (1 mL) was added ammonium acetate (77.1 mg, 1.0 mmol, 4.0 equiv) at room temperature. After stirring for 24 h, the reaction mixture was quenched with sat. $NaHCO_3$ aq., then the layers were separated. The aqueous layer was extracted with ethyl acetate and the combined organic layer was dried over Na_2SO_4 and concentrated *in vacuo*. The crude residue was purified by flash column chromatography ($CHCl_3$/MeOH = 30:1 to 20:1) and PTLC ($CHCl_3$/MeOH = 10:1) to produce **S0** as a yellow solid (46% yield). ^{1}H NMR (600 MHz, CD_3OD) δ 8.46 (d, J = 6.6 Hz, 2H), 7.60 (d, J = 6.0 Hz, 2H), 7.13 (s, 1H), 4.11 (t, J = 6.6 Hz, 2H), 3.00 (t, J = 7.2 Hz, 2H), 1.55 (s, 9H), one proton (NH) was not detected; ^{13}C NMR (150 MHz, CD_3OD) δ 165.3, 154.5, 150.5, 143.2, 141.4, 131.6, 119.5, 117.0, 108.8, 83.9, 46.9, 28.3, 23.4; HRMS (DART) m/z = 314.1505 calcd for $C_{17}H_{20}N_3O_3$ $[M+H]^+$, found: 314.1498.

***tert*-Butyl**

4-oxo-2-(pyridin-3-yl)-1,4,6,7-tetrahydro-5H-pyrrolo[3,2-*c*]pyridine-5-carboxylate (S1)

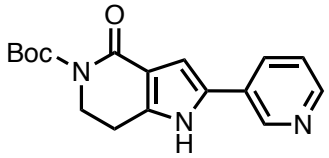

S1

Purification by flash column chromatography ($CHCl_3$/MeOH = 30:1) produced **S1** as a yellow solid (53% yield). ^{1}H NMR (600 MHz, $CDCl_3$) δ 11.56 (brs, 1H), 8.84 (d, J = 1.2 Hz, 1H), 8.37 (d, J = 4.8 Hz, 1H), 7.84 (dt, J = 7.2, 1.8 Hz, 1H), 7.25 (dd, J = 7.8,

4.8 Hz, 1H), 6.87 (d, *J* = 2.4 Hz, 1H), 4.06 (t, *J* = 6.0 Hz, 2H), 2.92 (d, *J* = 6.6 Hz, 2H), 1.51 (s, 9H); ^{13}C NMR (150 MHz, $CDCl_3$) δ 163.4, 153.1, 146.8, 144.8, 140.3, 131.8, 130.0, 128.5, 124.0, 115.9, 105.8, 82.6, 45.4, 28.1, 22.6; HRMS (DART) *m/z* = 314.1505 calcd for $C_{17}H_{20}N_3O_3$ $[M+H]^+$, found: 314.1505.

***tert*-Butyl**
4-oxo-2-phenyl-1,4,6,7-tetrahydro-5H-pyrrolo[3,2-c]pyridine-5-carboxylate (S2)

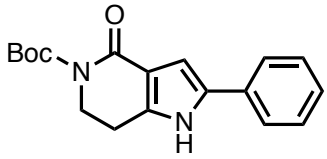

S2

Purification by flash column chromatography ($CHCl_3$/MeOH = 40:1) and PTLC ($CHCl_3$/MeOH = 10:1) produced **S2** as a white solid (34% yield). ^{1}H NMR (600 MHz, $CDCl_3$) δ 9.97 (brs, 1H), 7.50 (d, *J* = 7.2 Hz, 2H), 7.31 (t, *J* = 7.2 Hz, 2H), 7.19 (t, *J* = 7.2 Hz, 1H), 6.80 (d, *J* = 2.4 Hz, 1H), 4.08 (t, *J* = 6.0 Hz, 2H), 2.94 (t, *J* = 6.6 Hz, 2H), 1.51 (s, 9H); ^{13}C NMR (150 MHz, $CDCl_3$) δ 163.6, 153.4, 139.1, 133.5, 131.7, 128.8, 126.8, 124.1, 115.9, 104.4, 82.5, 45.4, 28.1, 22.7; HRMS (DART) *m/z* = 313.1552 calcd for $C_{18}H_{21}N_2O_3$ $[M+H]^+$, found: 313.1555.

***tert*-Butyl**
4-oxo-7-propyl-2-(pyridin-4-yl)-1,4,6,7-tetrahydro-5H-pyrrolo[3,2-c]pyridine-5-carboxylate (S3)

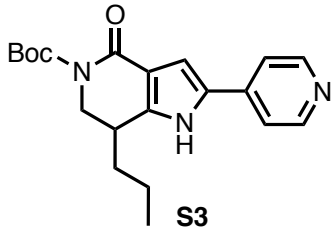

S3

Purification by flash column chromatography ($CHCl_3$/MeOH = 40:1 to 30:1) and PTLC ($CHCl_3$/MeOH = 10:1) produced **S3** as a yellow liquid (21% yield). ^{1}H NMR (600 MHz, $CDCl_3$) δ 11.06 (brs, 1H), 8.46 (d, *J* = 3.6 Hz, 2H), 7.46 (d, *J* = 3.6 Hz, 2H), 7.07 (d, *J* = 1.8 Hz, 1H), 4.10 (dd, *J* = 13.2, 4.8 Hz, 1H), 4.01 (dd, *J* = 12.6, 4.2 Hz, 1H), 3.02–2.96 (m, 1H), 1.79–1.71 (m, 1H), 1.65–1.57 (m, 1H), 1.54–1.48 (m, 10H), 1.39–1.32 (m, 1H), 0.89 (td, *J* = 7.2, 1.8 Hz, 3H); ^{13}C NMR (150 MHz, $CDCl_3$) δ 163.0, 153.2, 149.7,

145.0, 139.3, 130.5, 118.4, 115.8, 107.9, 82.7, 49.6, 33.5, 33.4, 28.1, 20.3, 14.0; HRMS (DART) *m/z* = 356.1974 calcd for $C_{20}H_{26}N_3O_3$ $[M+H]^+$, found: 356.1972.

***tert*-Butyl**
4-oxo-1-propyl-2-(pyridin-4-yl)-1,4,6,7-tetrahydro-5*H*-pyrrolo[3,2-*c*]pyridine-5-carboxylate (S4)

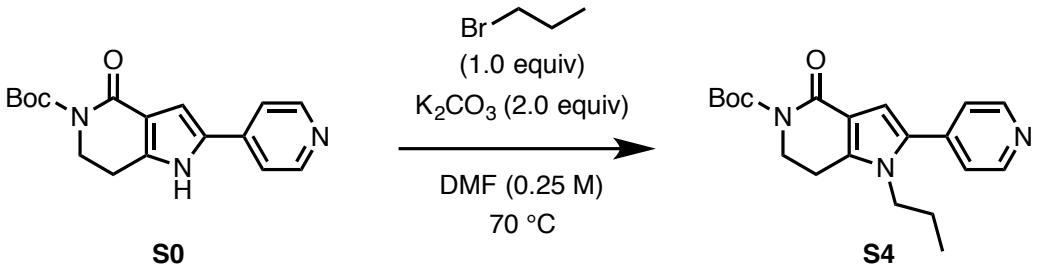

S0 **S4**

To stirred solution of *tert*-butyl 4-oxo-2-(pyridin-4-yl)-1,4,6,7-tetrahydro-5*H*-pyrrolo[3,2-*c*]pyridine-5-carboxylate (**S0**: 62.3 mg, 0.2 mmol, 1.0 equiv) and K_2CO_3 (55.3 mg, 0.4 mmol, 2.0 equiv) in *N*,*N*-dimethylformamide (DMF: 1 mL) was added 1-bromopropane (18.2 μL, 0.2 mmol, 1.0 equiv) at room temperature, and the mixture was stirred for 24 h. It was quenched by the addition of water. The reaction mixture was extracted with ethyl acetate, washed with brine, dried over Na_2SO_4, and concentrated *in vacuo*. The crude mixture was purified by flash column chromatography ($CHCl_3$/MeOH = 100:0 to 40:1) to produce **S4** as a brown oil (52% yield). ^{1}H NMR (600 MHz, $CDCl_3$) δ 8.66 (brs, 2H), 7.28 (d, *J* = 6.0 Hz, 2H), 6.78 (s, 1H), 4.14 (t, *J* = 6.0 Hz, 2H), 3.92 (t, *J* = 7.2 Hz, 2H), 2.91 (t, *J* = 6.0 Hz, 2H), 1.60–1.53 (m, 11H), 0.79 (t, *J* = 7.2 Hz, 3H); ^{13}C NMR (150 MHz, $CDCl_3$) δ 162.3, 153.6, 150.1, 140.5, 140.0, 133.0, 122.7, 115.6, 109.9, 82.5, 46.4, 44.7, 28.1, 24.1, 22.4, 10.8; HRMS (DART) *m/z* = 356.1974 calcd for $C_{20}H_{26}N_3O_3$ $[M+H]^+$, found: 356.1976.

***tert*-Butyl**
1-(11-azidoundecyl)-4-oxo-2-(pyridin-4-yl)-1,4,6,7-tetrahydro-5*H*-pyrrolo[3,2-*c*] pyridine-5-carboxylate (S5)

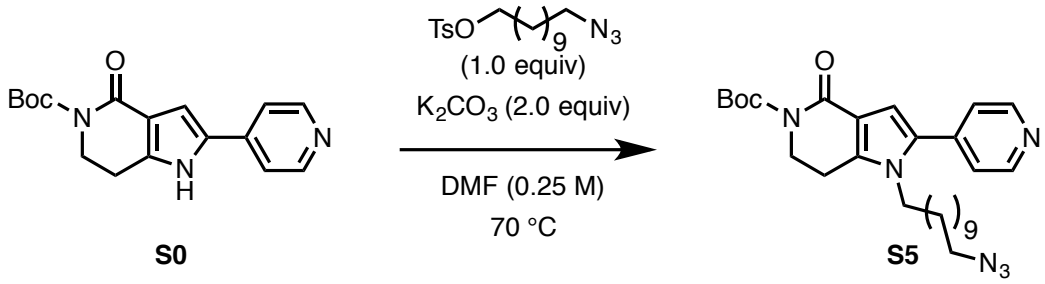

To a stirred solution of *tert*-butyl 4-oxo-2-(pyridin-4-yl)-1,4,6,7-tetrahydro-5*H*-pyrrolo[3,2-*c*]pyridine -5-carboxylate (**S0**: 62.3 mg, 0.2 mmol, 1.0 equiv) and K_2CO_3 (55.3 mg, 0.4 mmol, 2.0 equiv) in DMF (1 mL) was added 11-azidoundecyl 4-methylbenzenesulfonate (73.5 mg, 0.2 mmol, 1.0 equiv) at room temperature, and the mixture was stirred for an additional 23 h before being quenched by the addition of water. The reaction mixture was extracted with ethyl acetate, washed with brine, dried over Na_2SO_4, and concentrated *in vacuo*. The crude mixture was purified by flash column chromatography ($CHCl_3$/MeOH = 100:0 to 40:1) to produce **S5** as a brown oil (41% yield). ^{1}H NMR (600 MHz, $CDCl_3$) δ 8.65 (d, *J* = 6.0 Hz, 2H), 7.27 (d, *J* = 6.0 Hz, 2H), 6.77 (s, 1H), 4.14 (t, *J* = 6.0 Hz, 2H), 3.93 (t, *J* = 7.2 Hz, 2H), 3.25 (t, *J* = 6.6 Hz, 2H), 2.91 (t, *J* = 6.0 Hz, 2H), 1.60–1.53 (m, 11H), 1.39–1.09 (m, 16H); ^{13}C NMR (150 MHz, $CDCl_3$) δ 162.2, 153.6, 150.1, 140.3, 140.0, 133.0, 122.6, 115.6, 109.9, 82.5, 51.4, 44.9, 44.7, 30.7, 29.3, 29.2, 29.0, 28.9, 28.7, 28.1, 26.6, 26.3, 22.4, One carbon signal was not detected even with prolonged scans; HRMS (DART) *m/z* = 509.3240 calcd for $C_{28}H_{41}N_6O_3$ $[M+H]^+$, found: 509.3243.

2-(Pyridin-4-yl)-1,5,6,7-tetrahydro-4*H*-pyrrolo[3,2-*c*]pyridin-4-one hydrochloride (PHA767491)[1]

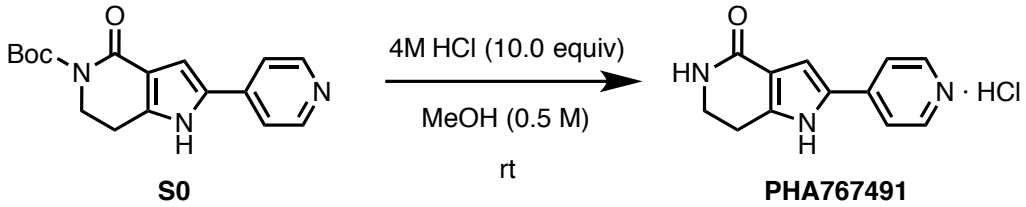

To a solution of *tert*-butyl 4-oxo-2-(pyridin-4-yl)-1,4,6,7-tetrahydro-5*H*-pyrrolo[3,2-*c*]pyridine-5- carboxylate (**S0**: 40.9 mg, 0.13 mmol, 1.0 equiv) in MeOH (0.26 mL) was added hydrogen chloride solution (4.0 M in 1,4-dioxane, 0.33 mL, 10.0 equiv) at 0 °C, and the mixture was allowed to warm to room temperature. After stirring for 1 h, the reaction mixture was

diluted with MeOH, then concentrated *in vacuo* to produce PHA767491 as a yellow solid (92% yield). ^{1}H NMR (600 MHz, DMSO-d_6) δ 8.69 (d, J = 7.8 Hz, 2H), 8.27 (d, J = 6.6 Hz, 2H), 7.55 (d, J = 1.8 Hz, 1H), 7.33 (brs, 1H), 3.42 (t, J = 7.2 Hz, 2H), 2.92 (t, J = 7.2 Hz, 2H), one proton (NH) was not detected; ^{13}C NMR (150 MHz, DMSO-d_6) δ 164.0, 146.8, 143.7, 140.8, 126.6, 118.8, 117.4, 113.3, 40.0, 21.9; HRMS (DART) *m/z* = 214.0980 calcd for $C_{12}H_{12}N_3O$ $[M+H]^+$, found: 214.0976.

2-(Pyridin-3-yl)-1,5,6,7-tetrahydro-4H-pyrrolo[3,2-c]pyridin-4-one hydrochloride (1)

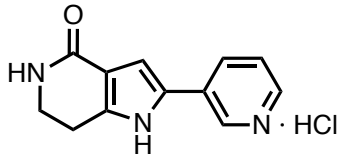

1

Compound **1** was obtained as a yellow solid (93% yield). ^{1}H NMR (600 MHz, DMSO-d_6) δ 9.31 (s, 1H), 8.89 (d, J = 8.4 Hz, 1H), 8.64 (d, J = 6.0 Hz, 1H), 8.02 (dd, J = 8.4, 5.4 Hz, 1H), 7.21 (d, J = 8.4 Hz, 1H), 3.41 (t, J = 7.2 Hz, 2H), 2.86 (t, J = 7.2 Hz, 2H), two protons (NH) were not detected; ^{13}C NMR (150 MHz, DMSO-d_6) δ 164.6, 140.2, 138.9, 137.3, 135.6, 131.9, 127.4, 124.9, 115.7, 108.0, 40.1, 21.7; HRMS (DART) *m/z* = 214.0980 calcd for $C_{12}H_{12}N_3O$ $[M+H]^+$, found: 214.0983.

2-Phenyl-1,5,6,7-tetrahydro-4*H*-pyrrolo[3,2-*c*]pyridin-4-one (2)[1]

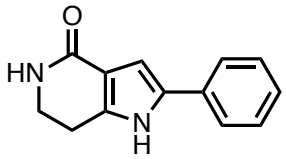

2

Compound **2** was obtained as a yellow solid (quant). ^{1}H NMR (600 MHz, DMSO-d_6) δ 11.9 (brs, 1H), 7.66 (d, J = 7.8 Hz, 2H), 7.36 (t, J = 7.8 Hz, 2H), 7.18 (t, J = 7.8 Hz, 1H), 6.73 (d, J = 2.4 Hz, 1H), 3.43 (t, J = 6.6 Hz, 2H), 2.85 (d, J = 6.6 Hz, 2H), one proton (NH) was not detected; ^{13}C NMR (150 MHz, DMSO-d_6) δ 165.5, 138.0, 132.1, 131.5, 128.8, 126.1, 123.6, 113.8, 103.0, 40.3, 21.7; HRMS (DART) *m/z* = 213.1028 calcd for $C_{13}H_{12}N_2O$ $[M+H]^+$, found: 213.1027.

7-Propyl-2-(pyridin-4-yl)-1,5,6,7-tetrahydro-4*H*-pyrrolo[3,2-*c*]pyridin-4-one

hydrochloride (5)

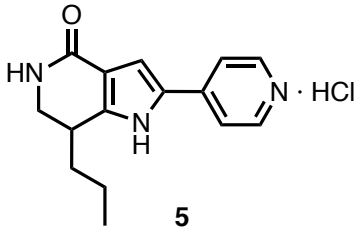

5

Compound **5** was obtained as a yellow solid (87% yield). ^{1}H NMR (600 MHz, DMSO-d_6) δ 8.70 (d, J = 6.6 Hz, 2H), 8.34 (d, J = 7.2 Hz, 2H), 7.55 (d, J = 1.8 Hz, 1H), 7.29 (brs, 1H), 3.52 (dd, J = 12.6, 5.4 Hz, 1H), 3.21 (dd, J = 12.6, 4.8 Hz, 1H), 3.05–2.99 (m, 1H), 1.82–1.73 (m, 1H), 1.60–1.52 (m, 1H), 1.48–1.39 (m, 1H), 1.34–1.24 (m, 1H), 0.90 (t, J = 7.2 Hz, 3H), one proton (NH) was not detected; ^{13}C NMR (150 MHz, DMSO-d_6) δ 163.6, 147.3, 146.8, 140.7, 126.8, 119.0, 116.7, 113.3, 44.3, 33.4, 32.3, 19.6, 14.0; HRMS (DART) m/z = 256.1450 calcd for $C_{15}H_{18}N_3O$ $[M+H]^+$, found: 256.1447.

1-Propyl-2-(pyridin-4-yl)-1,5,6,7-tetrahydro-4*H*-pyrrolo[3,2-*c*]pyridin-4-one (6)

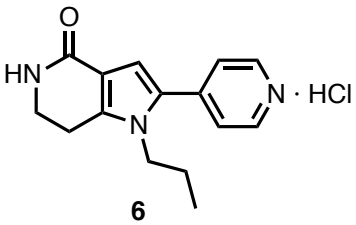

6

Compound **6** was obtained as a white solid (85% yield). ^{1}H NMR (600 MHz, CD_3OD) δ 8.83 (d, J = 6.0 Hz, 2H), 8.19 (d, J = 6.0 Hz, 2H), 7.32 (s, 1H), 4.31 (t, J = 7.2 Hz, 2H), 3.74 (t, J = 6.6 Hz, 2H), 3.16 (t, J = 7.2 Hz, 2H), 1.73 (sext, J = 7.2 Hz, 2H), 0.88 (t, J = 7.8 Hz, 3H); ^{13}C NMR (150 MHz, CD_3OD) δ 167.7, 150.2, 147.6, 142.5, 131.5, 124.6, 115.8, 114.3, 48.5, 41.4, 25.0, 22.4, 11.0, one carbon signal was not detected even with prolonged scans; HRMS (DART) m/z = 256.1450 calcd for $C_{15}H_{18}N_3O$ $[M+H]^+$, found: 256.1448.

1-(11-azidoundecyl)-2-(pyridin-4-yl)-1,5,6,7-tetrahydro-4*H*-pyrrolo[3,2-*c*]pyridin-4-one (S6)

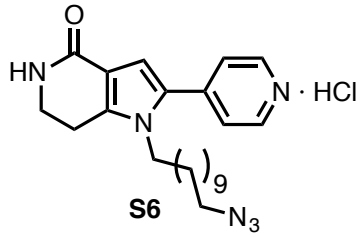

S6

Compound **S6** was obtained without purification as a yellow solid (93% yield). ^{1}H NMR (600 MHz, CD_3OD) δ 8.80 (d, *J* = 7.2 Hz, 2H), 8.16 (d, *J* = 7.2 Hz, 2H), 7.29 (s, 1H), 4.30 (t, *J* = 7.2 Hz, 2H), 3.72 (t, *J* = 7.2 Hz, 2H), 3.26 (t, *J* = 7.2 Hz, 2H), 3.12 (t, *J* = 7.2 Hz, 2H), 1.65 (quin, *J* = 6.6 Hz, 2H), 1.55 (quin, *J* = 6.6 Hz, 2H), 1.39–1.17 (m, 14H); ^{13}C NMR (150 MHz, CD_3OD) δ 167.7, 150.2, 147.6, 142.6, 131.6, 124.7, 115.8, 114.0, 52.4, 47.1, 41.4, 31.7, 30.48, 30.45, 30.4, 30.2, 30.1, 29.9, 27.7, 27.4, 22.4; HRMS (DART) *m/z* = 409.2716 calcd for $C_{23}H_{33}N_6O$ $[M+H]^+$, found: 409.2720.

2-(Pyridin-4-yl)-1,5,6,7-tetrahydro-4*H*-indol-4-one (3)

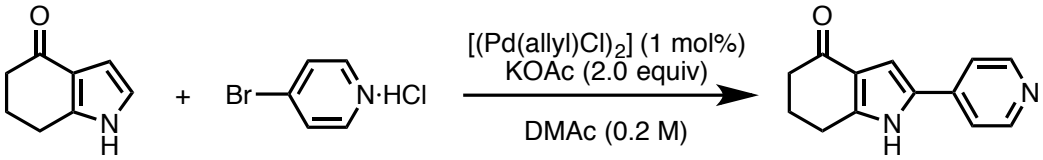

(1.5 equiv) **3**

To a 10-mL Schlenk tube containing a magnetic stirring bar, were added 4-bromopyridine hydrochloride (58.3 mg, 0.3 mmol, 1.0 equiv), 1,5,6,7-tetrahydro-4*H*-indol-4-one (60.8 mg, 0.45 mmol, 1.5 equiv), $Pd(OAc)_2$ (1.1 mg, 3 μmol, 1 mol%), KOAc (58.9 mg, 0.6 mmol, 2.0 equiv), and *N*,*N*-dimethylacetamide (DMAc: 1.5 mL). The mixture was stirred at 130 °C for 20 h. After cooling the reaction mixture to room temperature, it was quenched by the addition of sat. $NaHCO_3$ aq. The reaction mixture was extracted with ethyl acetate, washed with brine, dried over Na_2SO_4, and concentrated *in vacuo*. The residue was purified by flash column chromatography ($CHCl_3$/MeOH = 40:1 to 20:1) and PTLC ($CHCl_3$/MeOH = 10:1), resulting in **3** as a white solid (23% yield). ^{1}H NMR (600 MHz, CD_3OD) δ 8.44 (d, *J* = 6.6 Hz, 2H), 7.58 (d, *J* = 6.6 Hz, 2H), 7.04 (d, *J* = 4.2 Hz, 1H), 2.93–2.88 (m, 2H), 2.51–2.45 (m, 2H), 2.19–2.13 (m, 2H), one proton was not detected; ^{13}C NMR (150 MHz, CD_3OD) δ 197.5, 150.5, 149.5, 141.4, 131.4, 122.5, 119.6, 106.7, 38.7, 24.9, 23.5; HRMS (DART) *m/z* = 213.1030 calcd for $C_{13}H_{13}N_2O$ $[M+H]^+$, found: 213.1028.

2-(Pyridin-4-yl)-6,7-dihydrothieno[3,2-*c*]pyridin-4(5*H*)-one (4)

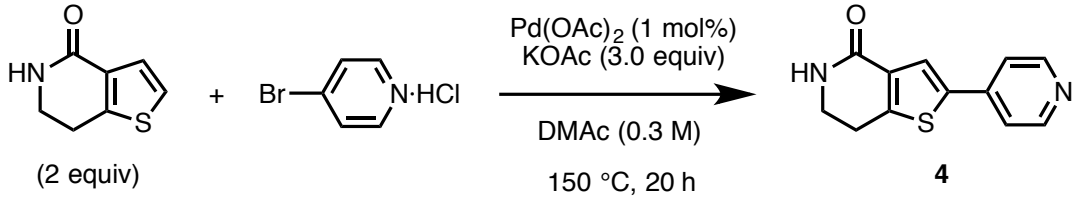

To a 10 mL Schlenk tube containing a magnetic stirring bar were added 4-bromopyridine hydrochloride (77.8 mg, 0.4 mmol, 1.0 equiv), 6,7-dihydrothieno[3,2-*c*]pyridin-4(5*H*)-one (122.6 mg, 0.8 mmol, 2.0 equiv), $Pd(OAc)_2$ (0.9 mg, 4 μmol, 1 mol%), KOAc (117.8 mg, 1.2 mmol, 3.0 equiv), and DMAc (1.3 mL). The mixture was stirred at 150 °C for 20 h. After cooling the reaction mixture to room temperature, it was quenched by the addition of sat. $NaHCO_3$ aq. The reaction mixture was extracted with ethyl acetate, washed with brine, dried over Na_2SO_4, and concentrated *in vacuo*. The residue was purified by PTLC ($CHCl_3$/MeOH = 10:1) to afford **4** as a white solid (47% yield). ^{1}H NMR (600 MHz, CD_3OD) δ 8.53 (d, *J* = 6.0 Hz, 2H), 7.89 (s, 1H), 7.67 (d, *J* = 6.6 Hz, 2H), 3.63 (t, *J* = 7.2 Hz, 2H), 3.13 (t, *J* = 7.2 Hz, 2H); ^{13}C NMR (150 MHz, CD_3OD) δ 163.2, 150.5, 147.5, 140.6, 138.9, 133.3, 123.8, 119.6, 41.0, 24.5; HRMS (DART) *m/z* = 231.0592 calcd for $C_{12}H_{11}N_2OS$ $[M+H]^+$, found: 231.0591.

1-(11-Aminoundecyl)-2-(pyridin-4-yl)-1,5,6,7-tetrahydro-4*H*-pyrrolo[3,2-*c*]pyridin-4-one (S7)

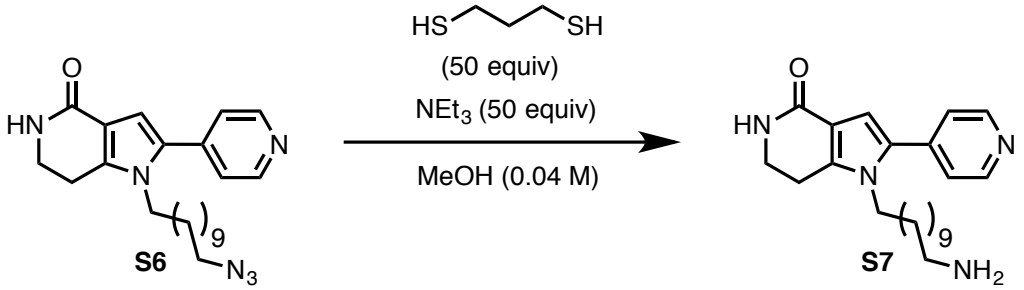

To a solution of 1-(11-azidoundecyl)-2-(pyridin-4-yl)-1,5,6,7-tetrahydro-4*H*-pyrrolo[3,2-*c*]pyridin-4-one hydrochloride (33.0 mg, 0.07 mmol) and triethylamine (NEt_3: 0.52 mL, 3.71 mmol, 50 equiv) in MeOH (1.85 mL) was added 1,3-propanedithiol (0.37 mL, 3.71 mmol, 50.0 equiv), and the mixture was stirred at room temperature for 39 h. The reaction mixture was diluted with MeOH and concentrated *in vacuo*. The residue was

purified by PTLC ($CHCl_3$/MeOH = 3:1) to afford **S7** as a colorless oil (90% yield). ^{1}H NMR (600 MHz, CD_3OD) δ 8.56 (d, *J* = 4.8 Hz, 2H), 7.91 (s, 1H), 7.50 (d, *J* = 4.8 Hz, 2H), 6.70 (s, 1H), 4.12 (t, *J* = 4.8 Hz, 2H), 3.59 (t, *J* = 4.8 Hz, 2H), 2.95 (t, *J* = 6.6 Hz, 2H), 2.91 (t, *J* = 7.2 Hz, 2H), 1.68–1.60 (m, 2H), 1.56–1.47 (m, 2H), 1.42–1.07 (m, 14H), one proton (NH) was not detected; ^{13}C NMR (150 MHz, CD_3OD) δ 168.6, 150.5, 142.9, 142.2, 133.3, 124.1, 115.0, 110.0, 79.5, 45.8, 41.6, 40.8, 31.5, 30.32, 30.28, 30.2, 29.8, 28.6, 27.4, 27.1, 22.7; HRMS (DART) *m/z* = 383.2811 calcd for $C_{23}H_{35}N_4O$ $[M+H]^+$, found: 383.2811.

Synthesis of PHA-probe (7)

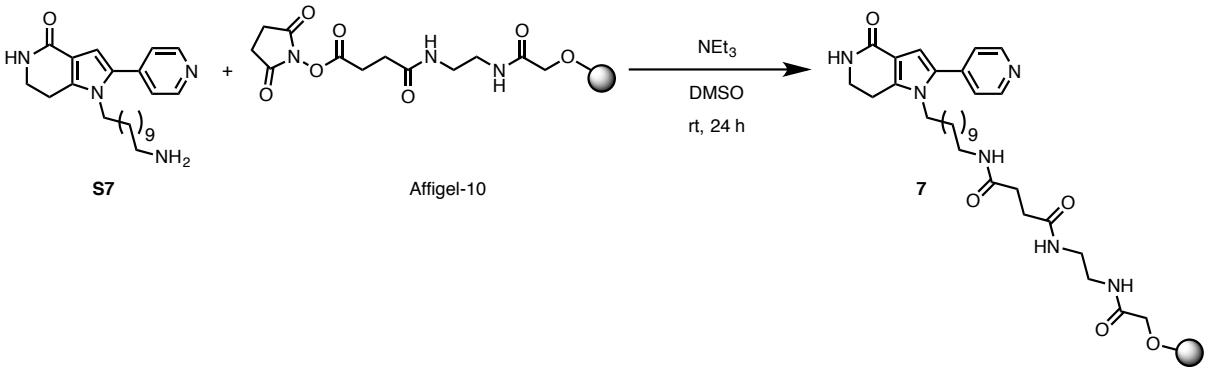

Affigel-10 ([153-6046, Bio-Rad], 1.5 mL, 22.5 μmol, 2.9 equiv) was washed 3x with DMSO. To a solution of Affigel-10 and NEt_3 (10 μL, 70 μmol, 9.0 equiv) in DMSO (1.5 mL) was added 1-(11-aminoundecyl)-2-(pyridin-4-yl)-1,5,6,7-tetrahydro-4*H*-pyrrolo [3,2-*c*] pyridin-4-one (**S7**: 3.0 mg, 7.8 μmol, 1.0 equiv), and the mixture was stirred at room temperature overnight. LC-MS indicated that all of **S7** was consumed. The reaction mixture was treated with 2-ethanolamine (4 μL, 0.07 mmol, 7 equiv) and stirred overnight. The PHA probe **7** was washed with DMSO and PBS, and stored at 4 °C in 2 mL PBS solution containing 0.05% NaN_3.

^{1}H NMR and ^{13}C NMR Spectra

^{1}H NMR of **S0** (600 MHz, CD_3OD)

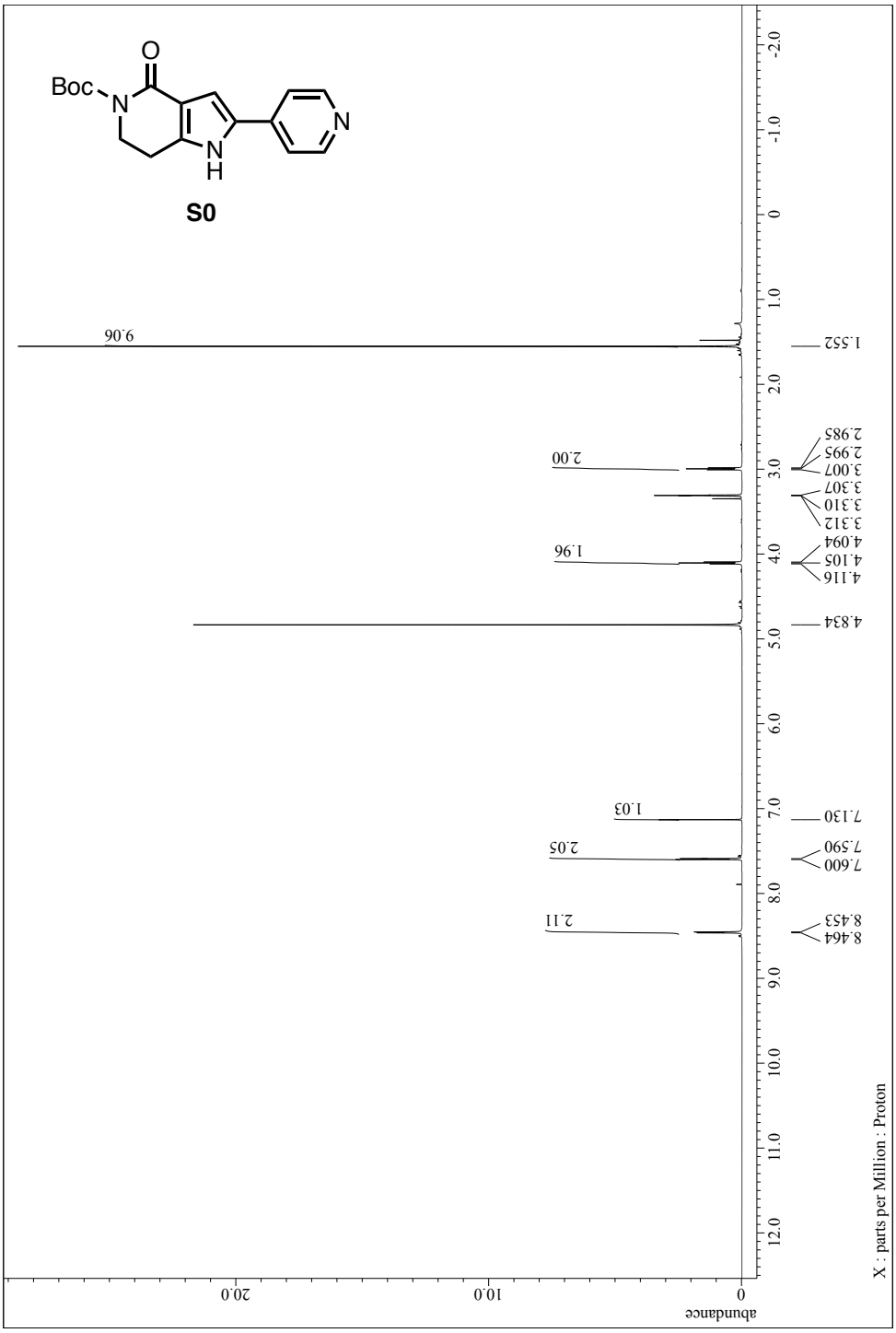

^{13}C NMR of **S0** (150 MHz, CD_3OD)

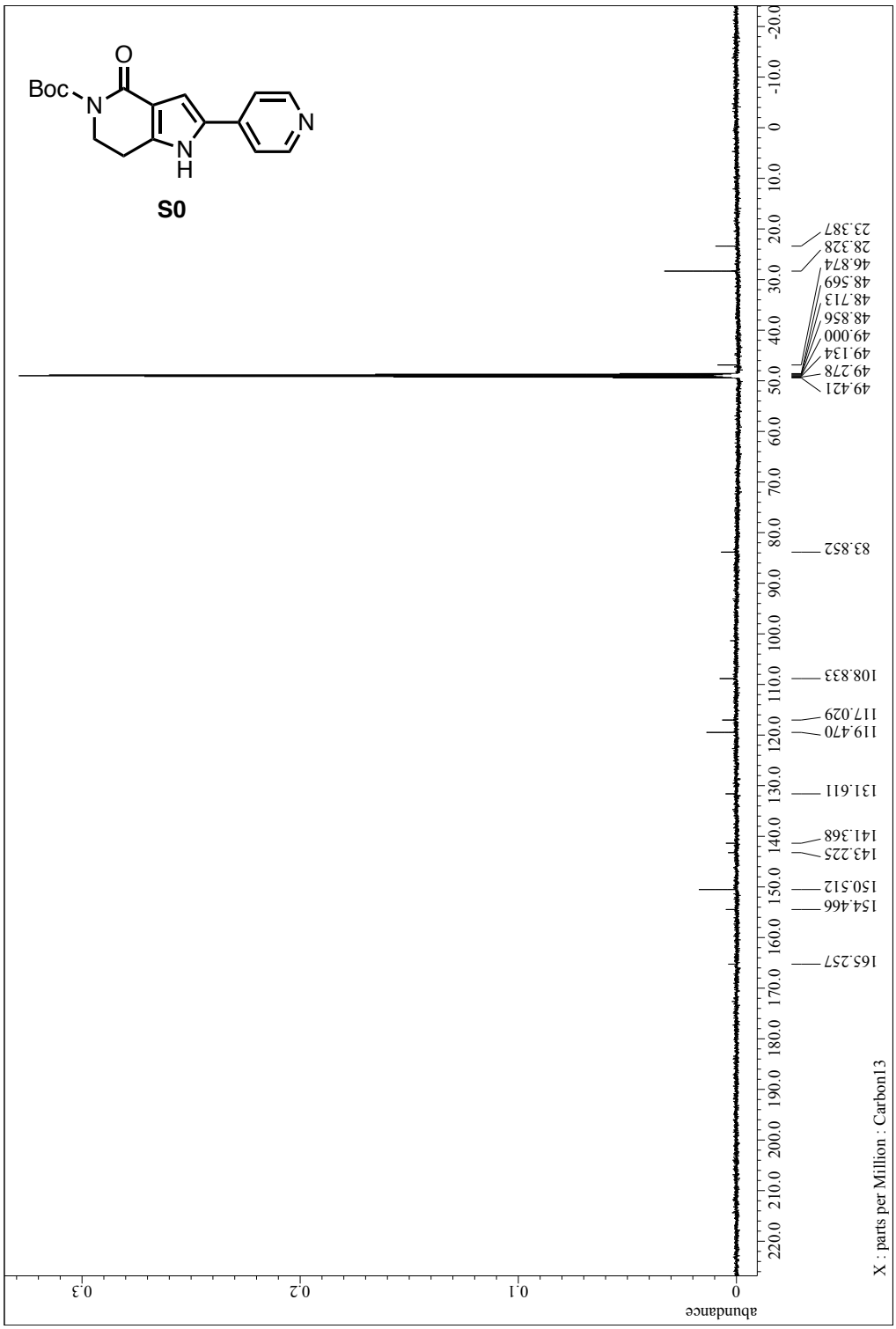

^{1}H NMR of **S1** (600 MHz, $CDCl_3$)

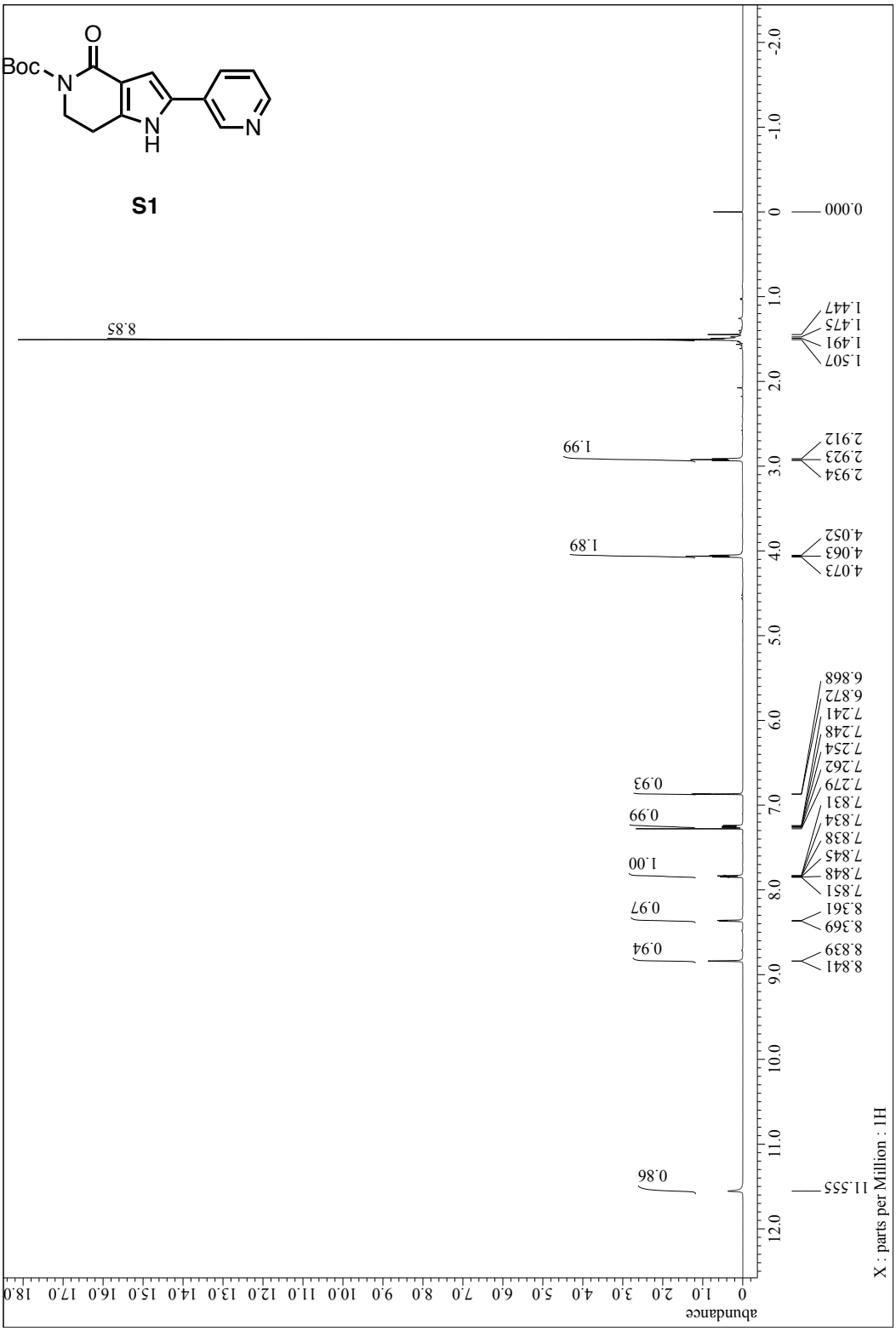

^{13}C NMR of **S1** (150 MHz, $CDCl_3$)

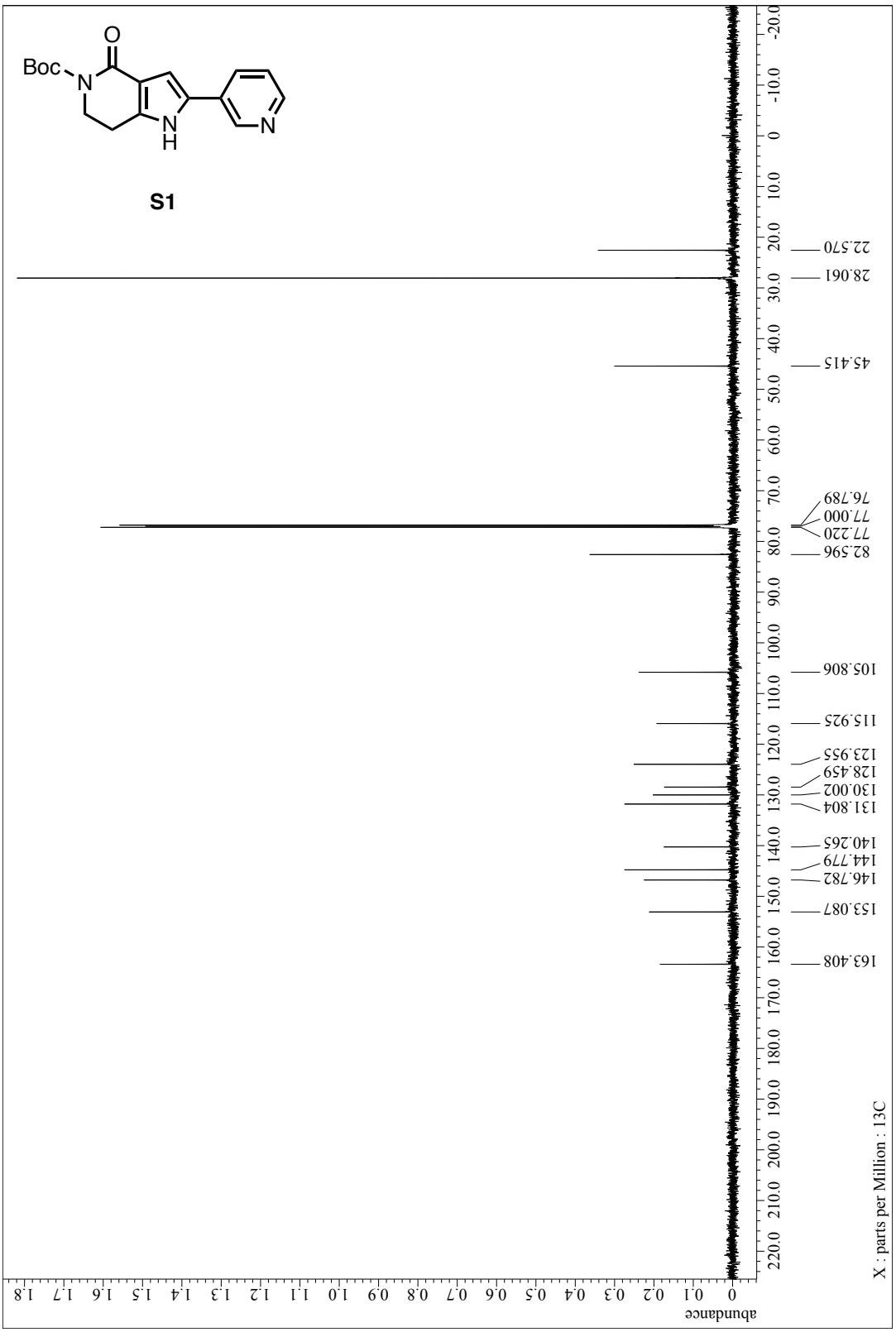

^{1}H NMR of **S2** (600 MHz, $CDCl_3$)

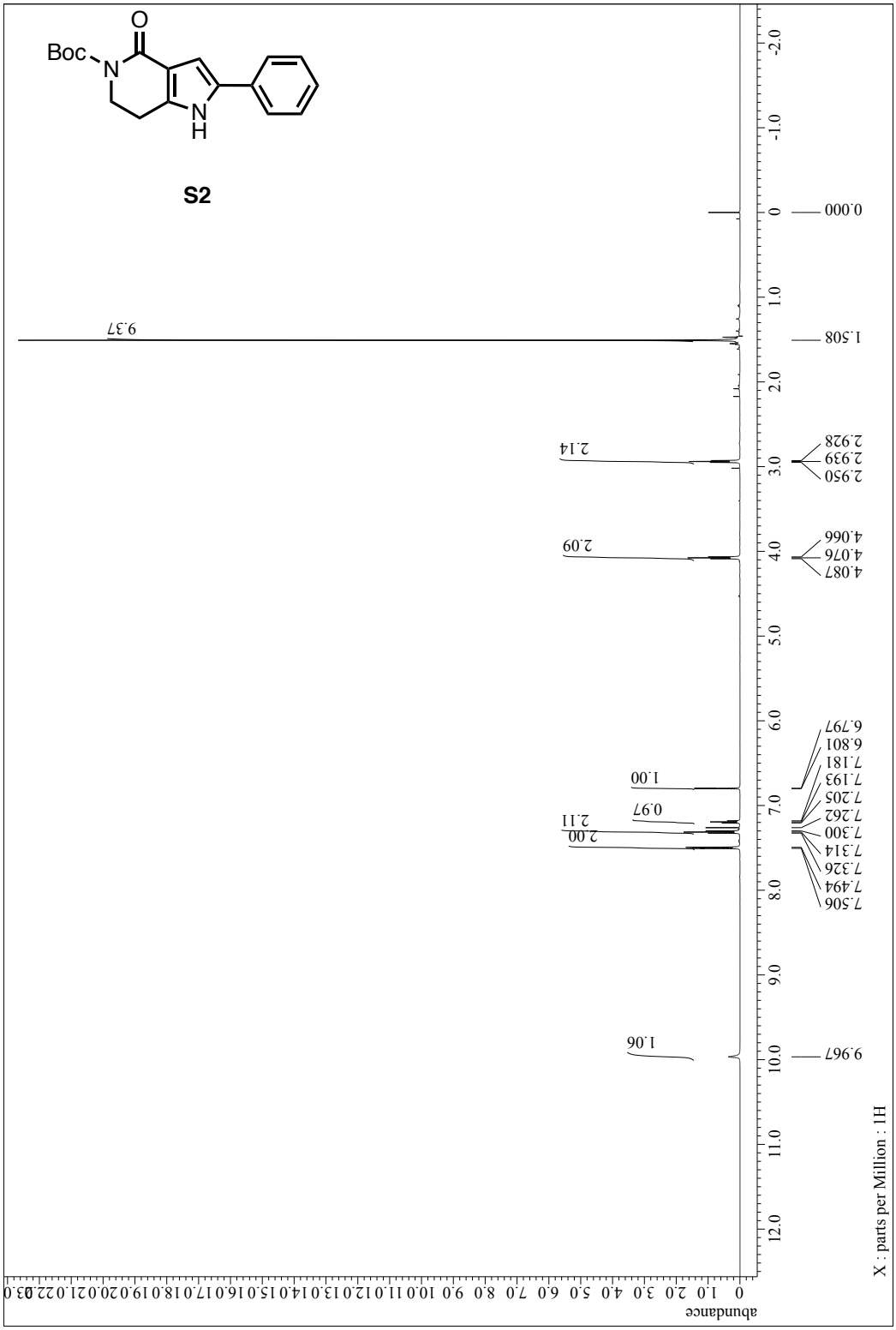

^{13}C NMR of **S2** (150 MHz, $CDCl_3$)

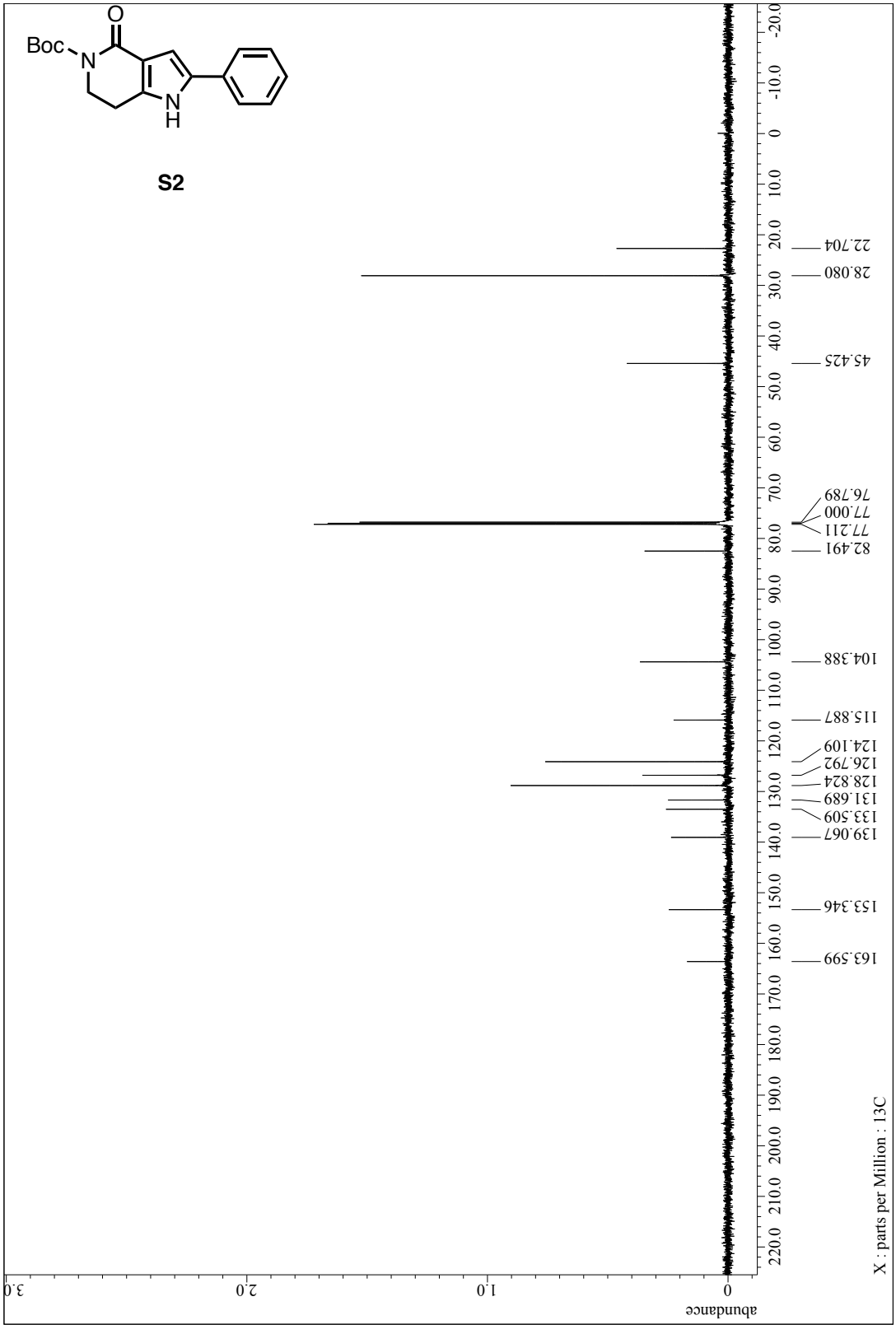

^{1}H NMR of **S3** (600 MHz, $CDCl_3$)

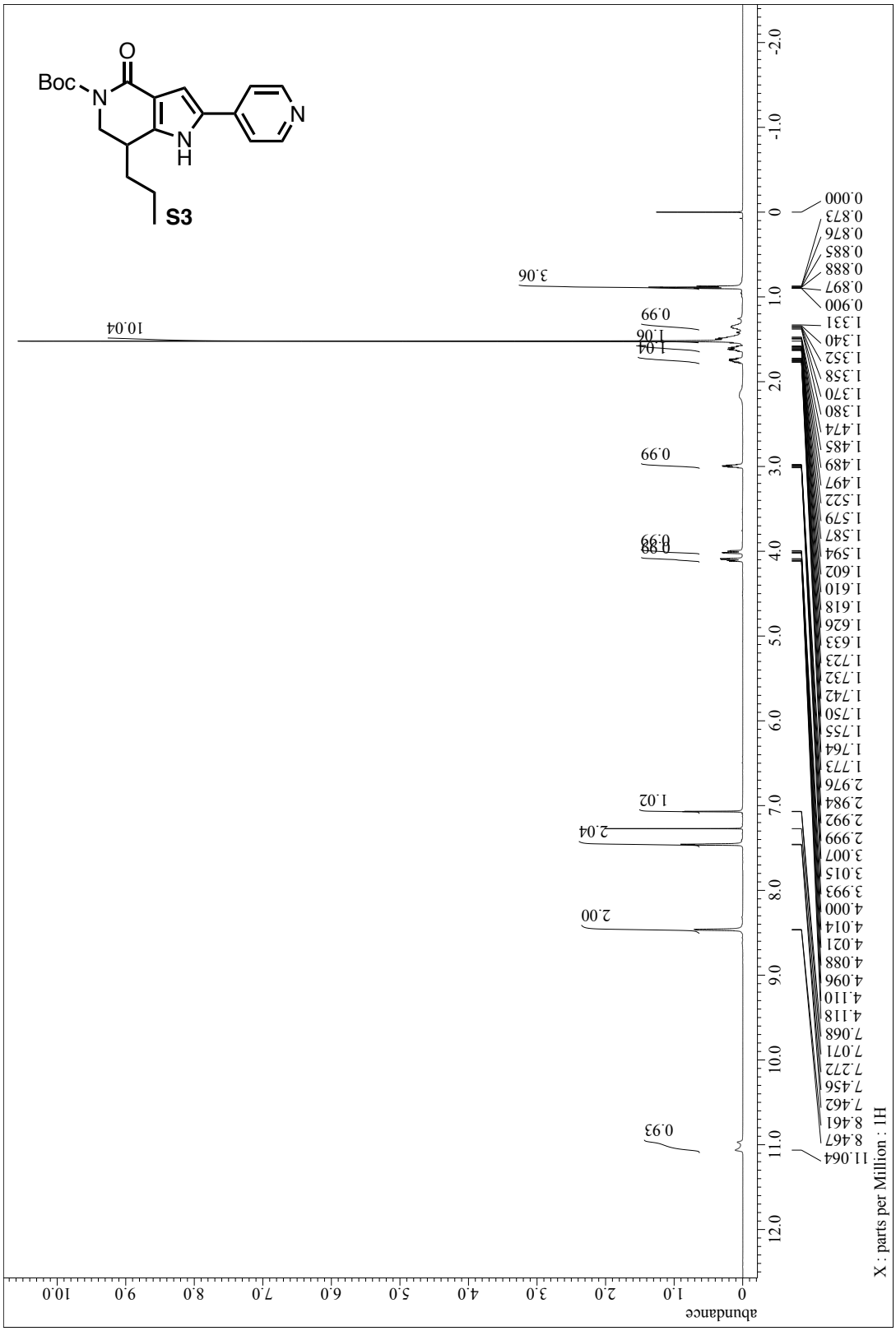

^{13}C NMR of **S3** (150 MHz, $CDCl_3$)

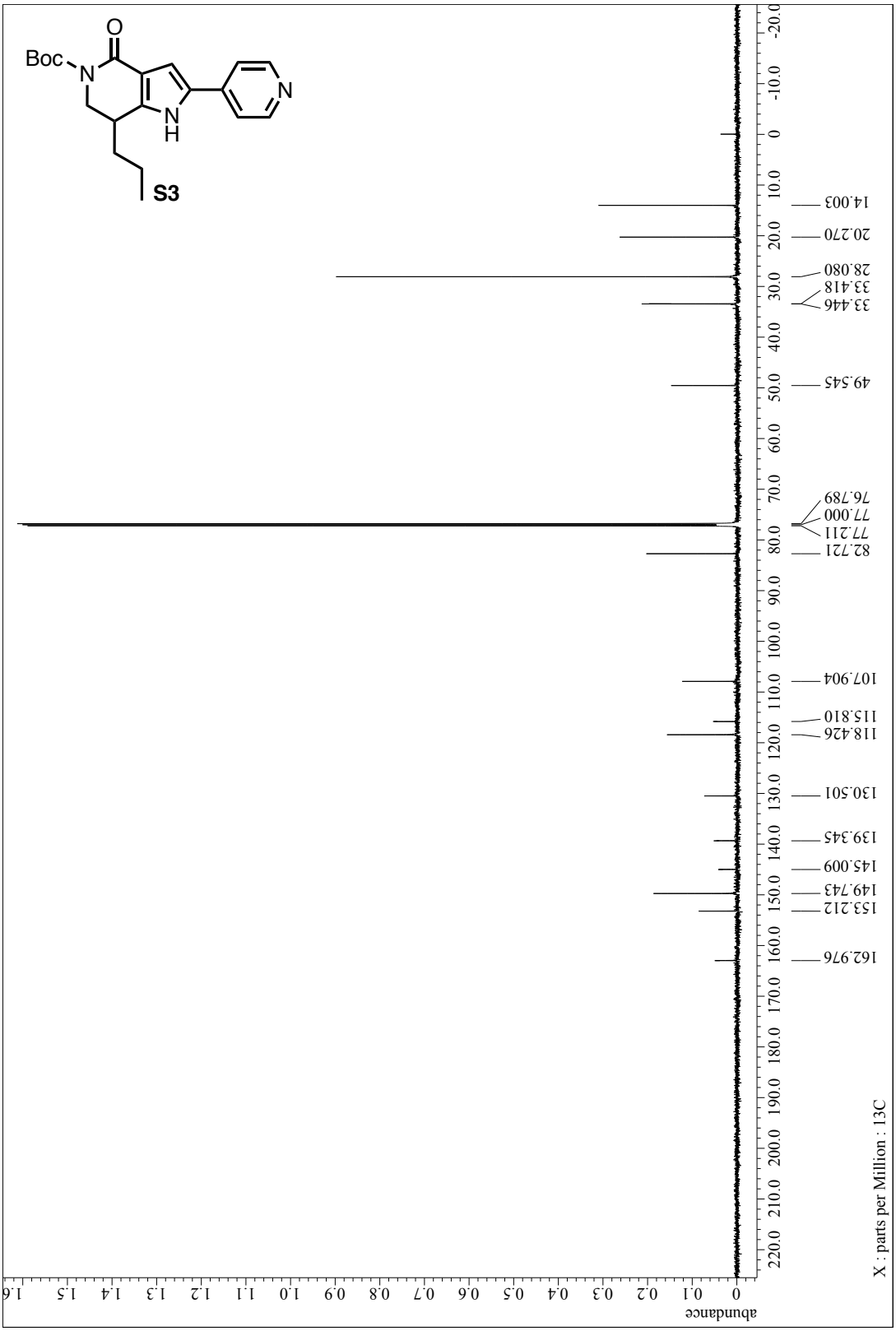

^{1}H NMR of **S4** (600 MHz, $CDCl_3$)

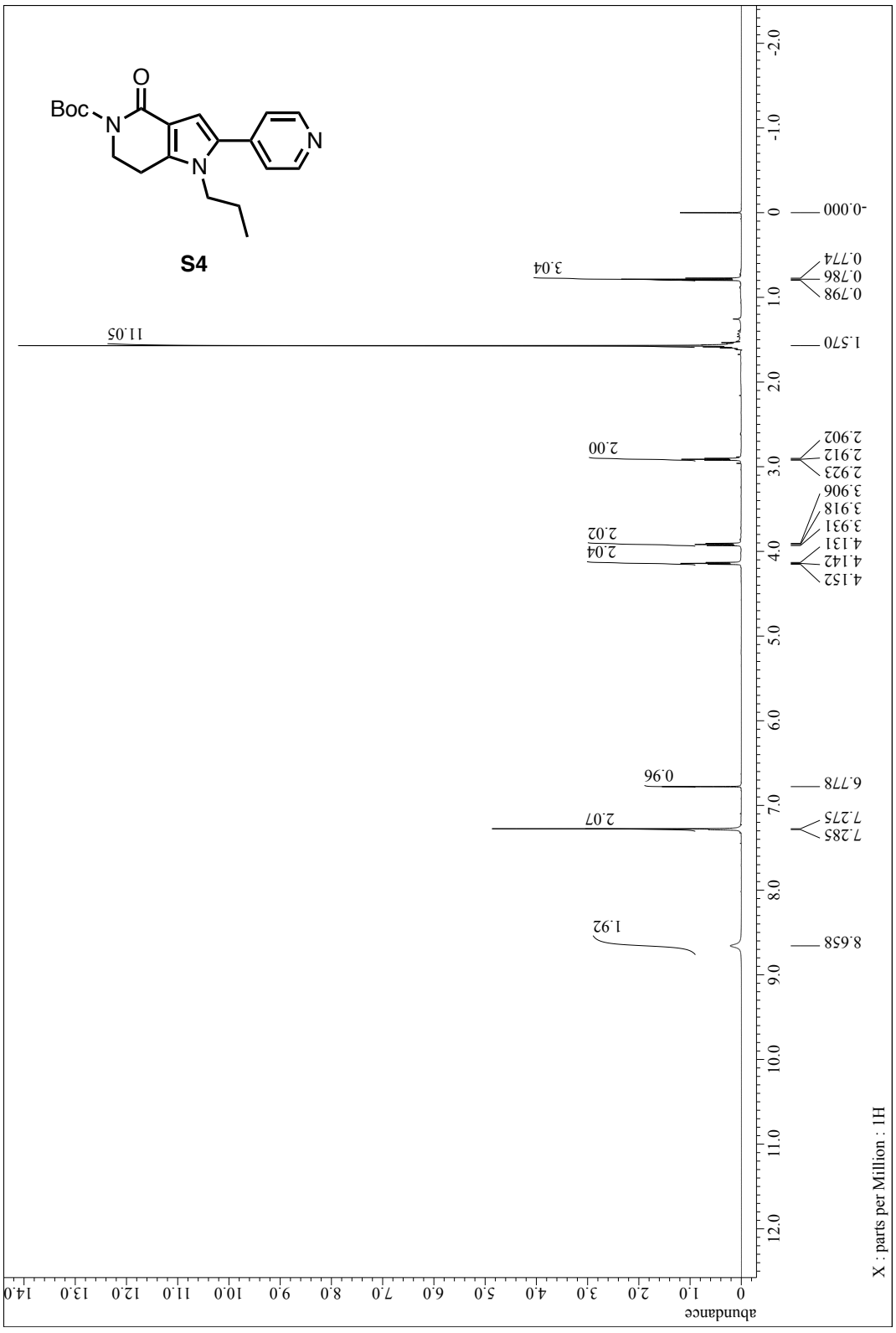

^{13}C NMR of **S4** (150 MHz, $CDCl_3$)

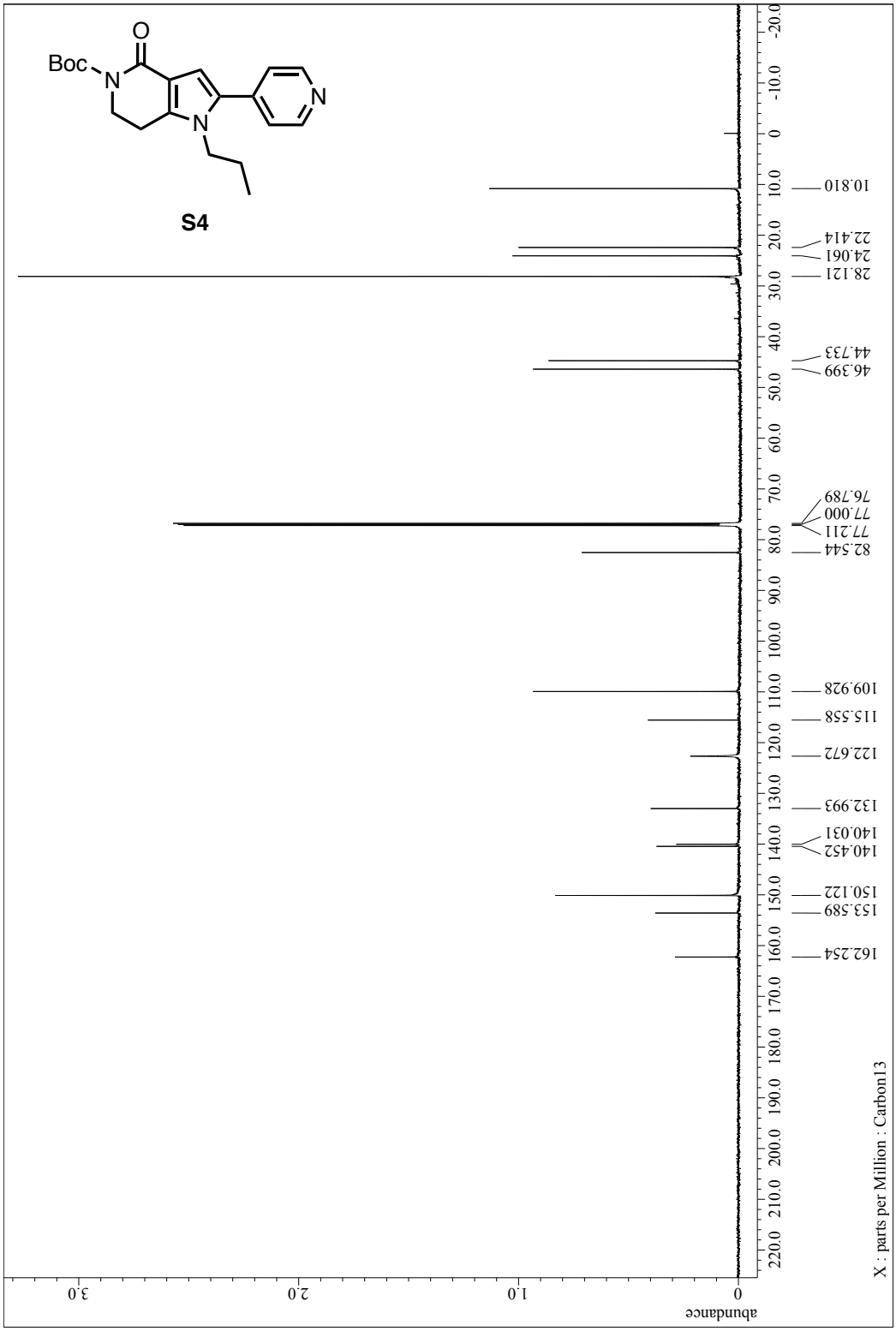

^{1}H NMR of **S5** (600 MHz, $CDCl_3$)

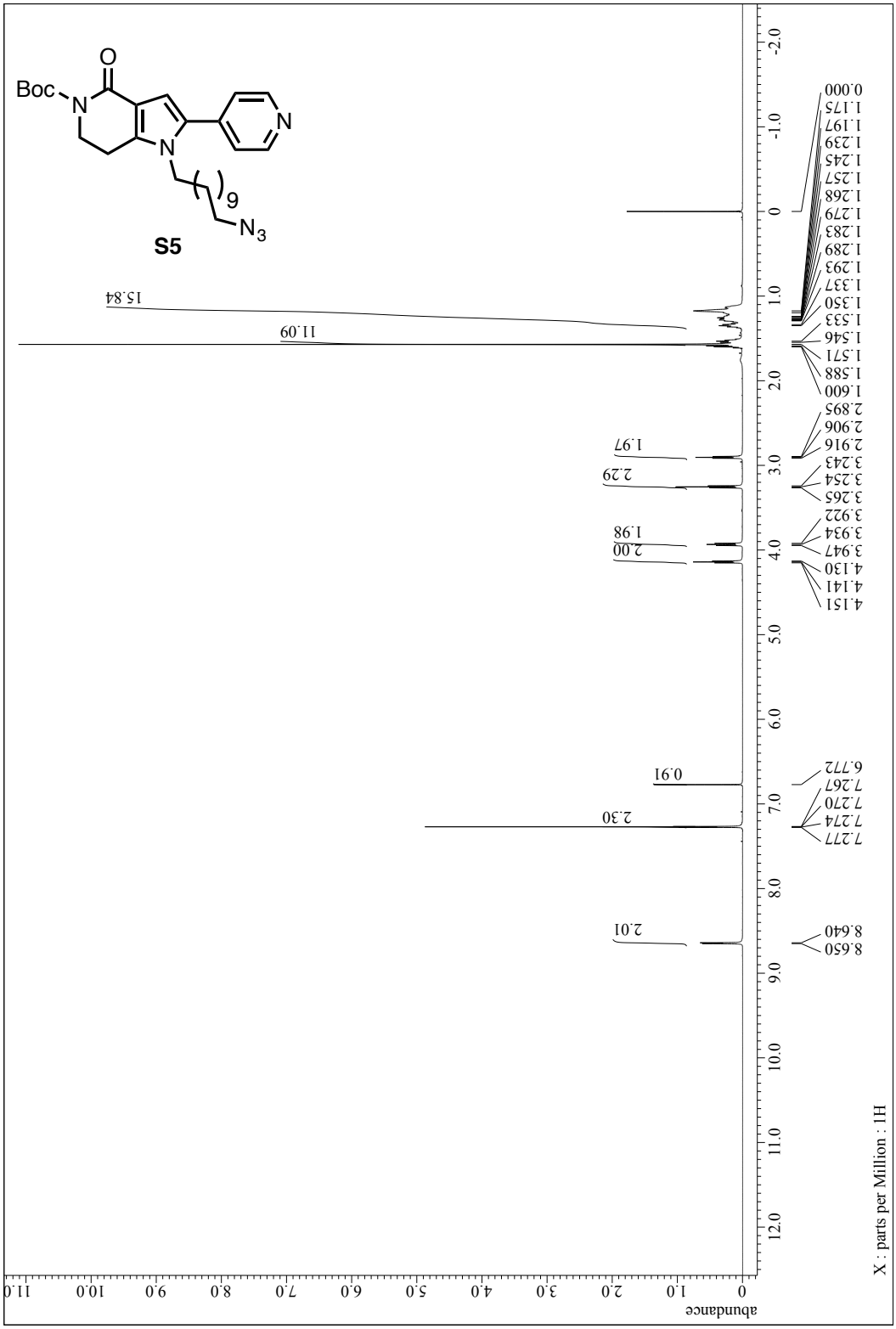

^{13}C NMR of **S5** (150 MHz, $CDCl_3$)

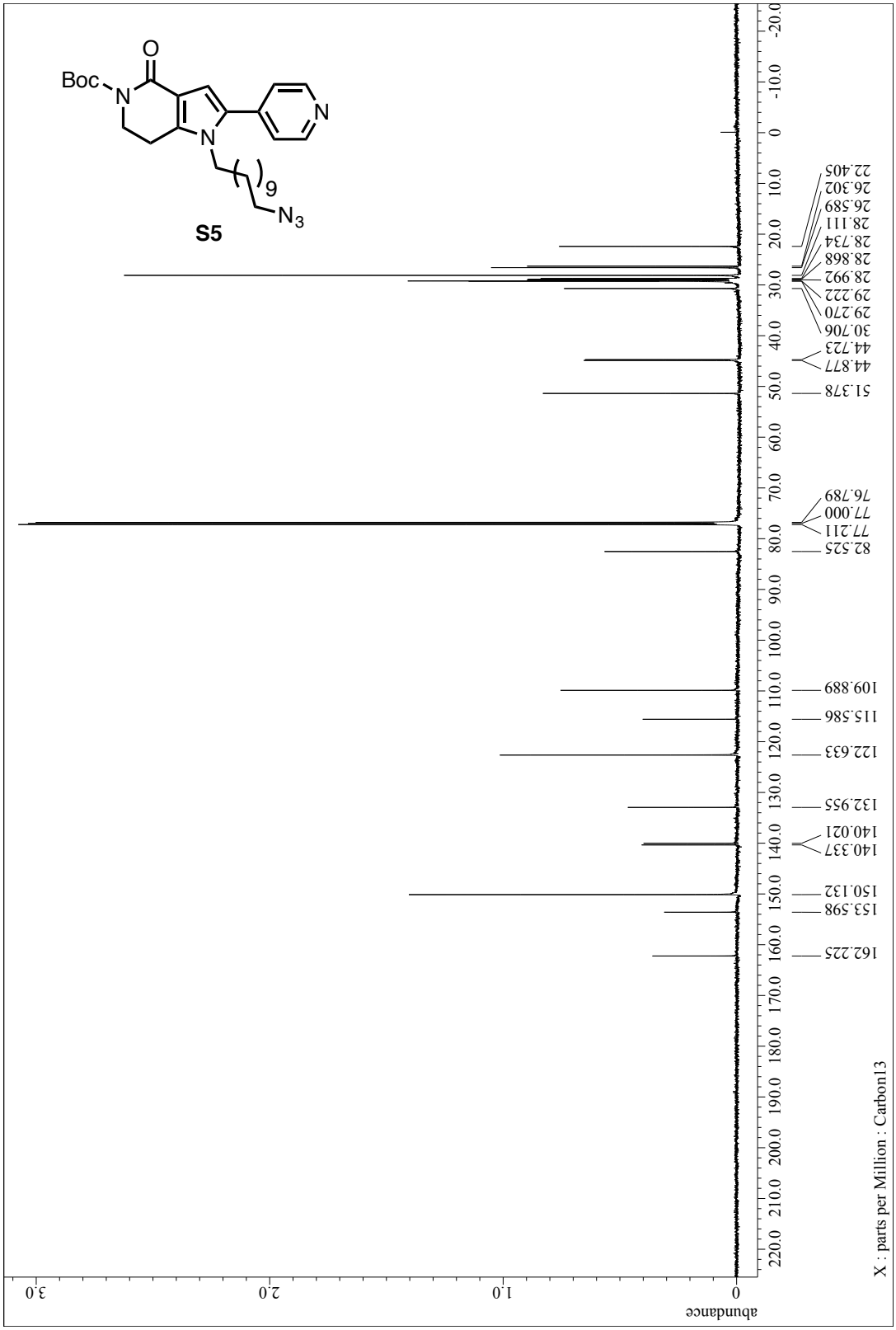

^{1}H NMR of PHA767491 (600 MHz, DMSO-d_6)

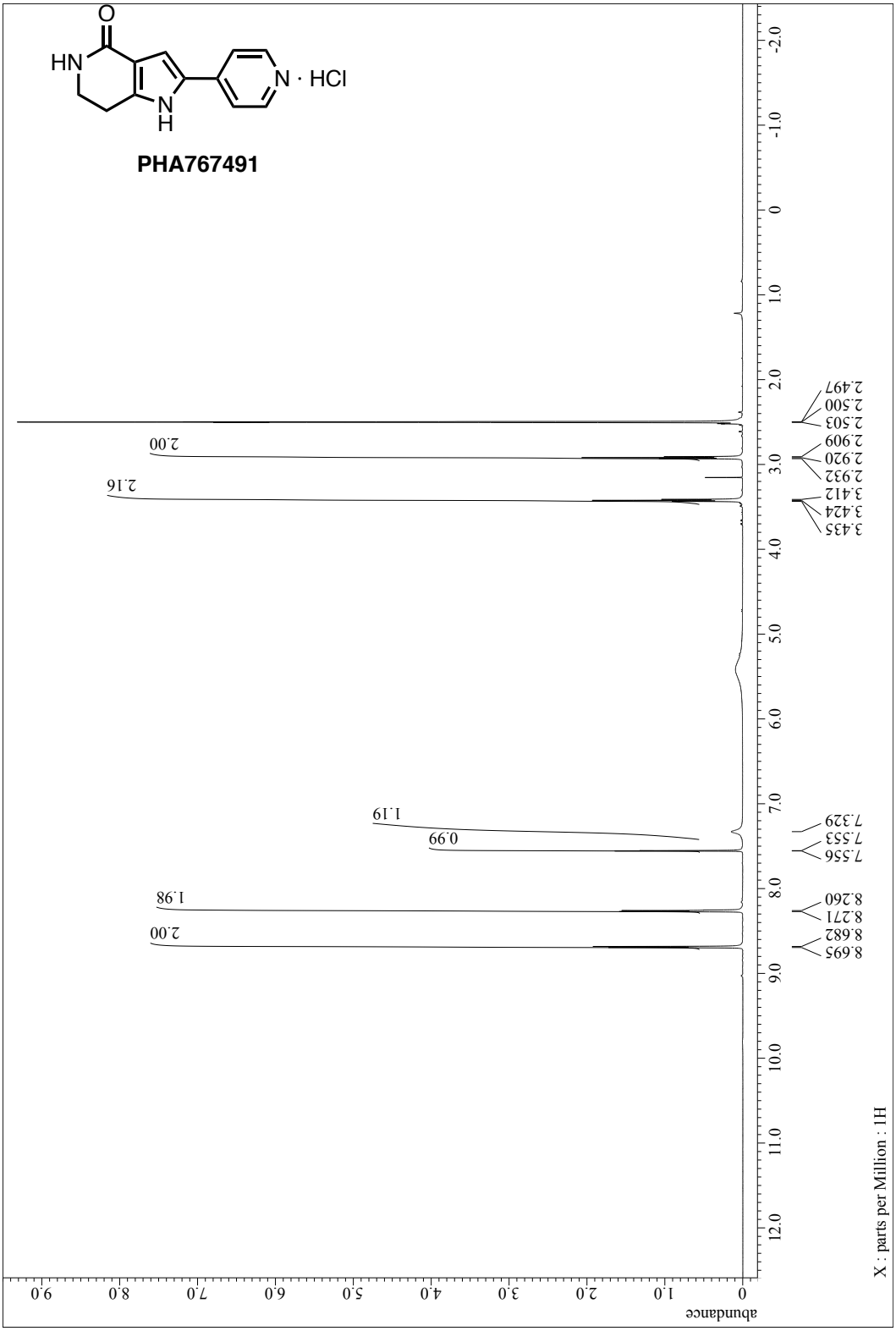

^{13}C NMR of PHA767491 (150 MHz, DMSO-d_6)

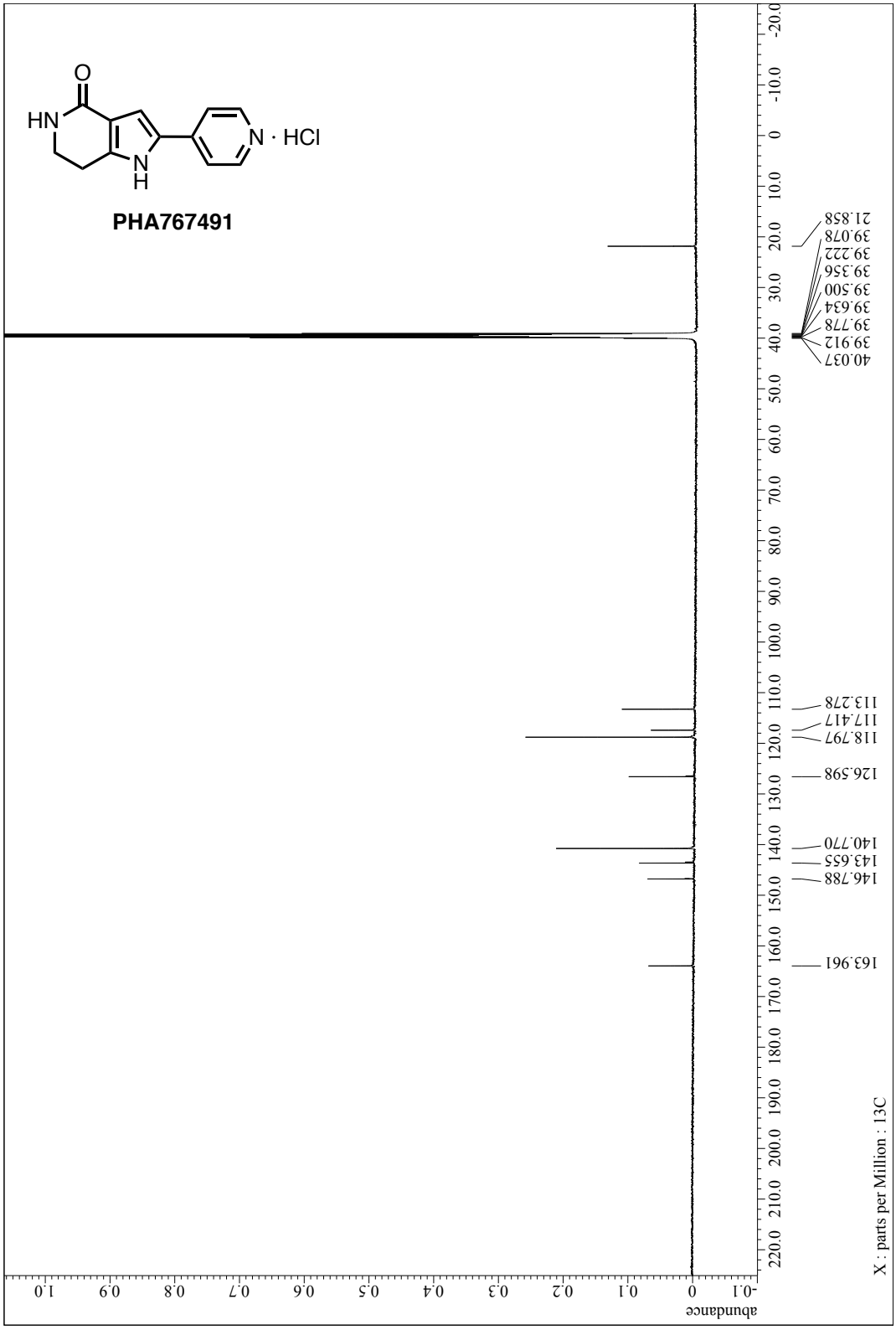

^{1}H NMR of **1** (600 MHz, DMSO-d_6)

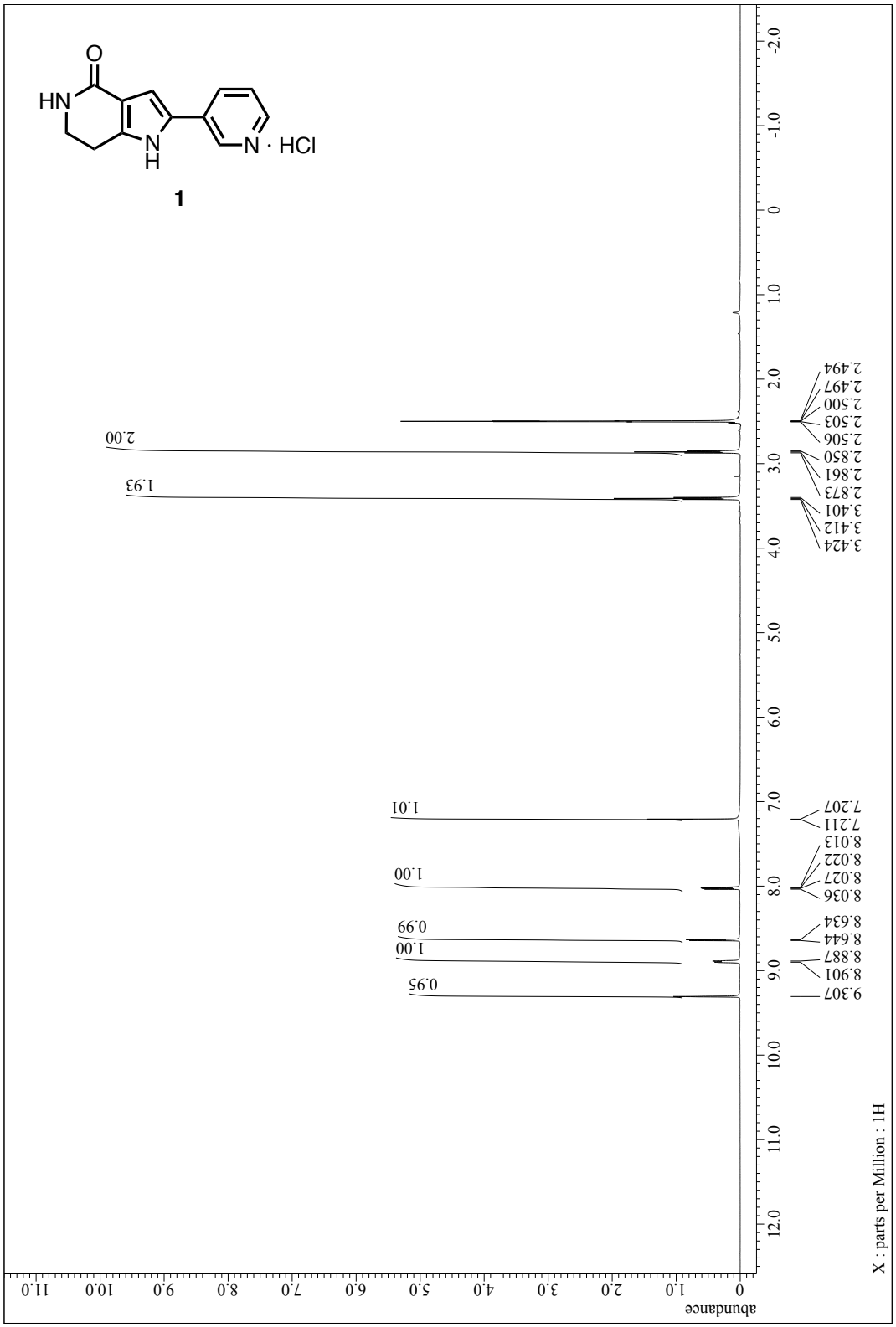

^{13}C NMR of **1** (150 MHz, DMSO-d_6)

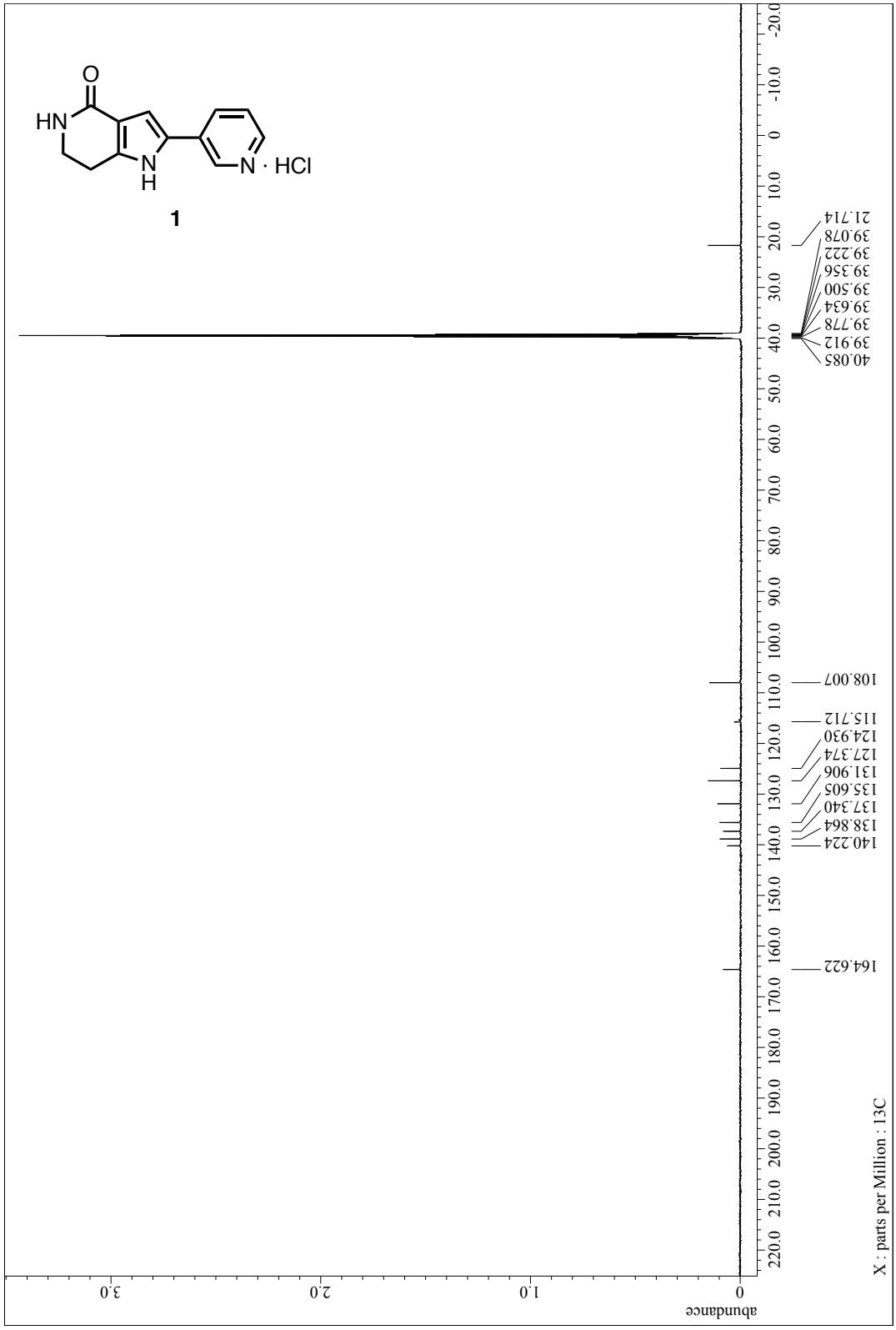

^{1}H NMR of **2** (600 MHz, DMSO-d_6)

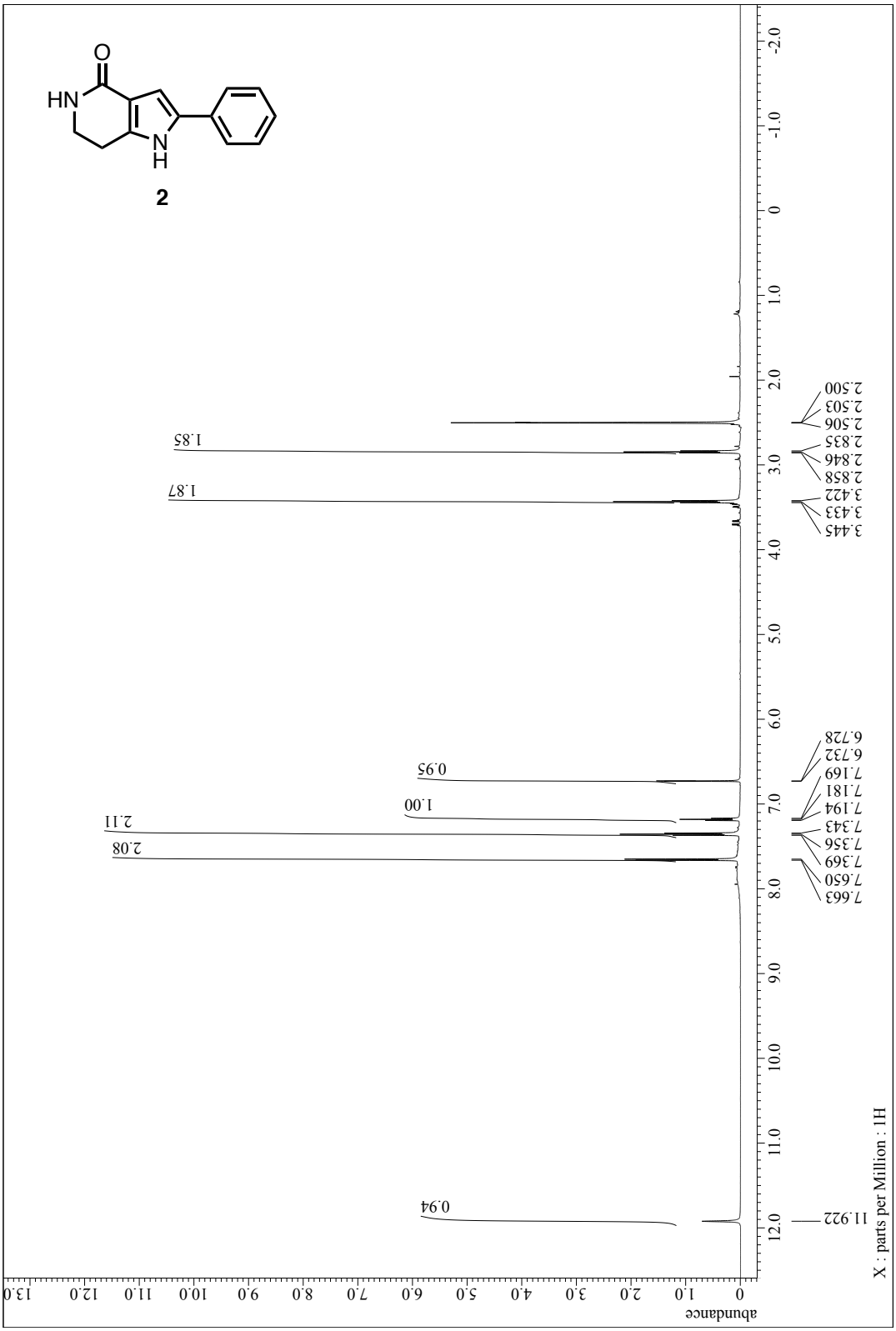

^{13}C NMR of **2** (150 MHz, DMSO-d_6)

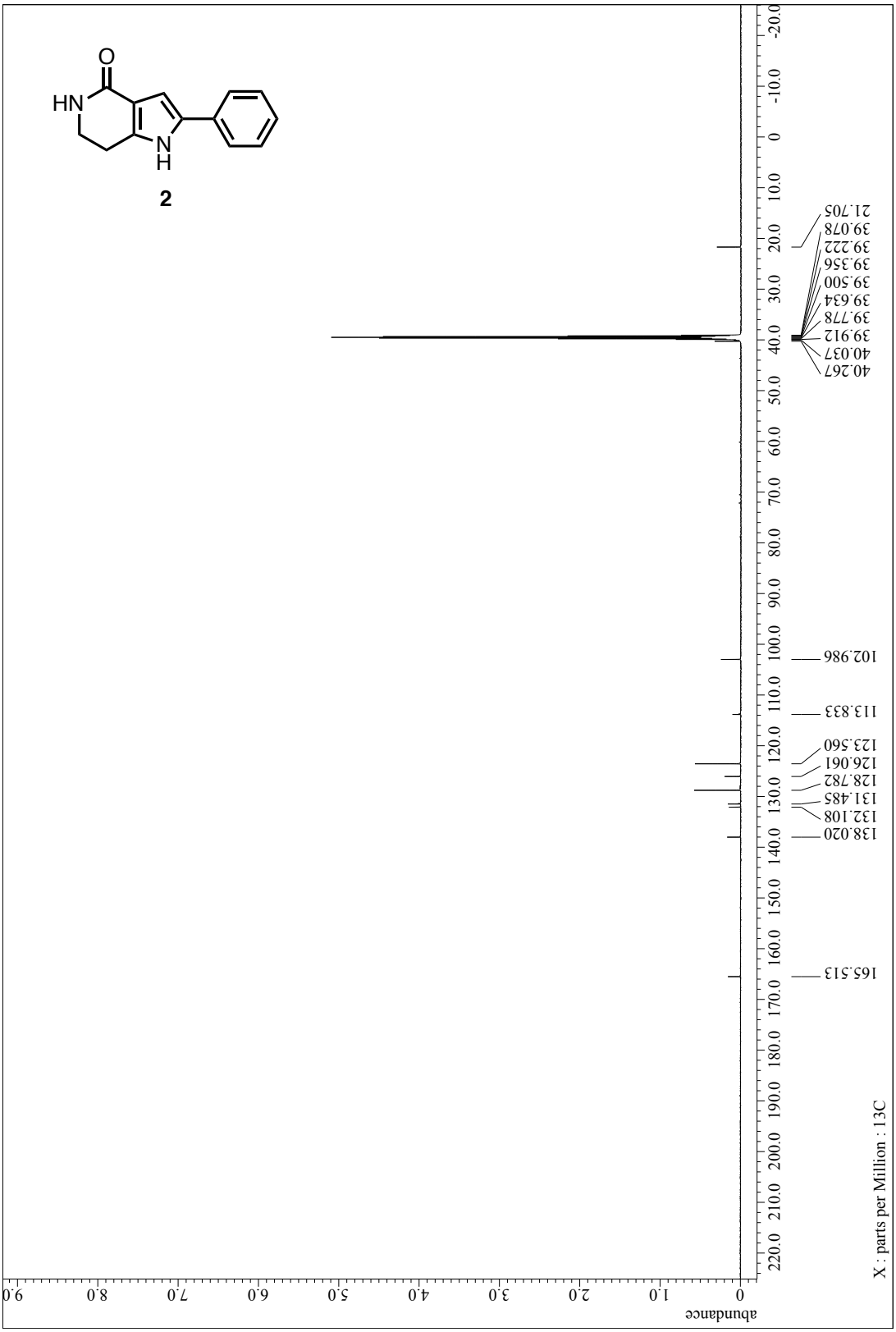

^{1}H NMR of **5** (600 MHz, DMSO-d_6)

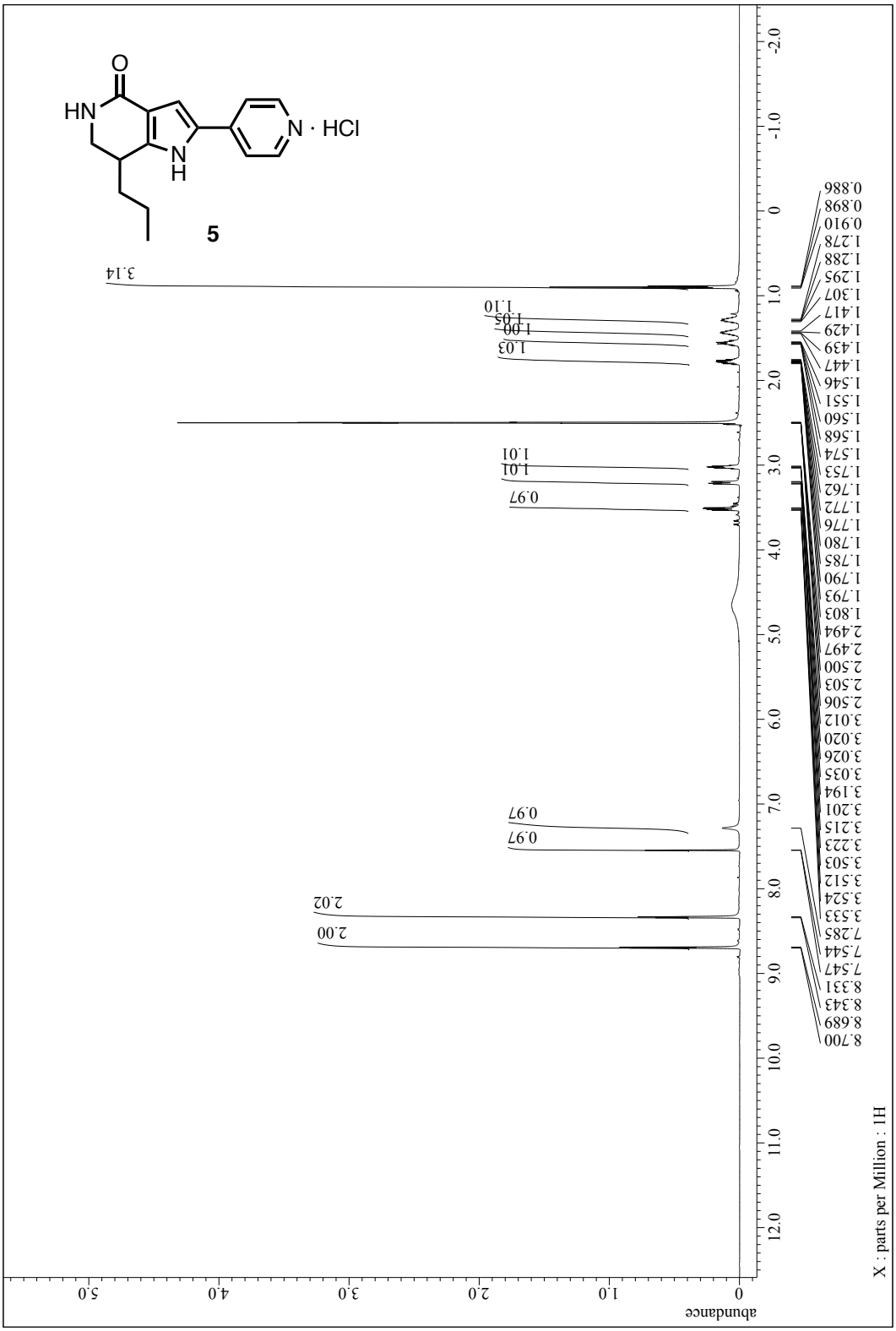

^{13}C NMR of **5** (150 MHz, DMSO-d_6)

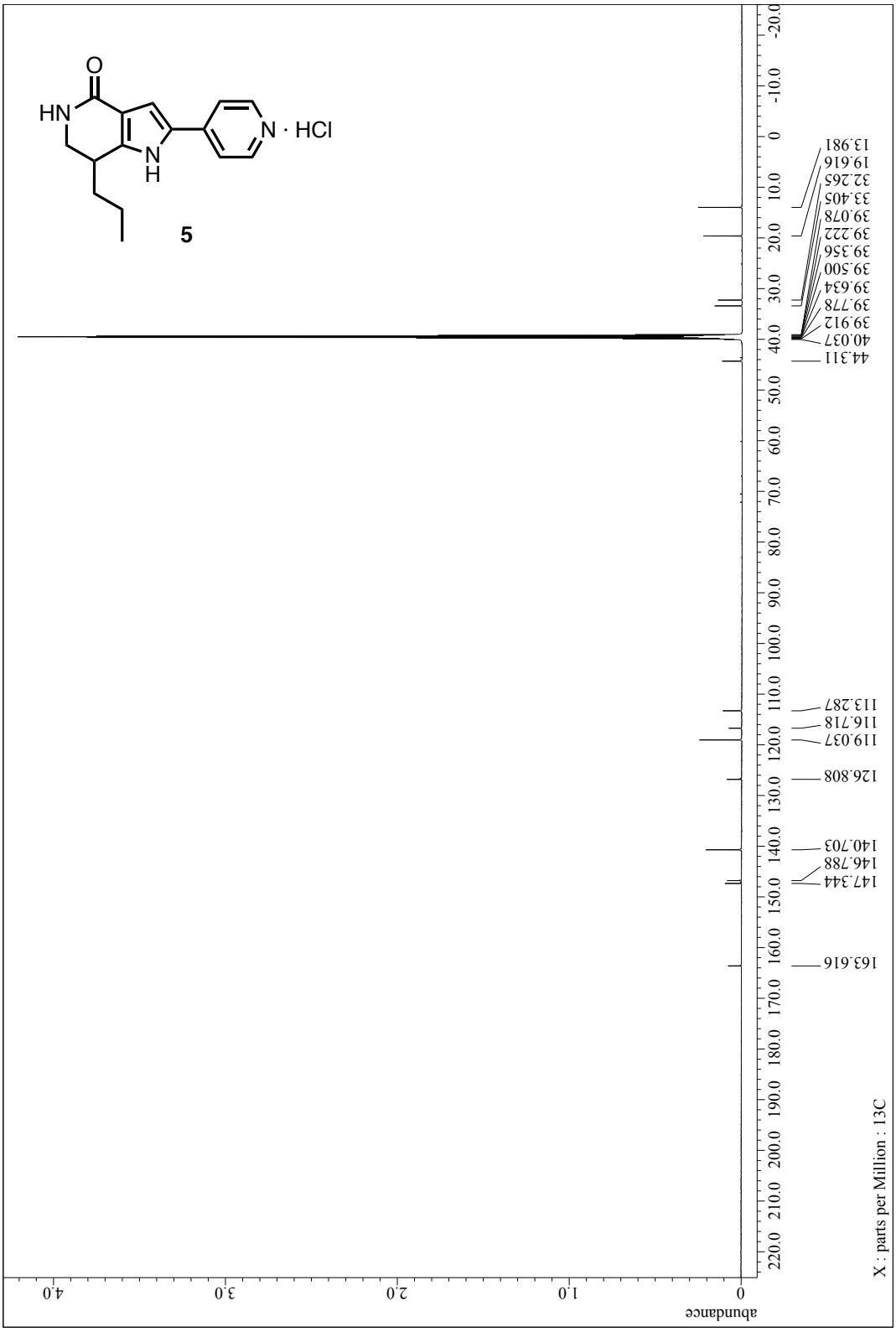

^{1}H NMR of **6** (600 MHz, CD_3OD)

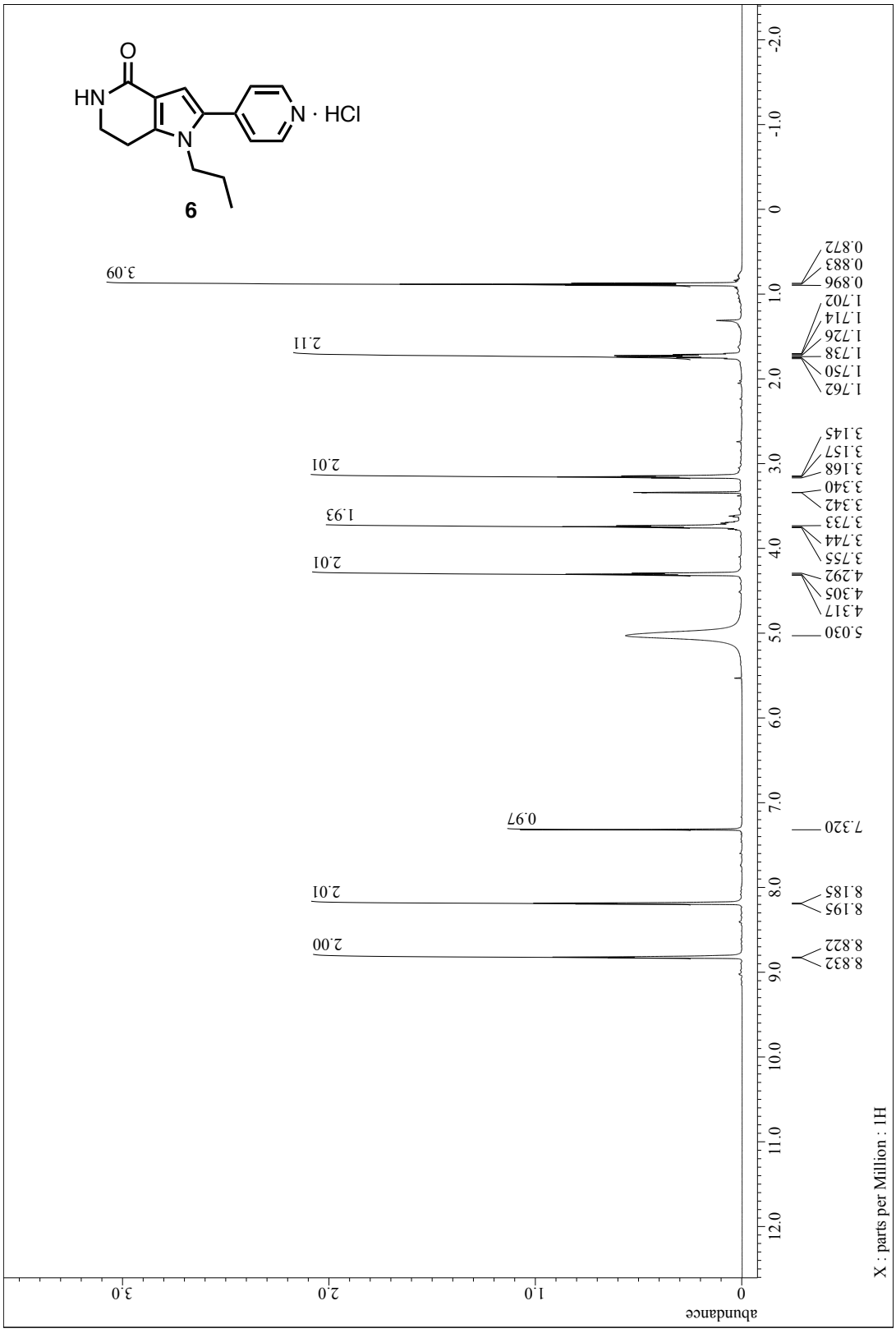

^{13}C NMR of **6** (150 MHz, CD_3OD)

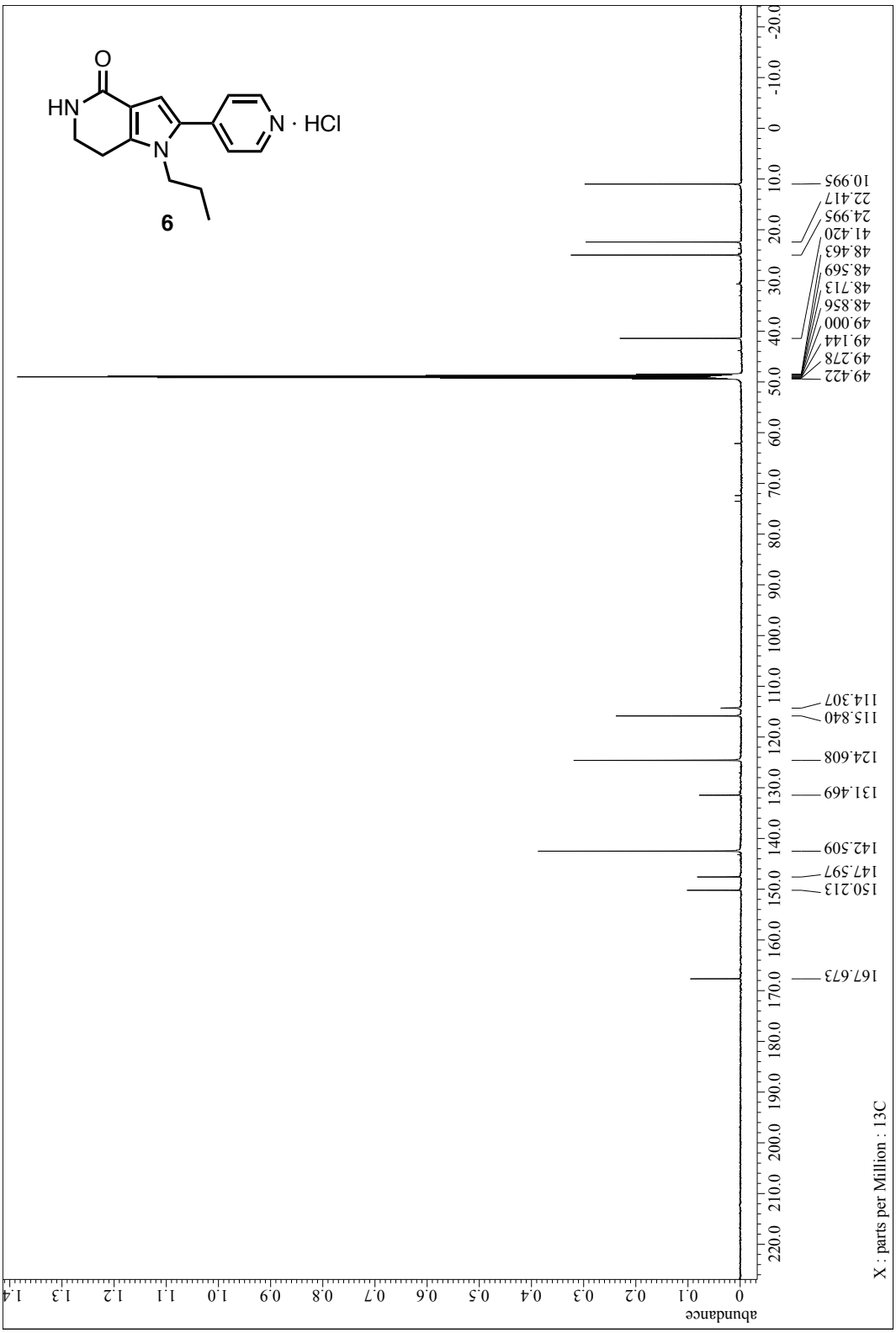

^{1}H NMR of **S6** (600 MHz, CD_3OD)

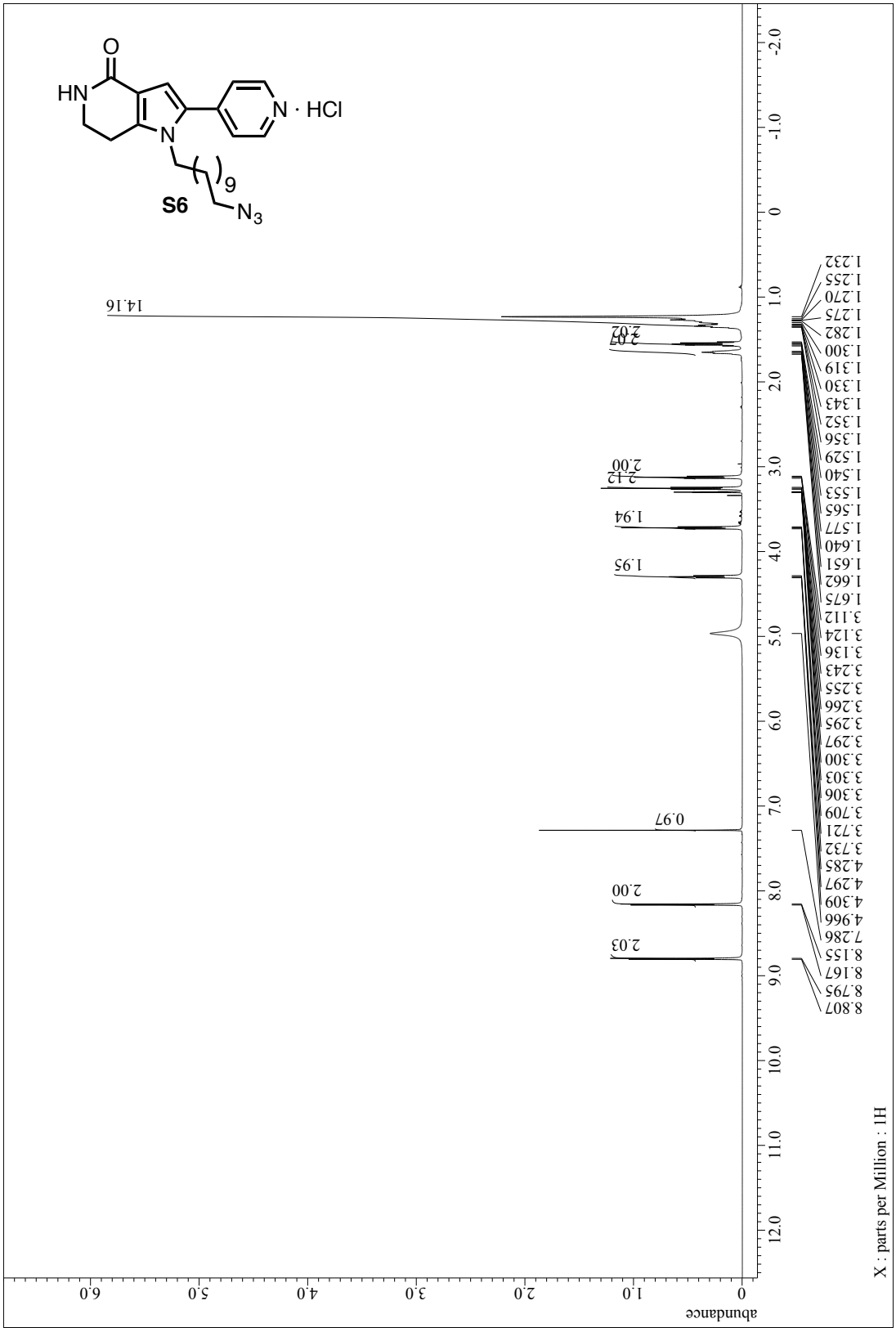

^{13}C NMR of **S6** (150 MHz, CD_3OD)

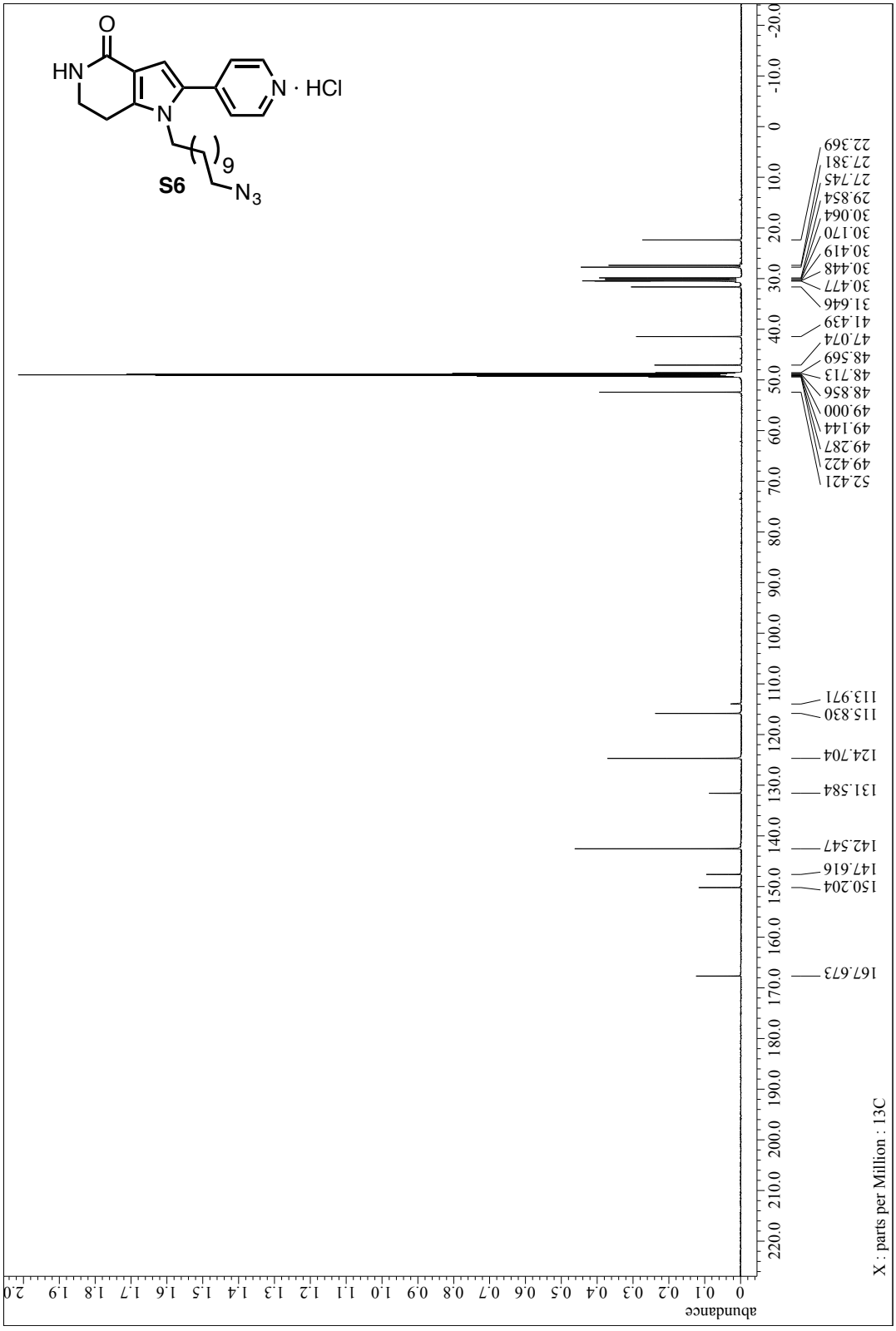

^{1}H NMR of **3** (600 MHz, CD_3OD)

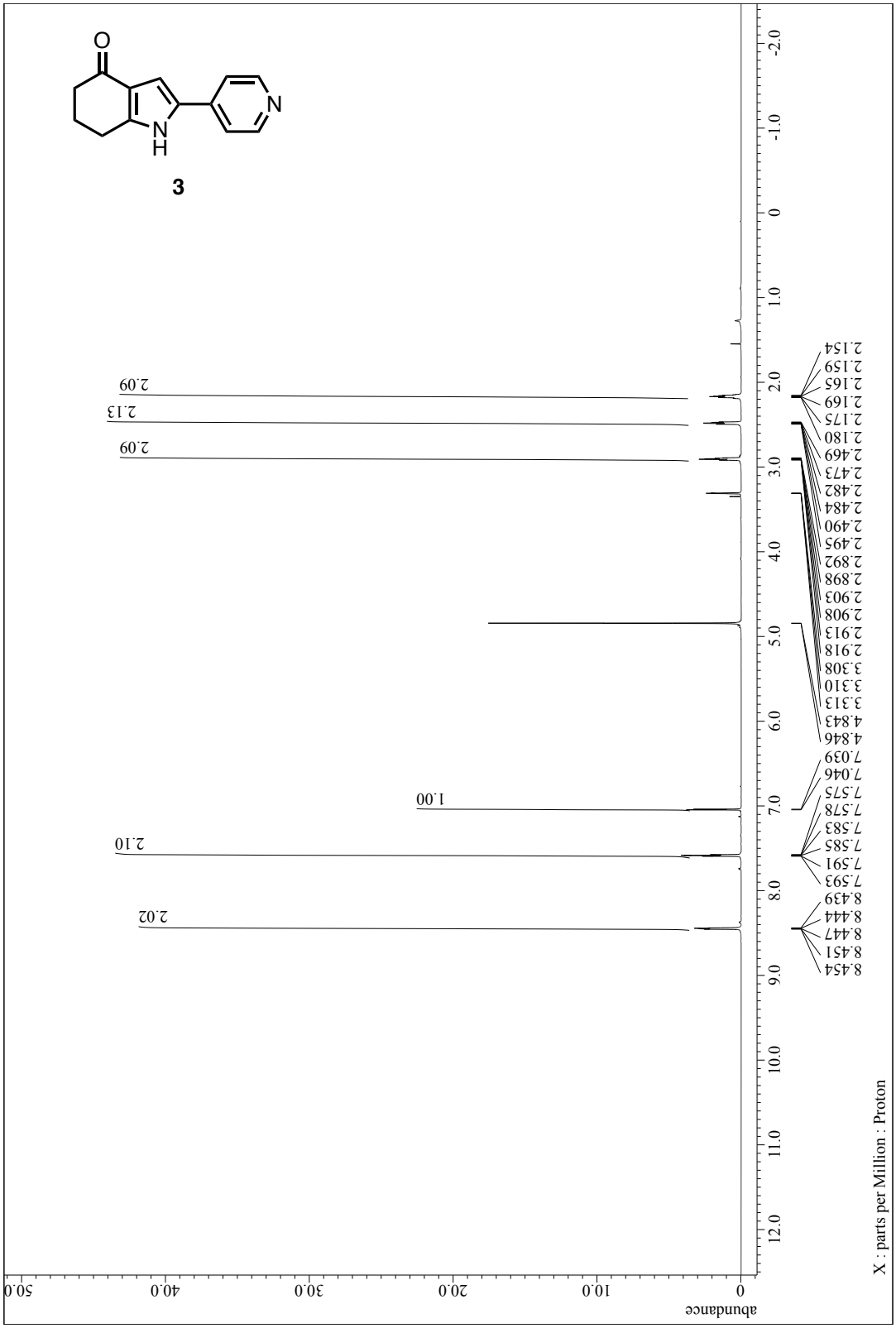

^{13}C NMR of **3** (150 MHz, CD_3OD)

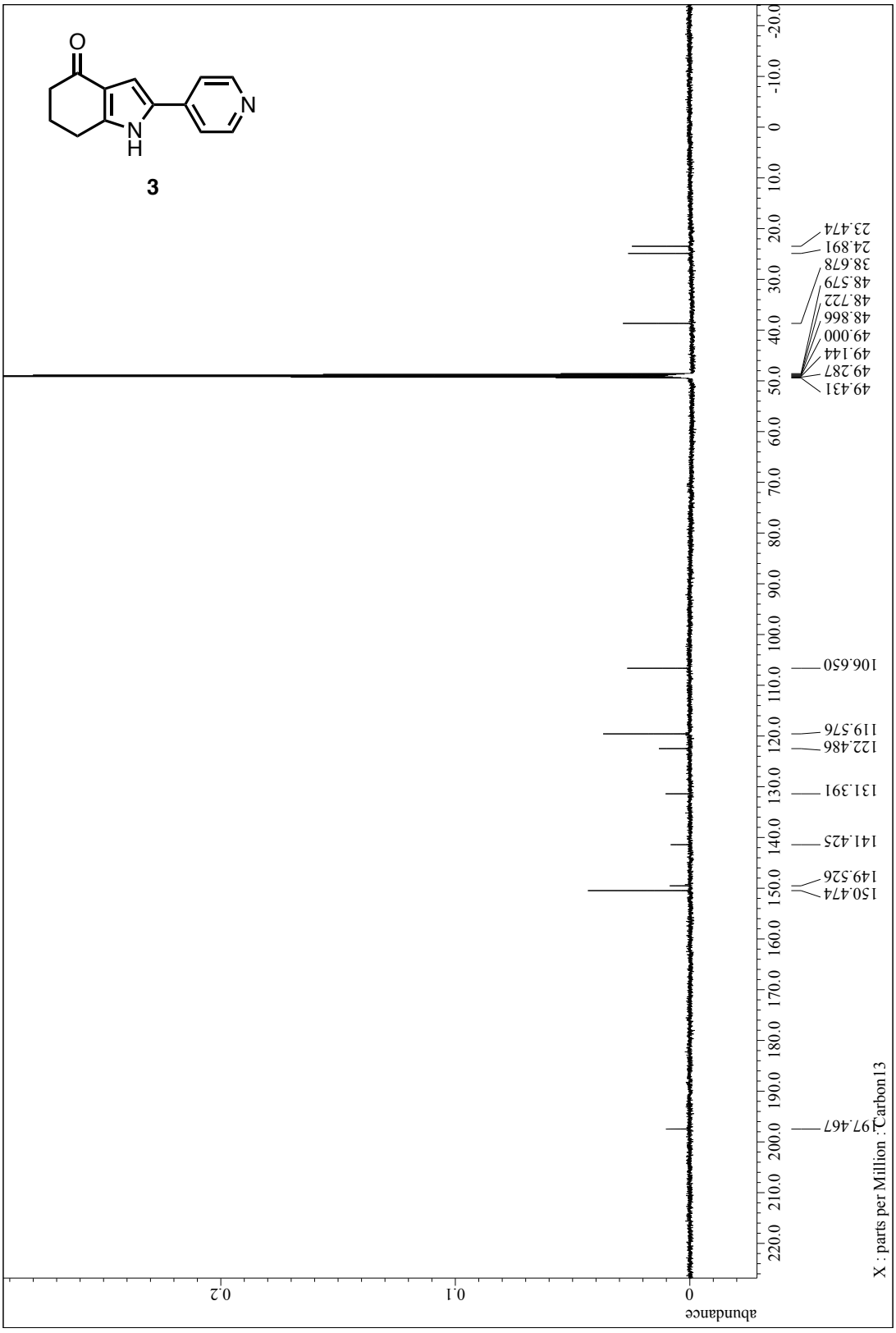

^{1}H NMR of **4** (600 MHz, $CDCl_3$)

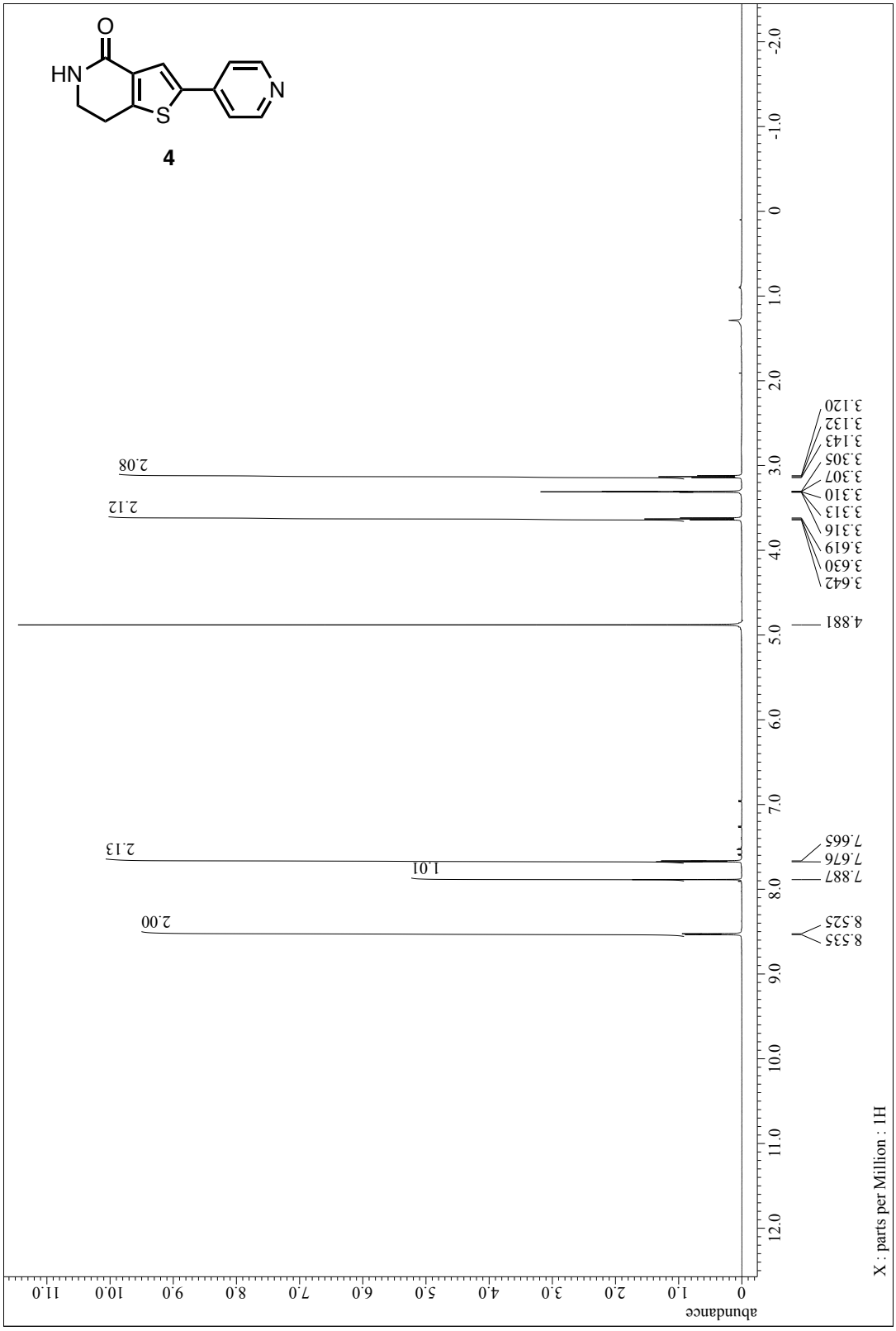

^{13}C NMR of **4** (150 MHz, $CDCl_3$)

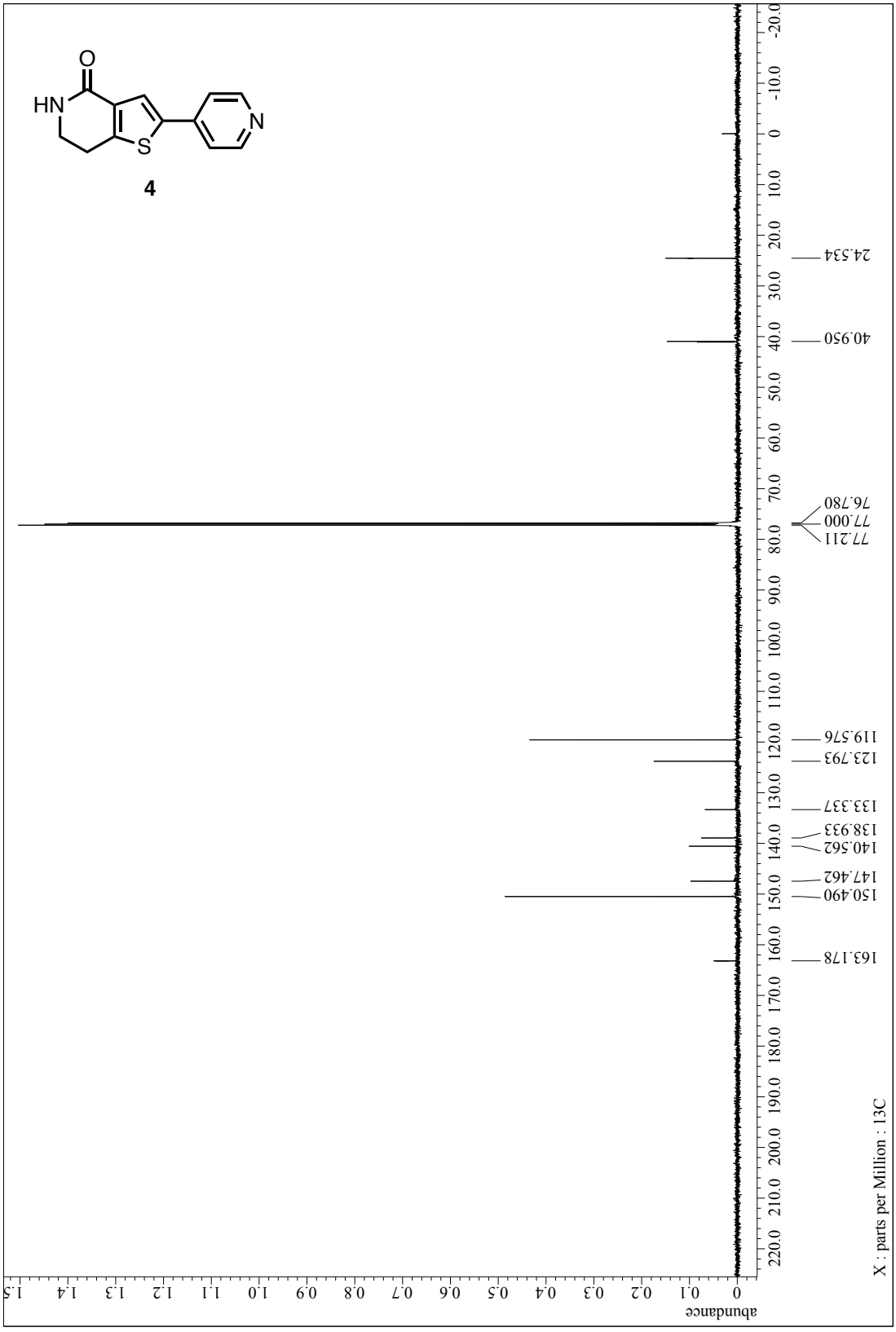

^{1}H NMR of **S7** (600 MHz, CD_3OD)

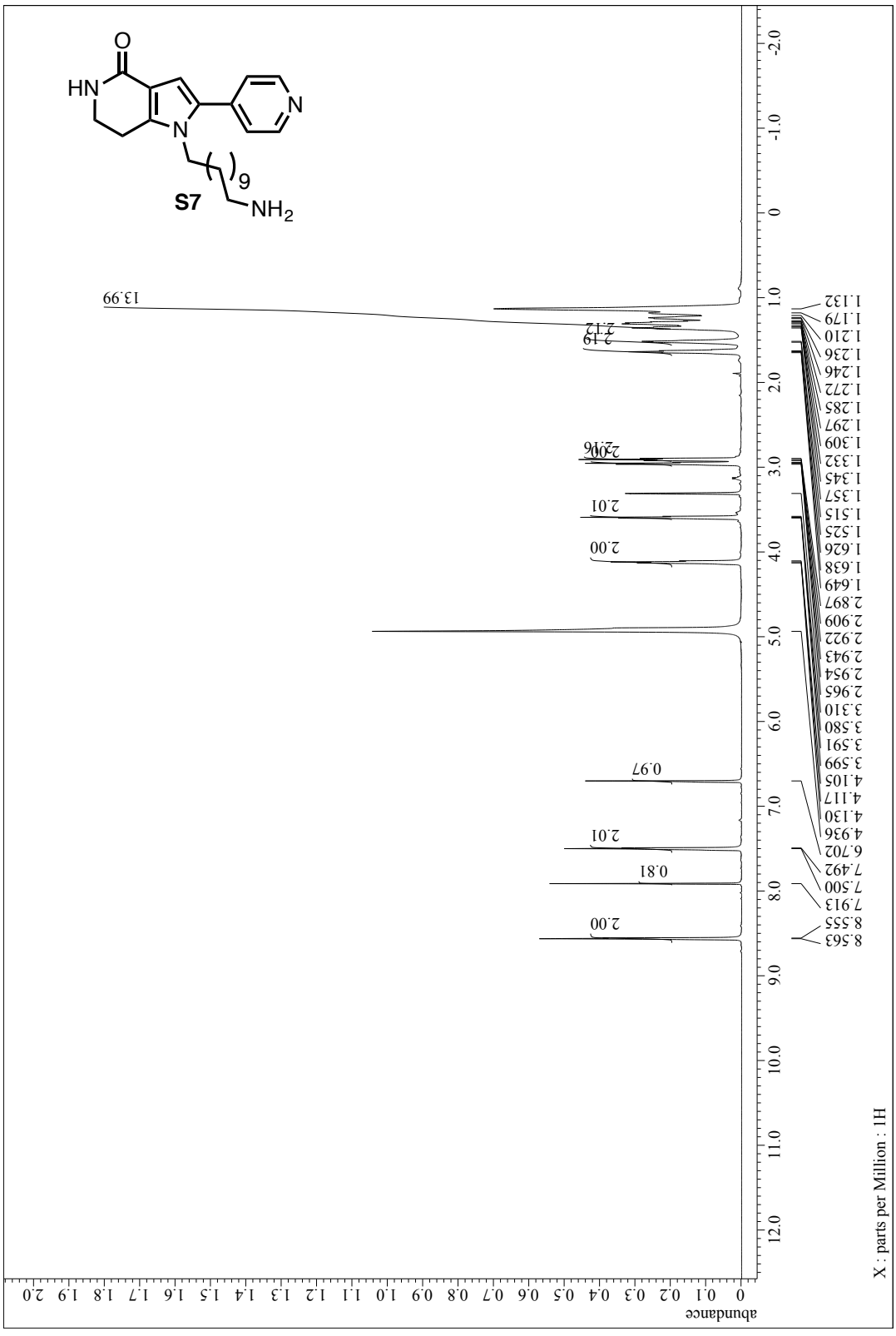

^{13}C NMR of **S7** (150 MHz, CD_3OD)

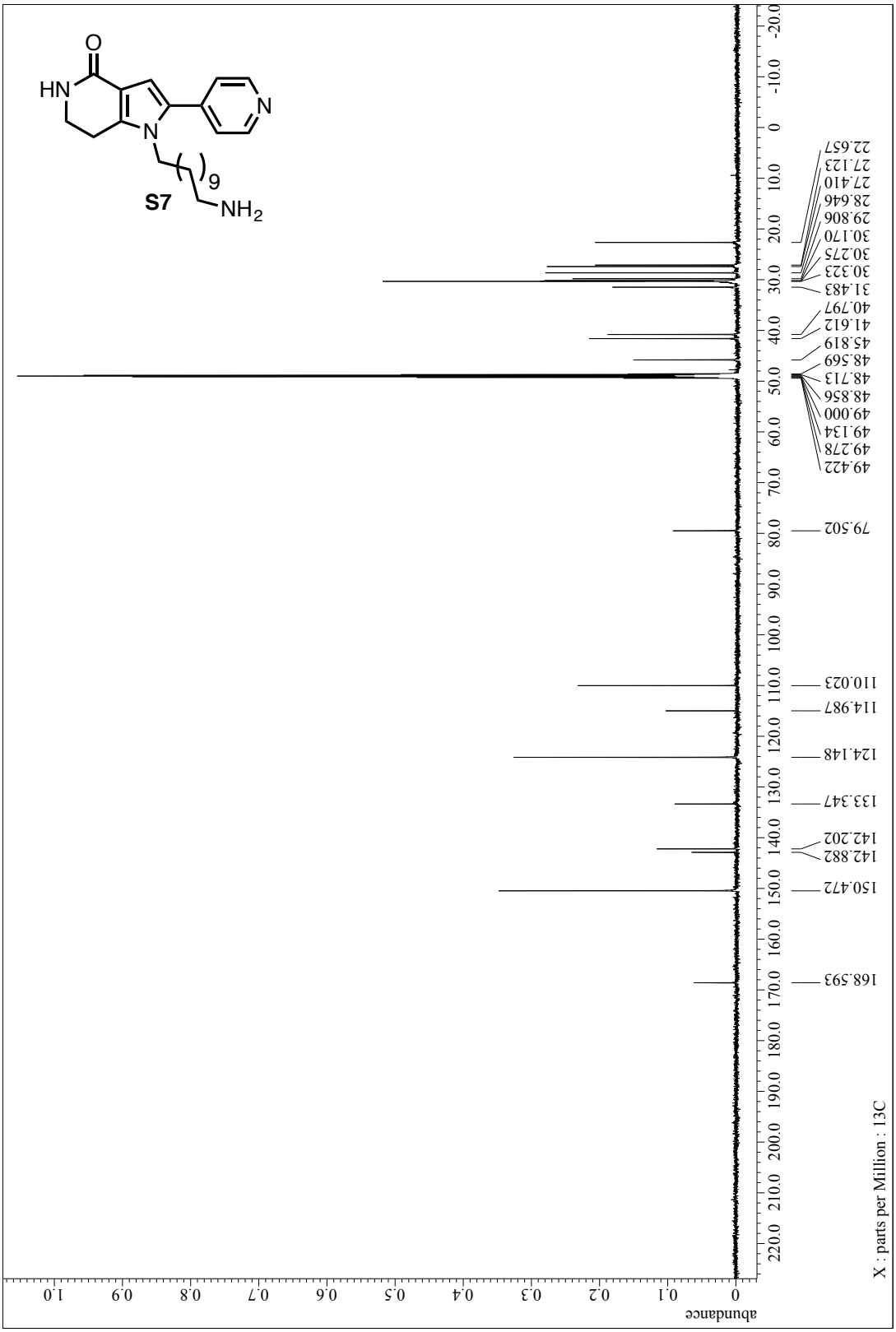

Screening proteins bound to PHA767491-beads

Two-week-old seedlings for pull-down assays (~ 1 g) grown under LD conditions were harvested at ZT0, 6, 12, and 18, and stored at -80˚C until use. These samples were mixed and ground to powder in liquid nitrogen. About 1 g of the powdered tissue was transferred to a 15 mL tube, lysed in 10 mL lysis buffer [150 mM Tris-HCl pH 7.5, 15 mM $MgCl_2$, 15 mM EGTA, 1 mM DTT, protease inhibitor mixture (P9599; Sigma-Aldrich), and 50 μM 26S protease inhibitor MG132 (C2211; Sigma-Aldrich)], then sonicated. After sonication, 300 μL of 10% (v/v) NP40 was added to each tube (0.5%, final concentration). Samples were incubated on ice for 5 min, and centrifuged at 13,000 g at 4˚C for 10 min. Protein samples (3 mg) were incubated with or without 60 μM PHA767491 (0.5% DMSO, final concentration) at 4˚C for 30 min with rotary mixing. A 250 μL aliquot of PHA-beads, **7**, suspended in PBS was washed with bead buffer [100 mM Tris-HCl pH 7.5, 250 mM NaCl, 5 mM EDTA, 5 mM EGTA, 0.1% (v/v) NP40, protease inhibitor mixture, and 50 μM 26S protease inhibitor MG132] three times, and re-suspended in 250 μL of bead buffer. PHA-beads were equally divided into two tubes, and added to cell lysates that were incubated with or without PHA767491. Samples were gently rotated at 4˚C for 1 h. PHA-bead resins were washed with bead buffer six times. The resultant resins were suspended in SDS sample buffer, and boiled at 95˚C for 8 min. Supernatants were collected and subjected to proteomic analysis.

SDS-PAGE and in-gel digestion of protein samples

SDS-PAGE was carried out according to the method described by Laemmli (9). After boiling protein-bound PHA-beads in SDS sample buffer, released proteins were partially separated (~2 cm) using a slab gel. Each lane was divided into six pieces, with about 0.2 cm^3 of each piece. In-gel digestion was performed according to the method described by Rosenfeld (10).

Mass Spectroscopy, chromatographic methods, instrumentation, and analysis

Samples were analyzed by nano-flow reverse phase liquid chromatography followed by tandem MS, using a Q Exactive Hybrid Quadrupole-Orbitrap Mass Spectrometer (ThermoFisher Scientific). A capillary reverse-phase HPLC-MS/MS system was composed of a Dionex U3000 gradient pump equipped with a VICI CHEMINERT

valve, and a Q Exactive equipped with a Dream Spray nano-electrospray ionization (NSI) source (AMR, Tokyo, Japan). Samples were automatically injected using a PAL System autosampler (CTC Analytics, Zwingen, Switzerland) and a peptide L-trap column (Trap and Elute mode, Chemical Evaluation Research Institute, Tokyo) attached to an injector valve for desalinating and concentrating peptides. After washing the trap with MS-grade water containing 0.1% (v/v) trifluoroacetic acid and 2% (v/v) acetonitrile (solvent C), the peptides were loaded onto a separation capillary C18 reverse-phase column (NTCC-360/100-3-125, 125×0.1 mm, Nikkyo Technos, Tokyo). The eluents used were: A, 100% water containing 0.5% (v/v) acetic acid, and B, 80% (v/v) acetonitrile containing 0.5% (v/v) acetic acid. The column was developed at a flow rate of 0.5 μL min^{-1} with an acetonitrile concentration gradient of 5% B to 35% B for 20 min, then 35% B to 95% B for 1 min, 95% B for 3 min, 95% B to 5% B for 1 min, and finally re-equilibrating with 5% B for 10 min. Xcalibur 3.0.63 (ThermoFisher Scientific) was used to record peptide spectra over a mass range of m/z 350–1500. MS spectra were recorded followed by 20 data-dependent high-energy collisional dissociation (HCD) MS/MS spectra generated from the 20 highest intensity precursor ions. Multiply-charged peptides were chosen for MS/MS experiments due to their good fragmentation characteristics. MS/MS spectra were interpreted and peak lists were generated using Proteome Discoverer 2.0.0.802 (ThermoFisher Scientific). Searches were performed using SEQUEST (ThermoFisher Scientific) against the *Arabidopsis thaliana* (TAIR TaxID=3702) peptide sequence database. Search parameters were set as follows: enzyme selected with two maximum missing cleavage sites, a mass tolerance of 10 ppm for peptide tolerance, 0.02 Da for MS/MS tolerance, fixed modification of carbamidomethyl (C) and variable modification of oxidation (M). Peptide identifications were based on a significant Xcorr values (high confidence filter). Peptide identification and modification information returned from SEQUEST were manually inspected and filtered to obtain confirmed peptide identification and modification lists of HCD MS/MS.

Proteins whose unique peptides were enriched 10-fold by the PHA-bead bound samples without PHA767491 treatment compared to those from a PHA767491-treated sample were selected as PHA767491-bound proteins (Experiment 1). We discarded proteins whose unique peptide numbers were lower than four in samples without the PHA767491 treatment in Experiment 1. We then performed target

ID using different biological samples (Experiment 2) to validate the initial screening. Only reproducible proteins are shown in Supplementary Table1.

Pull-down assays for recombinant GST-CKL

To construct the vector for producing recombinant GST-CKL1 protein, the *CKL1* coding sequence (CDS) was amplified with KOD-Plus-Neo DNA polymerase (Toyobo) from a cDNA pool of Arabidopsis Col-0 using primers and cloned in pGEX-2T at the *Eco*RI and *Bam*HI sites, generating pGEX-CKL1. The DNA sequence of the pGEX-CKL1 was confirmed by Sanger sequencing. The plasmid was transformed into *E. coli* BL21 and GST-CKL1 protein was purified according to the supplier's protocol (GE Healthcare). For pull-down assays using purified GST-CKL1, 100 ng of GST-CKL1 was suspended in binding buffer [50 mM Tris-HCl pH 7.5, 150 mM NaCl, 1 mM DTT, 0.5% (v/v) NP40] and pre-incubated with free PHA767491 at a final concentration of 50 μM for 1 h. PHA-beads (25 μL) were added, and the mixture was further incubated for 30 min. PHA-beads resins were then collected and washed with wash buffer [100 mM Tris-HCl pH 7.5, 250 mM NaCl, 5 mM EDTA, 5 mM EGTA, 0.1% (v/v) NP40] six times. Proteins bound by the beads were analyzed by western blotting. GST-CKL1 protein was detected by the same method as reported previously (11).

For pull-down assays for GST-CKL (Fig. 2B upper panel), we cloned all *CKL* genes, except for *CKL1*, into pENTR/D-TOPO (LifeTechnologies) with the primers listed in Supplementary Table 5, generating pENTR/D-CKL. pENTR/D-CKL constructs were incubated with pGEX-GW, in which a Gateway cassette was integrated downstream of GST and LR clonase (LifeTechnologies), generating pGEX-CKL. pGEX-CKL constructs were transformed into *E. coli* BL21, and GST-CKL proteins were purified using methods as described above. Only GST-CKL2, GST-CKL4, and GST-CKL7 were purified at high enough concentrations using the supplier's protocol, and could thus be used for pull-down assays. About 20 to 100 ng of GST-CKL were used for pull-down assays using PHA-beads as described above. Detection of GSL-CKL proteins in input or pull-down fractions with PHA-beads was performed as described above.

In vitro phosphorylation assays of Arabidopsis CKLs

To perform in vitro phosphorylation assays, 50 mM Tris-HCl pH 7.5, 10 mM $MgCl_2$, 0.5 mM DTT, 5 μCi of [γ-^{32}P] ATP (NN-NEG502A, PerkinElmer), 20 to 100 ng recombinant GST-CKL, 500 ng casein (C8032, Sigma), and inhibitors (see figure legends, all samples contained 4% (v/v) DMSO as solvent for PHA767491) were incubated at 37˚C for 30 min. SDS sample buffer was added after the reaction, and the resulting samples were boiled for 5 min. Samples were resolved on 10% SDS-polyacrylamide gels. Dried gels were exposed to an imaging plate (BAS IP-MS 2040) and ^{32}P incorporation was detected with a Typhoon FLA 7000 Laser Scanner/Imager (GE Healthcare). Each protein sample without [γ-^{32}P] ATP was analyzed by western blotting with anti-GST antibody. Each intensity for ^{32}P incorporation on casein was normalized to amounts of full length GST-CKL4 as determined by western blotting. These values were used to calculate the IC_{50} (the half-maximal inhibitory concentration) of CKL4 kinase activity from the means three separate experiments.

Phylogenic analysis

Amino acid sequences of Arabidopsis CKL were obtained from TAIR (http://www.arabidopsis.org/), and those from other organisms were from NCBI (http://www.ncbi.nlm.nih.gov/) with the following IDs: Ot CK1 (Ot02g06160), Ot CK1-like (Ot02g06100), Nc CK1a (XP_011392814.1), CrCK1(XM_001693947.1), OsCK1/OsHBD2 (Os02g0622100/ LOC_Os02g40860), OsHD16 (Os03g0793500/ LOC_Os03g57940) Human CK1α (CCDS47304), Human CK1δ (CCDS11805), Human CK1ε (CCDS13970), Human CK1γ1 (CCDS10192), CK1γ2 (CCDS12077), CK1γ3 (CCDS4135). CKL evolutionary history was inferred using the Neighbor-Joining method (12). The optimal tree with the sum of branch length = 3.18412757 is shown. The percentage of replicate trees in which the associated taxa clustered together in the bootstrap test (500 replicates) are shown next to the branches (13). The tree is drawn to scale, with branch lengths in the same units as those of the evolutionary distances used to infer the phylogenetic tree. Evolutionary distances were computed using the Poisson correction method (14) and are expressed as the number of amino acid substitutions per site. The analysis involved 29 amino acid sequences. All positions containing gaps and missing data were eliminated. There were a total of 240 positions in the final dataset. Evolutionary analyses were conducted in MEGA7 (15).

Expression analyses of *CKL*s using the Diurnal database

Expression of *CKL* genes was analyzed using the Diurnal database (http://mocklerlab.org/tools) (16) for diurnal (LDHH_ST) and circadian (LL12_LDHH) conditions, eFP browser (http://bar.utoronto.ca/efp/cgi-bin/efpWeb.cgi) (17) for developmental distribution, light responses, and temperature changes. Expression data for *CKL3*, *CKL7*, and *CKL12* were absent from all datasets.

Circadian rhythm assays using mesophyll protoplasts

To construct the effector plasmid for RNA interference of the *CK1* gene family, 214 bp to 613 bp (where the adenine of the start codon is 1) of the *CKL1* CDS was cloned into pCR8 (LifeTechnologies) and integrated into pYU501 (18) by LR clonase (LifeTechnologies), generating pYU501-CKL-RNAi-1. By a similar method, 676 bp to 1075 bp of the *CKL1* CDS was cloned into pYU501, making pYU501-CKL-RNAi-2. Similarly, pYU501-TOC1-RNAi and pYU501-ZTL-RNAi vectors were constructed with primers listed in Supplementary Table 5. Empty pYU501 vector was used as the control vector. Construction of the reporter vectors *CCA1:LUC* and *PRR5:LUC* was previously reported (2).

The mesophyll cell protoplast circadian rhythm assay was performed as described previously with minor modifications (2, 19). We used 14- to 21-day old *Arabidopsis* plants grown under a 16 h L/ 8 h D photoperiod to prepare protoplasts. Reporter (2 μg) and effector (10 μg) plasmids were added to 5.0 x 10^4 to 5.0 x 10^5 protoplasts. Transfected protoplasts were collected and re-suspended in 1 mL of W5 solution (19) containing 500 μM luciferin and 50 μg/mL ampicillin. Protoplasts were then transferred into single wells of a white 96-well plate (136101 Nunc MicroWell White plate, ThermoFisher Scientific) (200 μL protoplasts per well) and incubated in the dark for 12 h. After incubation, the assay was analyzed with a CL96 automated bioluminometer under LL. Period length estimations were calculated using R (https://CRAN.R-project.org) (20).

To analyze the expression of *CKL* genes, transfected protoplasts used for circadian assays were harvested at ZT72 for RNA isolation and reverse transcription as described above. RNA isolation was performed as described previously (21). RT-qPCR was performed to measure the expression of the *CKL* family of genes in protoplasts.

Expression of *CKL* genes determined by RT-qPCR analyses were normalized with *ISOPENTENYL PYROPHOSPHATE: DIMETHYLALLYL PYROPHOSPHATE ISOMERASE 2* (*IPP2, AT3G02780*), a gene that is constitutively expressed under diurnal and circadian conditions (16). Expression analyses were performed using independent three biological replicates. Primers used for RT-qPCR are listed in Table S5.

RT-qPCR analysis of seedlings treated with PHA767491 for 3 h

Seedlings of Arabidopsis Col-0 were grown on MS under 12 h light/ 12 h dark (LD) conditions at 22˚C for 4 days. Seedlings were transferred to constant light (LL) at ZT0, and about 20 seedlings were submersed in 5 mL MS 2% sucrose liquid containing 200 μM PHA767491 or DMSO control, under vacuum for 5 min (PHA767491/DMSO was treated at 1, 7, 13, and 19 h after lights on). After 3 h incubation under light at 22˚C (4, 10, 16, and 22 h after lights on), seedlings were flash-frozen in liquid nitrogen. RNA isolation, reverse transcription, and quantitative PCR (qPCR) were performed as described previously (21). Gene expression was normalized to the expression of *IPP2*. Primers used for qPCR were described previously (21) or are listed in Table S5. Three biological replicates were analyzed for RT-qPCR analysis.

RNAseq analysis to identify genes differentially expressed by PHA767491

Four-day-old seedlings of Arabidopsis Col-0 grown on MS under LD conditions at 22˚C were transferred into LL conditions at ZT0. About 20 seedlings were submersed in 5 mL of MS 2% sucrose liquid containing 200 μM PHA767491 or DMSO control under vacuum for 5 min at 15 h after lights on. After 3 h incubation under light at 22˚C (ZT18), seedlings were frozen in liquid nitrogen. RNA isolation and generation of RNAseq libraries were performed as reported previously (2). Deep sequencing was performed with Illumina NextSeq 500 according to the supplier's protocol (Illumina). Only sequence reads over the quality (continuous 50 nucleotides with quality values >25) were used, and further procedures were performed as previously reported (2). Genes differentially expressed between three biological replicates of PHA767491-treated seedlings and non-treated seedlings were obtained by EdgeR (22) with FDR $q < 10^{-4}$. Enrichments of expression peaks for genes differentially expressed due to PHA767491 treatment, or 'light-response genes' in down-regulated genes by

PHA767491, were analyzed by Phaser (16), with a cutoff value of 0.7 in LL12_LDHH conditions. RNAseq data of PHA767491-treated Arabidopsis has been deposited in the DDBJ Sequence Read Archive (DRA, http://trace.ddbj.nig.ac.jp/dra/index_e.html) with accession number DRA006077.

Yeast two-hybrid assay

The *PRR5* coding sequence containing its termination codon was amplified from a cDNA pool and cloned into pENTR/D-TOPO (Life Technologies), generating pENTR/D-PRR5 (+ter). The DNA sequence of the pENTR/D-PRR5 (+ter) was confirmed by Sanger sequencing. The plasmid was treated with Gateway LR clonase (Life Technologies) and pEG202 (DupLEX-A^{TM}, OriGene) harboring the Gateway cassette, generating pEG202-PRR5. pEG202-PRR5 was delivered into yeast strain RFY206, resulting in RFY206/pEG202-PRR5 according to supplier's protocol (OriGene). RFY206/pEG202-TOC1, RFY206/pEG202-PRR3, RFY206/pEG202-PRR7, and RFY206/pEG202-PRR9 were prepared with similar methods. The *CKL4* coding sequence containing its termination codon was cloned into pENTR/D-TOPO, generating pENTR/D-CKL4 (+ter). The plasmid and pJG4-5 harboring a Gateway cassette were used to make pJG4-5-CKL4. pJG4-5-CKL4 was delivered into yeast strain EGY48, resulting EGY48/pJG4-5-CKL4. LacZ reporter assays were performed according to the manufacturer's protocol (OriGene).

Analysis of PRR-fusion proteins in plants treated with PHA767491

Four-day-old Arabidopsis seedlings over-expressing PRR5-FLAG (*35Spro:PRR5-FLAG*) (21) grown under LD at 22˚C were transferred into a 96-well plate by a dropper. Seedlings were treated with 20 μL of MS liquid containing 2% sucrose and PHA767491 at 500 μM with a final concentration of 5% (v/v) DMSO. As a control experiment, MS containing 2% sucrose and 5% DMSO was used to treat the seedlings. Seedlings were harvested after one day of treatment, and stored at ZT12 under light. Additional 'dark' samples of PHA767491-treated or non-treated seedlings were further kept in the dark for 24 h, and then harvested. Detection of PRR5-FLAG was performed using 10-20% gradient acrylamide gel (198-15041, Wako), as previously described (21) with anti-FLAG antibody (F3165, Sigma-Aldrich). PRR5-VP, TOC1-VP, and PRR7-VP protein in corresponding seedlings was analyzed by a similar method

with anti-VP16 antibody (ab4808, Abcam) as described (23). Note that the acrylamide concentrations used for separating PRR-fusion proteins in Figs. 4E and S12 did not allow determination of phosphorylation levels.

To analyze PHA767491-induced band shifts of PRR5-FLAG *in vivo*, four-day-old seedlings grown under constant white light were transferred into a 96-well plate by a dropper, and seedlings were treated with 500 μM PHA767491 as above. Seedlings were harvested after one day of treatment. Total proteins were extracted from seedling and treated either with or without lambda protein phosphatase (P0753S, New England Biolabs) as previously described (24). The protein samples were separated in 6 % acrylamide gels (195-15171, Wako) to segregate PRR5-FLAG bands as distinctly as possible. PRR5-FLAG was detected by anti-FLAG antibody (F3135, Sigma-Aldrich). The intensity of each lane was normalized by setting the peak value as 1 using Image J software (https://imagej.nih.gov/ij/). Analyses of PRR-VP fusion band shifts were likewise performed but with anti-VP16 antibody (ab4808, Abcam). Note that the amounts of PRR-fusion proteins in Figs. 4D and S11 were not the same as in vivo, due to additional steps required during sample preparation.

CKL4 phosphorylation of PRR5 and TOC1

Recombinant MBP-PRR5-His and MBP-TOC1-His were examined as substrates of CKL4. To prepare MBP-PRR5-His protein, pMAL-PRR5-His plasmid was generated by a Gateway LR reaction with pENTR/D-PRR5 (without its stop codon) (25) and pMAL-GW-His, in which a gateway cassette was integrated between MBP and His-tag. pMAL-PRR5-His was transformed into *E. coli* strain BL21. BL21/pMAL-PRR5-His was pre-cultured in Luria-Bertani medium (LB) at 37˚C overnight. The pre-culture (1 mL) was added to 100 mL of fresh LB and further incubated overnight at 20˚C with presence of 0.4 mM IPTG to induce MBP-PRR5-His. BL21/pMAL-PRR5-His cells were harvested, and lysed in lysis buffer [50 mM NaH2PO4 pH8.0, 300 mM NaCl, and 10% Glycerol]. Cell extracts were sonicated and amended with NP40 to a final concentration of 0.1%. Extracts were incubated at 4˚C to lyse cells efficiently, then centrifuged at 3,300 g for 30 min at 4˚C. MBP-PRR5-His protein was purified from the supernatant according to the manufacturer's protocol (156-0131, Bio-Rad). MBP-TOC1-His was purified with similar methods. To perform in vitro phosphorylation assays, 50 mM Tris-HCl pH 7.5, 10 mM $MgCl_2$, 0.5 mM DTT, 5 μCi

of [γ-^{32}P] ATP (NN-NEG502A, PerkinElmer), 100 ng recombinant GST-CKL4, 100 ng MBP-PRR5-His (or 20 ng MBP-TOC1-His), and 400 μM PHA767491 (or 4 % v/v DMSO) were incubated at 37˚C for 3 h. ^{32}P incorporation for proteins were detected as described above.

Overlap between PRR5 or TOC1 downstream genes and PHA767491-affected genes

Overlaps between genes mis-expressed in PHA767491 (Supplemental table 2) and genes mis-expressed in plants over-expressing PRR5-VP (*35Spro:PRR5-VP*) (21)or those in *toc1-2* (26) were analyzed by Fisher's exact test in R (http://www.r-project.org/).

Gene expression analysis of *prr5 toc1* treated with PHA767491

Wild type and *prr5-11 toc1-2* seedlings (27) were grown under LD for 4 days after germination, and transferred into LL at ZT0. Seedlings were submersed in 5 mL of MS 2% sucrose liquid containing 50, 200, or 500 μM PHA767491 or DMSO control under vacuum for 5 min at 19 h after lights on. After 3 h incubation under light at 22˚C, seedlings were frozen in liquid nitrogen. RNA isolation and RT-qPCR were performed as described above. Expression levels in DMSO treatment were normalized to 1, and relative expression was plotted from three biological replicates.

Gene expression analysis of *ztl*

Four-day-old seedlings of Arabidopsis Col-0 as wild-type, or *ztl* (*ztl-3*) (28) grown under LD conditions were transferred to 96-well plates and treated with MS 2% sucrose containing 5 % DMSO, and further grown under LD. Plants were harvested at ZT18, 2 days after DMSO treatment. RNAseq was performed using three biological replicates. Genes that were expressed significantly lower in the *ztl* mutant compared to wild-type were obtained by EdgeR (FDR $q < 10^{-4}$). Overlaps between down-regulated genes in *ztl*, and down-regulated or up-regulated genes due to PHA767491 treatment were analyzed by Fisher's exact text in R. Expression of 452 *ztl*-down-regulated genes was surveyed in RNAseq data of plants treated with PHA767491 and shown in a heatmap drawn by R as described previously(21). RNAseq data of *ztl* mutants has been deposited in the DRA with accession number DRA006078.

Sensitivity of *prr5 toc1* and *ztl* to PHA767491

prr5-11 toc1-2 CCA1:LUC plants were generated by transforming a binary vector harboring *CCA1:LUC* into *prr5-11 toc1-2* (27), via an *Agrobacterium*-mediated method (29). *ztl CCA1:LUC* plants were generated by crossing *ztl-3* (28) and *CCA1:LUC* (1). Four day old seedlings were transferred into a 96 well plate by a dropper. Luciferin and PHA767491 were applied to the seedling well, and *CCA1:LUC* luminescence was monitored as described above. Period lengths were normalized to the period length of each mutant treated with the DMSO control, because period lengths of the mutants were different from wild-type (circadian time (CT) controlled period change).

Circadian rhythm of U2OS cells

Circadian rhythm assays of U2OS cells were performed as described previously (30).

In vitro mammalian CK1δ-kinase assays

In vitro CK1δ-kinase assays were performed as described previously (30).

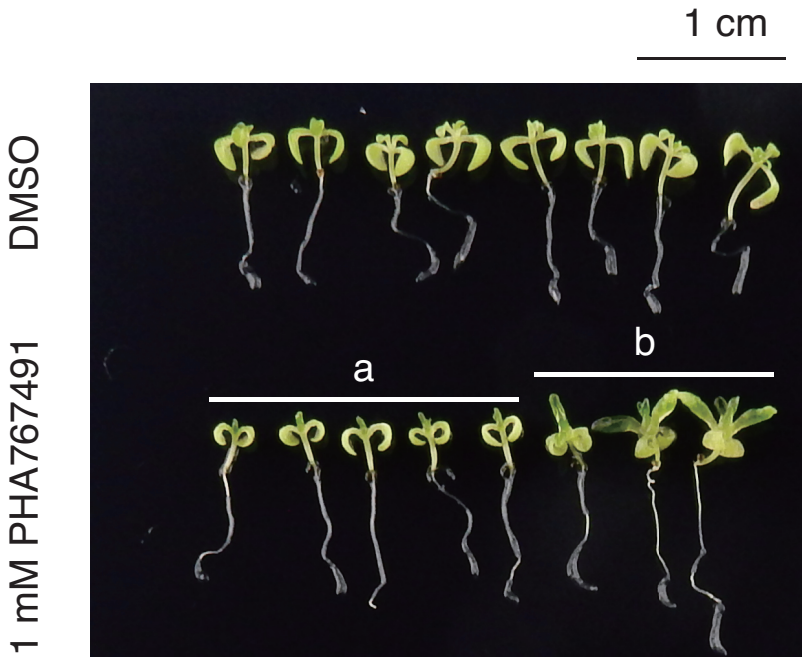

Figure S1. Treatment with high concentrations of PHA767491 retarded the growth of Arabidopsis seedlings.
Individual seedlings were transferred into wells of a 96-well plate, treated with 1 mM PHA767491, and photographed after two weeks. Seedlings treated with PHA767491 did not form rosette leaves (a), or they generated large and abnormally-shaped leaves (b).

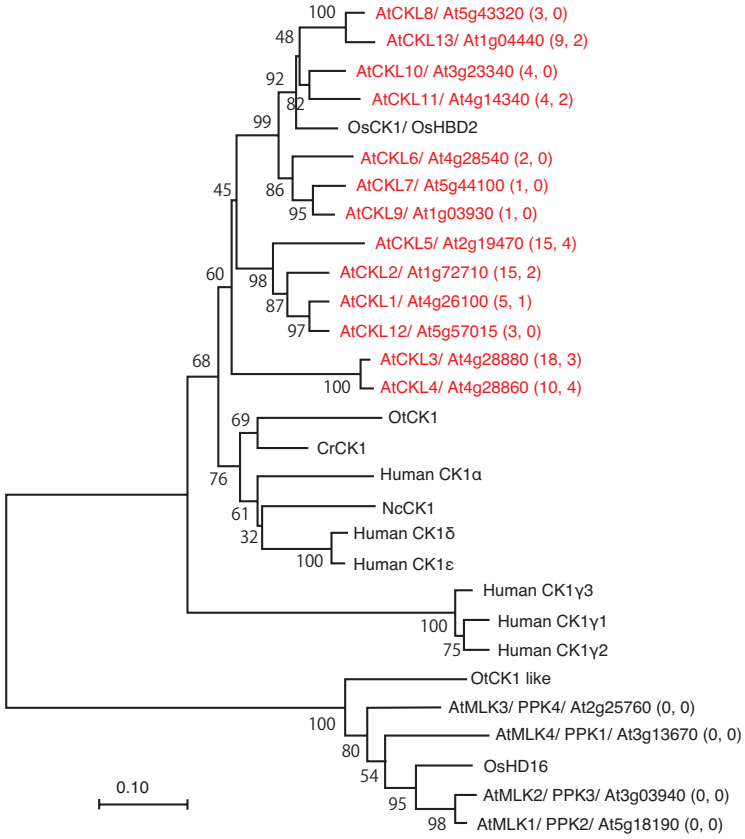

Figure S2. Phylogenetic tree of CKL kinases.
The evolutionary history was inferred by using the Neibhbor-Joining method (see Methods in detail). Gene phylogeny of CKL kinases and MLK kinases from Arabidopsis, and several CK1 kinases from human, fungi (Neurospora crassa), green algae (Ostreococcus tauri, Chlamydomonas reinhardtii), and rice (Oryza sativa). Kinase domains of protein sequences were used to make the phylogenetic tree. The percentage of replicate tree I which the associated taxa clustered together in the bootstrap test (500 replicates) are shown next to the branches. Red color indicates proteins interact with PHA-beads at least one experiment (see also Supplementary Table 1). Numbers in parenthesis show unique Arabidopsis peptides specifically bound by PHA-beads.

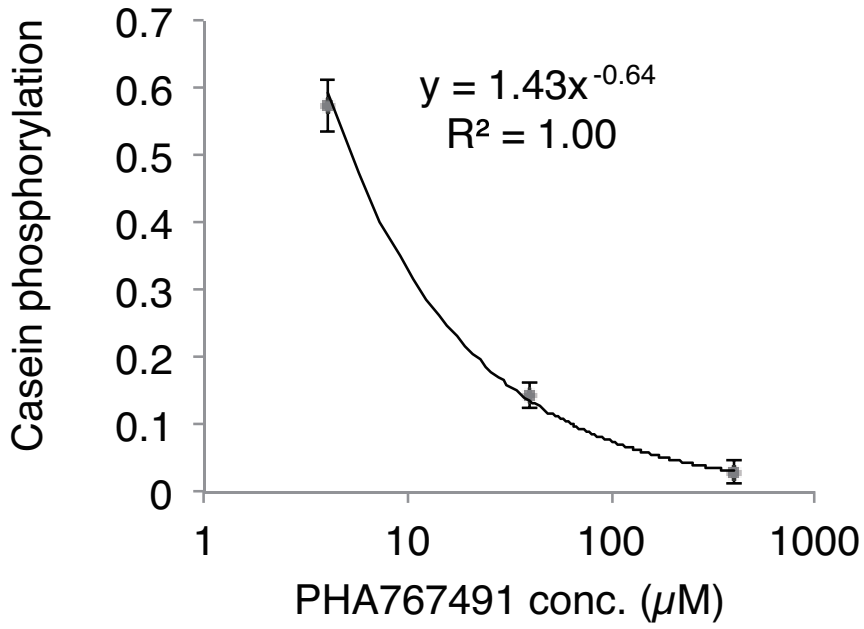

Figure S3. Inhibition of CKL4 kinase activity by PHA767491.
IC_{50} (the half-maximal inhibitory concentration) of PHA767491 on CKL4 kinase activity to casein was determined from three independent trials including data shown in Fig. 2d.

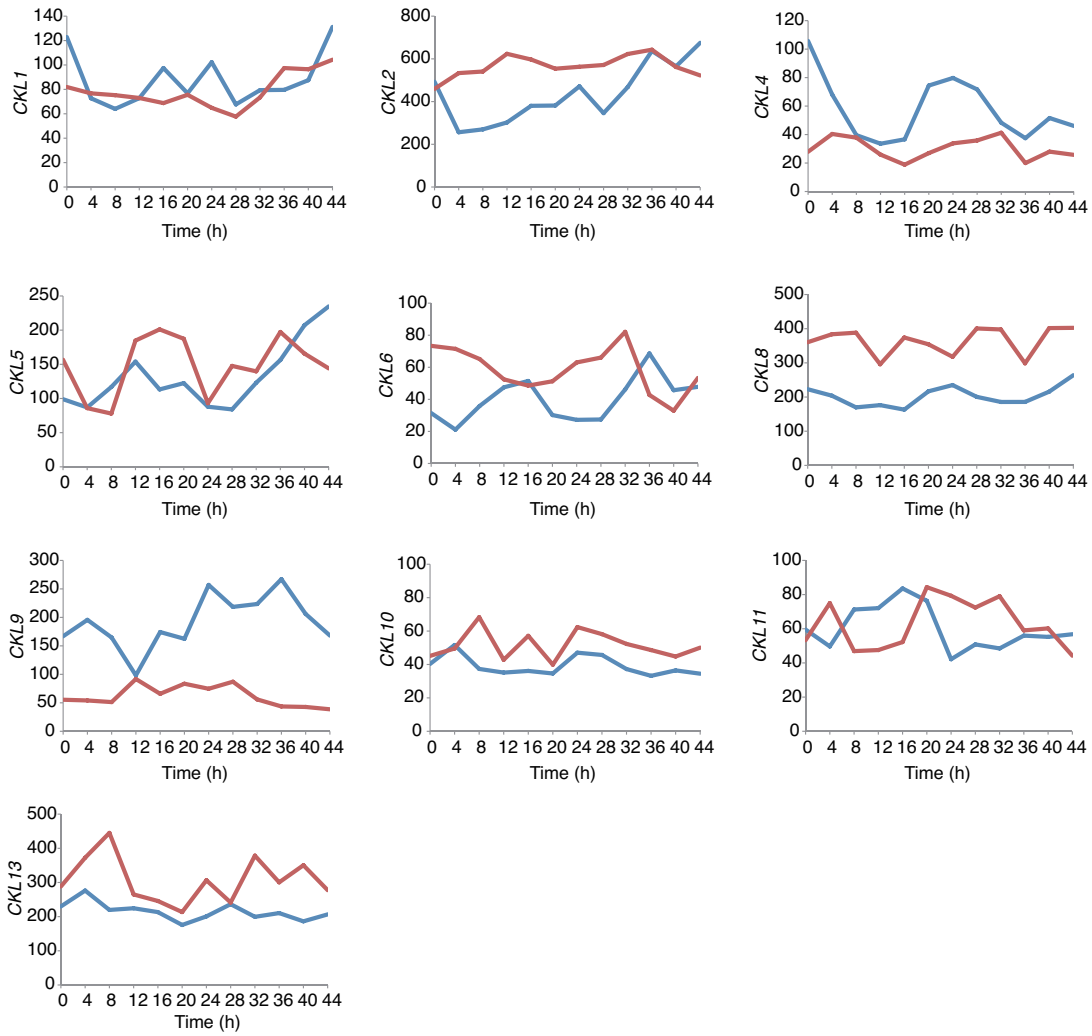

Figure S4. Expression of *CKL*s under diurnal and circadian cycles.
Expression of ten *CKL* family gene under diurnal (LDHH_ST, blue), and circadian conditions (LL12_LDHH, red) derived from the Diurnal database (http://diurnal.mocklerlab.org/). Expression of *CKL3*, *CKL7*, and *CKL12* are not represented in the database.

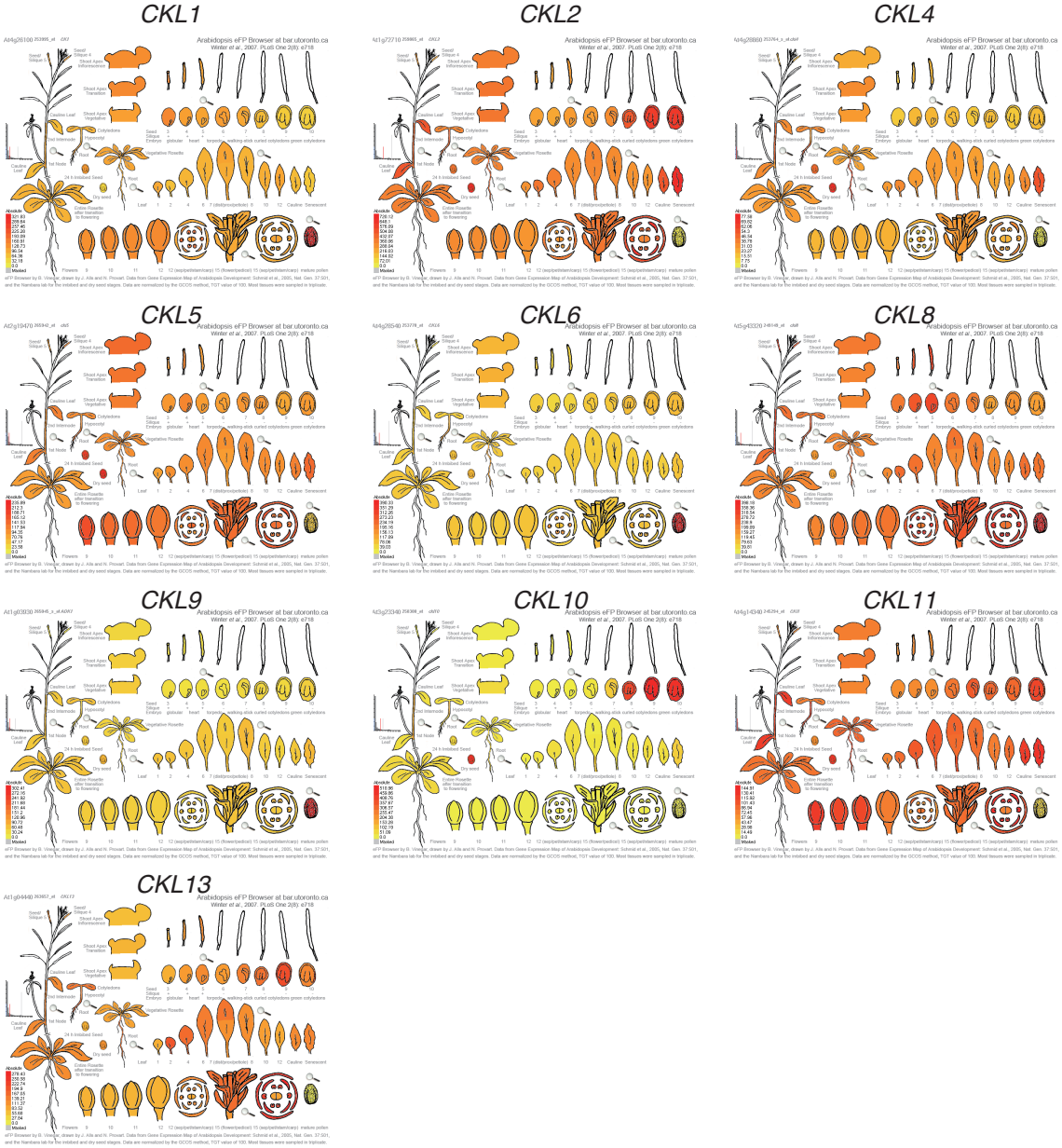

Figure S5. Expression of *CKL*s in various organs.

CKL genes expression were analyzed in Developmental map in Arabidopsis eFP Browser (http://www.bar.utoronto.ca/efp/cgi-bin/efpWeb.cgi).

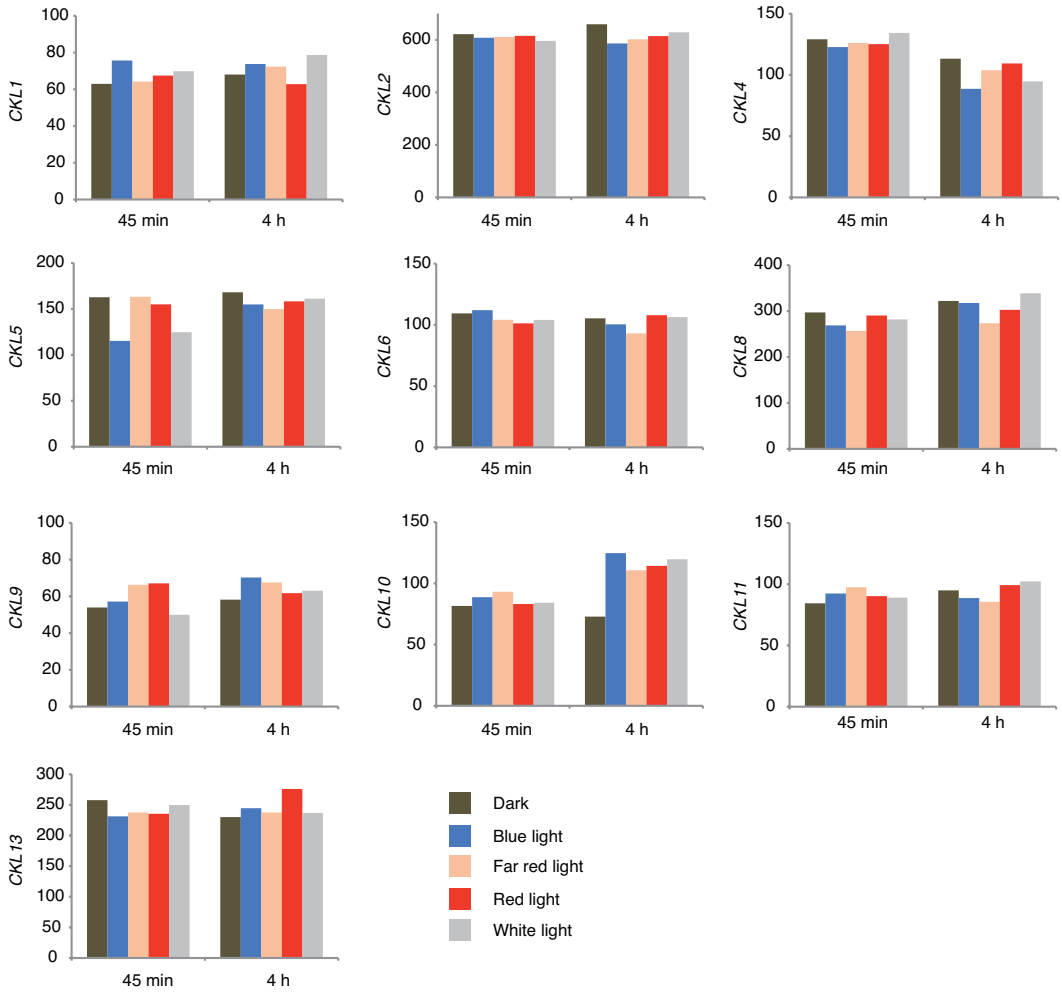

Figure S6. Expression of *CKL*s under various light treatments.
CKL genes expression after 45 min or 4 h light treatments in Arabidopsis eFP Browser. Fluences are 10 μmol s^{-1} m^{-2}.

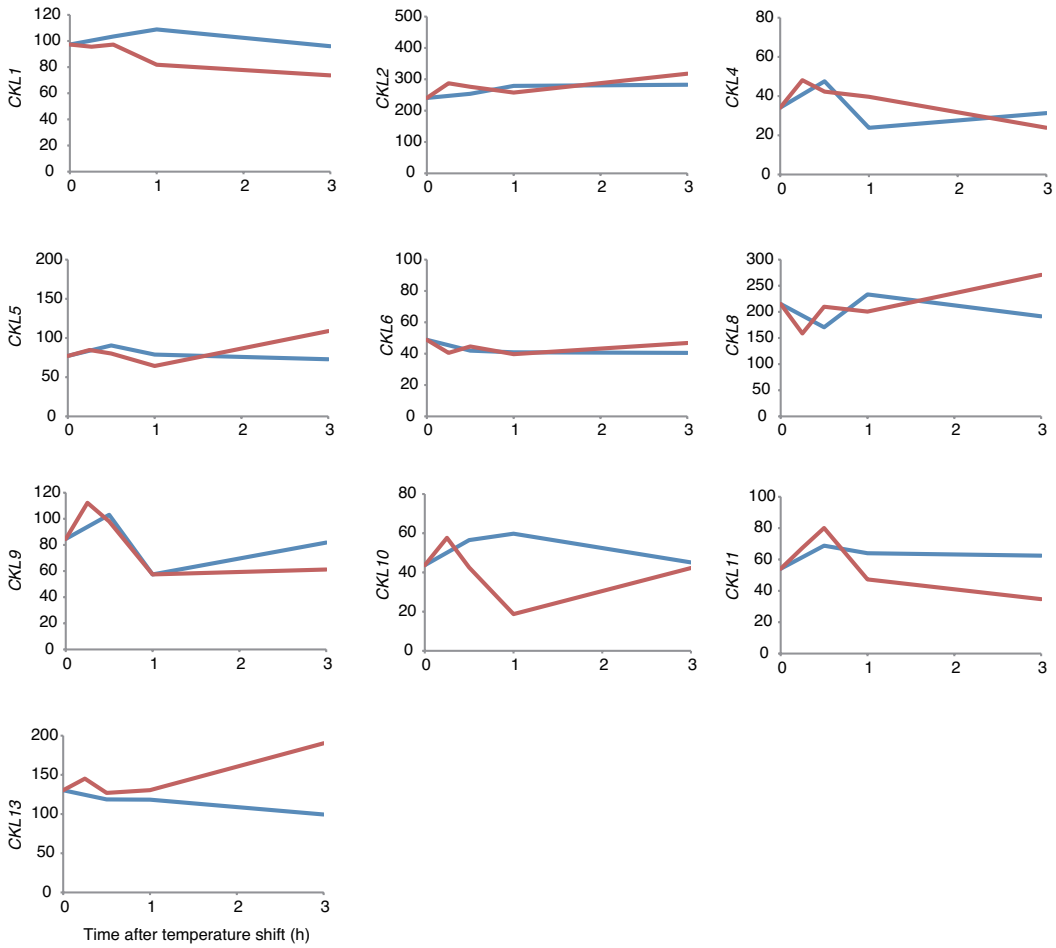

Figure S7. Changes in *CKL* expression in Arabidopsis plants following a shift in temperature. Time-course expression profiling of *CKL* genes resulting from a shift from warm to cold temperature (24˚C to 4˚C, blue) or warm to hot (24˚C to 30˚C, red). Data were obtained from Arabidopsis eFP Browser (University of Toronto, http://bar.utoronto.ca/efp2/Arabidopsis/Arabidopsis_eFPBrowser2.html).

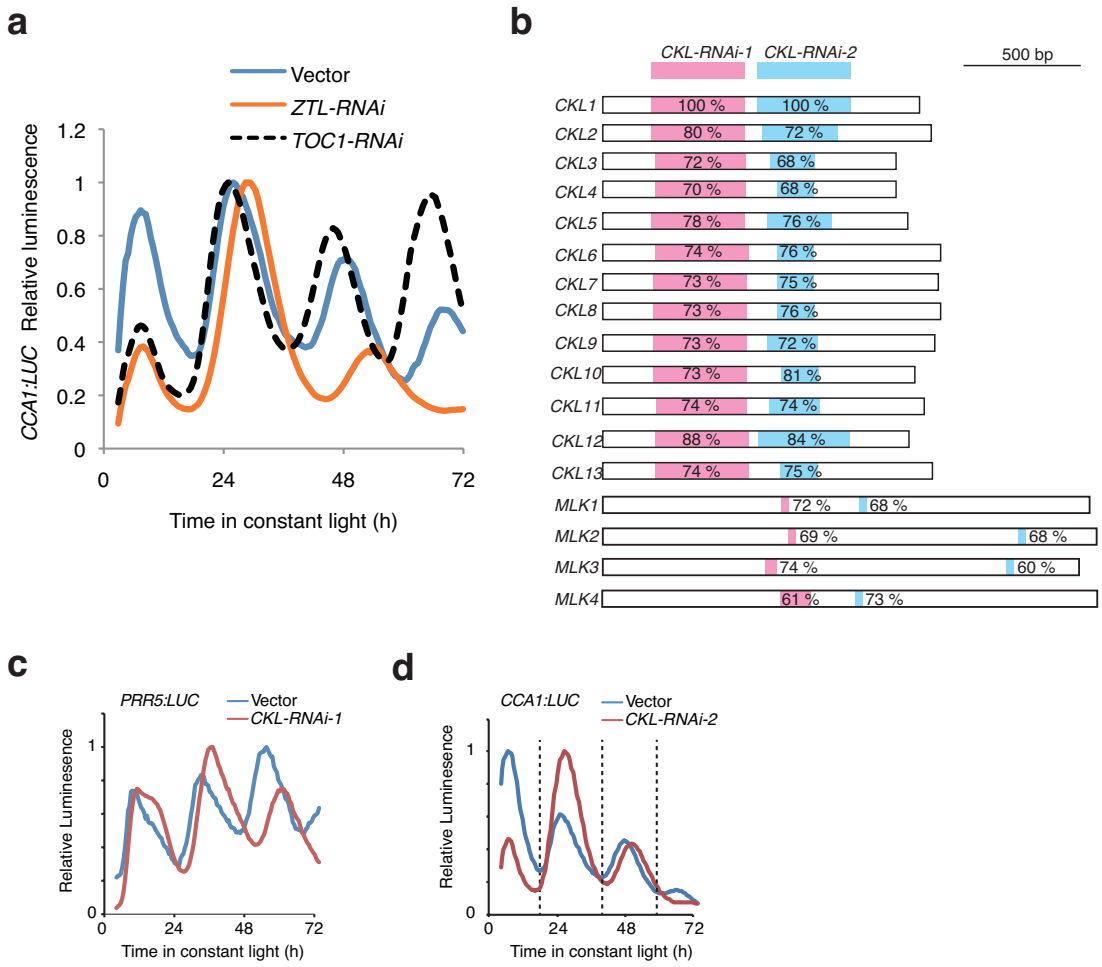

Figure S8. Co-transfection of *CCA1:LUC* and RNAi constructs for knock-down experiments with *CKL* family genes and their effects on circadian rhythms.
a, Bioluminescence of *CCA1:LUC* in mesophyll cell protoplasts (MCP) co-transfected with *ZTL-RNAi*, *TOC1-RNAi*, or empty vector . **b**, *CKL-RNAi-1* and *CKL-RNAi-2* constructs used for knock-down of *CKL* family gene expression. Pink and blue bars are regions with high sequence similarity (percent similarities are indicated within each bar) to *CKL-RNAi-1* and *CKL-RNAi-2*, respectively. **c,** *PRR5:LUC* circadian rhythm of MCPs transfected with *CKL-RNAi-1* (red) and vector control (blue). **d,** *CCA1:LUC* circadian rhythm of MCPs transfected with *CKL-RNAi-2* (red) and its vector control (blue). Dashed lines indicate the trough' s lowest point of *CCA1:LUC* expression in control MCPs. Representative traces are shown in **a**, **c**, and **d** for similar results obtained in other trials.

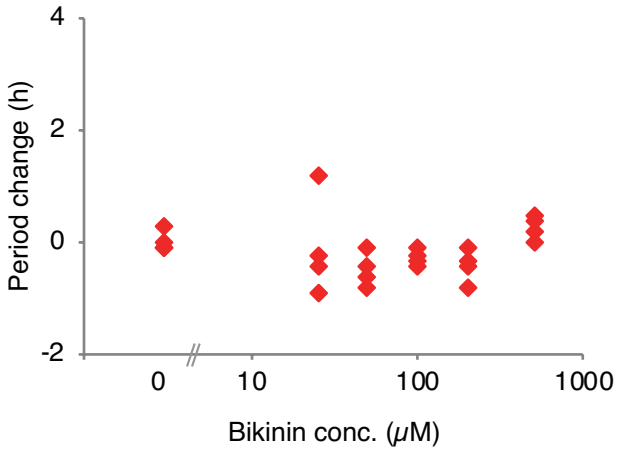

Figure S9. Effect of a GSK3 inhibitor, Bikinin, on circadian period.
Effect of Bikinin on circadian period of *CCA1:LUC* was analyzed.

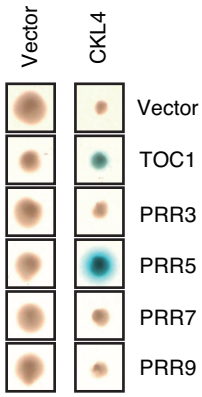

Figure S10. Interaction between CKL4 and PRRs in a yeast two hybrid assay.

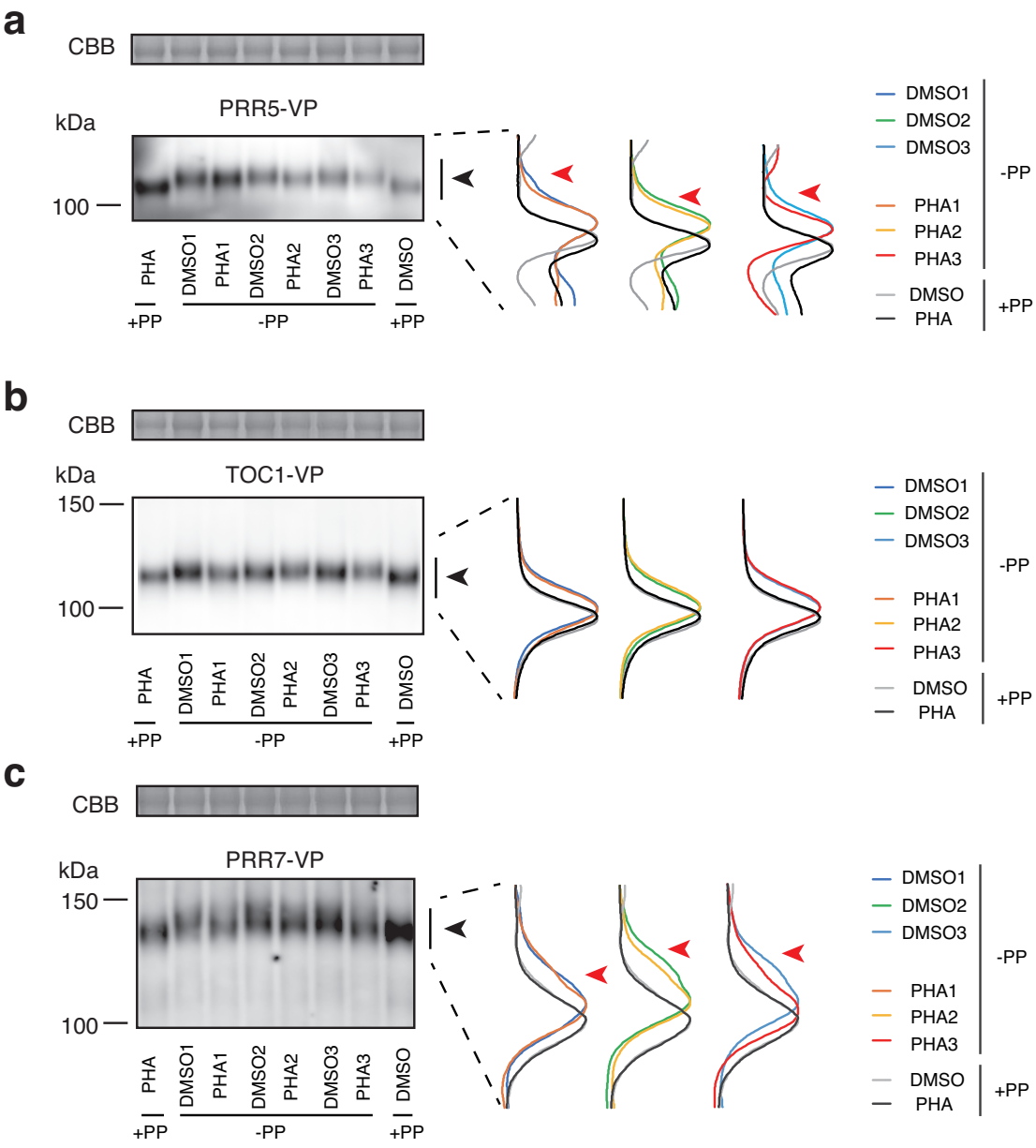

Figure S11. Band shifts of PRR5-VP, TOC1-VP, and PRR7-VP by PHA767491 treatment in vivo.

Band shift of PRR5-VP ***(A)***, TOC1-VP ***(B)***, and PRR7-VP ***(C)*** by PHA767491 treatment. Black arrows indicate PRR fusion proteins. Intensity profile of each PRR-fusion protein band is shown in the panel by setting the peak value as 1. Red arrow indicates electrophoretic mobility shifts of PRR-fusion proteins by PHA767491. Three biological replicates were examined.

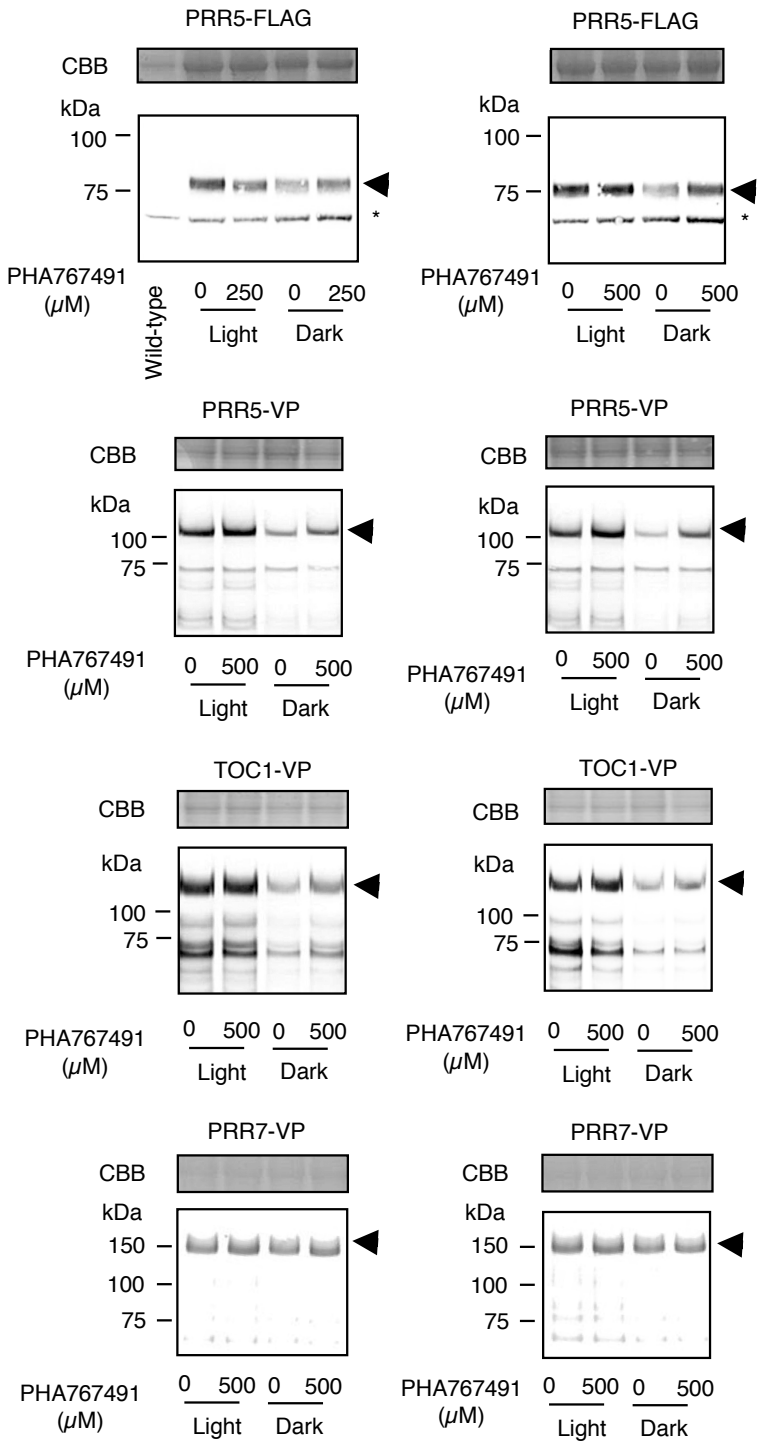

Figure S12. PRR5-FLAG, PRR5-VP, TOC1-VP, and PRR7-VP in plants treated with PHA767491.

Arrows indicate PRR-fusion protein bands detected by western blotting analysis. Asterisks are non-specific bands even observed in Wild-type plants. Non-specific bands by anti-FLAG antibody was used as control to proof that similar amount of protein samples were used.

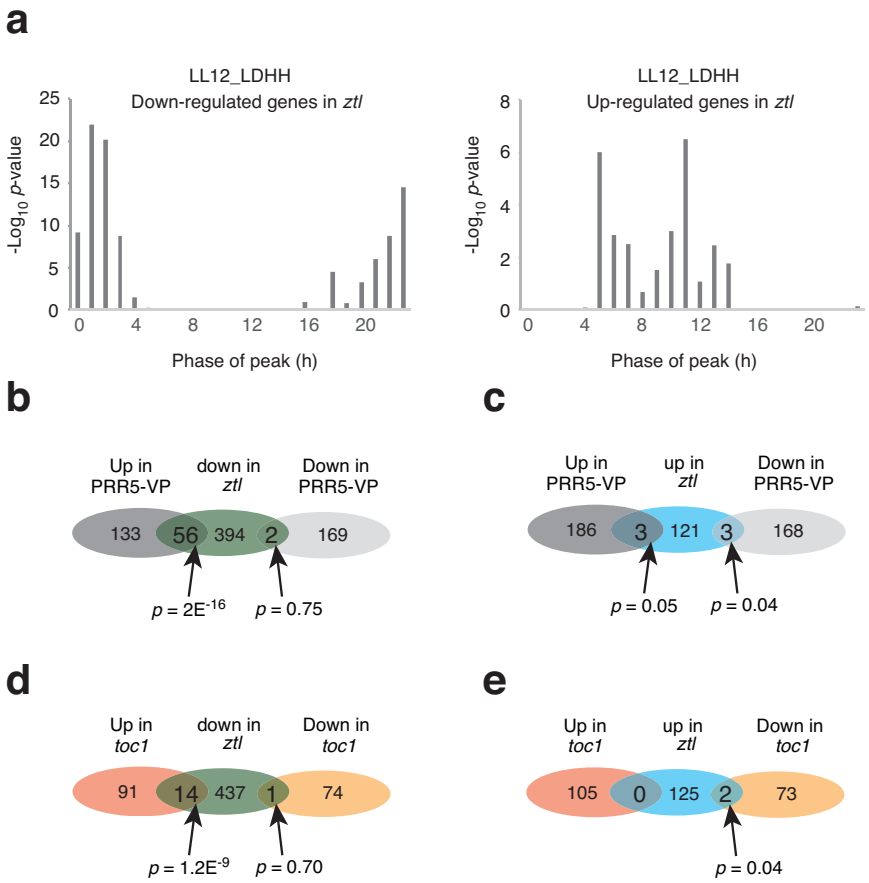

Figure S13. Mis-expressed genes in ztl mutants overlapwith downstream genes of PRR5 and TOC1. ***(A)*** Phase enrichment analysis of mis-expressed genes in ztl mutants (*ztl-3*) under free-running conditions (LL12_LDHH), as determined by Phaser. ***(B)*** Comparison between down-regulated genes in ztl and genes mis-expressed in PRR5-VP-overexpressing plants (*35Spro:PRR5-VP*). Fisher' s exact test was performed between the two gene groups. ***(C)*** Comparison between up-regulated genes in *ztl* and genes mis-expressed in PRR5-VP. ***(D)*** Comparison between down-regulated genes in *ztl* and mis-expressed genes in *toc1* (*toc1-2*). ***(E)*** Comparison between up-regulated genes in *ztl* and mis-expressed genes in *toc1*.

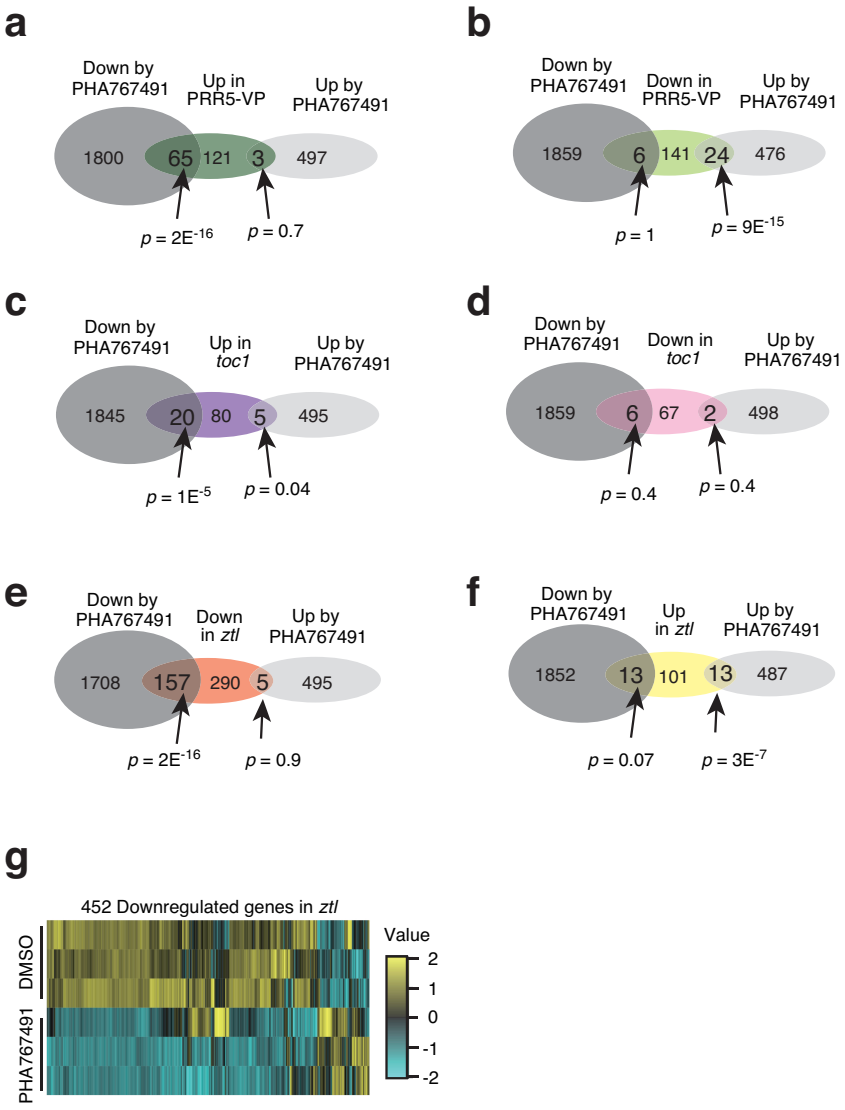

Figure S14. Action mechanism of PHA767491 on gene expression is related to PRR5 and TOC1 function. ***(A)*** Comparison between up-regulated genes in PRR5-VP and genes mis-expressed by PHA767491 treatment. Fisher' s exact test was performed between the two gene groups. ***(B)*** Comparison between down-regulated genes in PRR5-VP plants and genes mis-expressed with PHA767491 treatment. ***(C)*** Comparison between up-regulated genes in *toc1* and mis-expressed genes expressed with PHA767491 treatment. ***(D)*** Comparison between down-regulated genes in *toc1* and mis-expressed genes expressed with PHA767491 treatment. ***(E)*** Comparison between down-regulated genes in *ztl* and mis-expressed genes expressed with PHA767491 treatment. ***(F)*** Comparison between up-regulated genes in *ztl* and mis-expressed genes expressed with PHA767491 treatment. ***(G)*** Expression of 452 down-regulated genes in *ztl* in response to PHA767491 treatment.

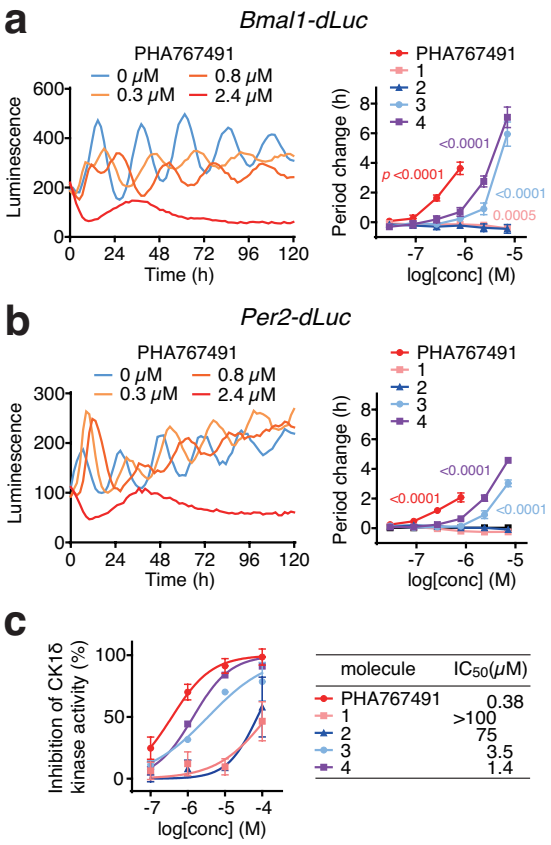

Figure S15. PHA767491 inhibits mammal CK1.

Circadian luciferase activities of *Bmal1-dLuc* (**a**) and *Per2-dLuc* (**b**) reporters in mammalian U2OS cells treated with PHA767491 and its analogues (mean ± SD, n = 3 ~ 4, with One-way ANOVA *p* for each analogue, right). Representative traces treated with PHA767491 were shown in left. **c**, Inhibition of human CK1δ kinase activity by PHA767491 and its analogues.

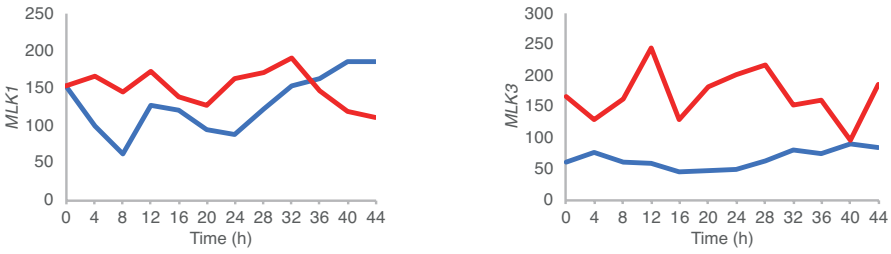

Figure S16. Expression of MLKs under diurnal and circadian cycles.

MLK genes expression under diurnal (LDHH_ST, blue) and circadian (LL12_LDHH, red) cycles in the Diurnal database (http://diurnal.mocklerlab.org/). MLK2 and MLK4 expression were not found due to lack of probes in the microarray analyses.

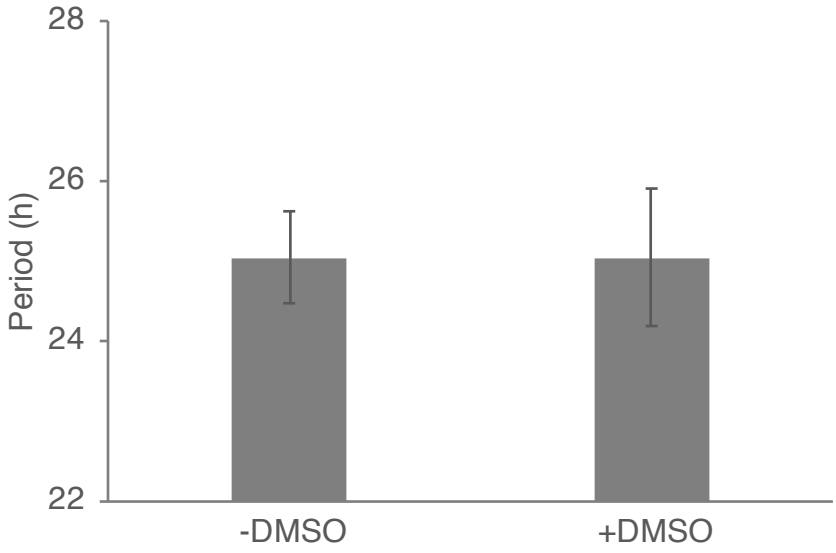

Figure S17. Circadian period of plants treated with DMSO.
Circadian period of *CCA1:LUC* seedlings treated with MS liquid containing 5% (v/v) DMSO. No significant change of period length was observed between two groups, by students' t-test $p > 0.05$. Error bars indicate SD (n=4).

Family	Description	AGI code	Experiment 1		Experiment 2	
			Unique peptides, -PHA767491	Unique peptides, +PHA767491	Unique peptides, -PHA767491	Unique peptides, +PHA767491
CK1	CKL1	AT4G26100	5	0	1	0
	CKL2	AT1G72710	15	0	2	0
	CKL3	AT4G28880	18	0	3	0
	CKL4	AT4G28860	10	0	4	0
	CKL5	AT2G19470	15	0	4	0
	CKL11	AT4G14340	4	0	2	0
	CKL13	AT1G04440	9	0	2	0
GSK3	ATSK13	AT5G14640	6	0	1	0
	BIL1	AT2G30980	4	0	5	0
	BIL2	AT1G06390	4	0	5	0
	BIN2	AT4G18710	7	0	6	0
CPK	CPK6	AT2G17290	5	0	9	0
	CPK26	AT4G38230	6	0	14	0
MPK	MPK2	AT1G59580	6	0	1	0
	MPK7	AT2G18170	7	0	3	0
Other kinases	Protein kinase	AT2G32850	112	2	40	0
	MAPKKK	AT3G58640	22	0	5	0
	RAF10	AT5G49470	20	0	8	0
	Protein kinase	AT3G61160	6	0	2	0
Others	MTK1	AT1G49820	48	0	29	0
	Acetolactate synthase	AT2G31810	8	0	5	0
	IBR3	AT3G06810	7	0	2	0
	FBA6	AT2G36460	4	0	2	0
	HCF109	AT5G36170	6	0	3	0

Supplementary Table 1. PHA-bead binding proteins in Arabidopsis. Unique peptides enriched in the PHA-bead fraction in samples without and with an excess of PHA767491 (-PHA767491) are shown.

Dataset S1. RNAseq data of *ztl* mutants.

Dataset S2. RNAseq data of plants treated with PHA767491.

Dataset S3. Expression of 452 down-regulated or 127 up-regulated genes in *ztl*, in response to PHA767491.

Dataset S4. Primers and plasmids used in this stydy.

References for methods

1. Nakamichi N, Kita M, Ito S, Yamashino T, & Mizuno T (2005) PSEUDO-RESPONSE REGULATORS, PRR9, PRR7 and PRR5, together play essential roles close to the circadian clock of Arabidopsis thaliana. *Plant Cell Physiol* 46(5):686-698.
2. Kamioka M*, et al.* (2016) Direct Repression of Evening Genes by CIRCADIAN CLOCK-ASSOCIATED1 in the Arabidopsis Circadian Clock. *Plant Cell* 28(3):696-711.
3. Vanotti E*, et al.* (2008) Cdc7 kinase inhibitors: pyrrolopyridinones as potential antitumor agents. 1. Synthesis and structure-activity relationships. *J Med Chem* 51(3):487-501.
4. Orsini P, Maccario A, & Colombo N (2007) Regioselective γ Alkylation of ter-Butyl 2,4-dioxopiperidine-1-carboxylate. *Synthesis* 20:3185-3190.
5. Milen M, Ábrányi-Balogh P, Dancsó A, & G. K (2012) Microwave-assisted synthesis of thioamides with elemental sulfur. *Journal of Sulfur Chemistry* 33(1):33-41.
6. Milen M, Ábrányi-Balogh P, Dancsó A, Drahos L, & Keglevich G (2013) Synthesis of New Thienopyridine Derivatives by a Reaction of 4-(Methylsulfanyl)-6,7-dihydrothieno[3,2-c]pyridine with Amino Acids. *Heteroatom Chemistry* 24:124-130.
7. Jishkariani D*, et al.* (2015) Dendron-Mediated Engineering of Interparticle Separation and Self-Assembly in Dendronized Gold Nanoparticles Superlattices. *J Am Chem Soc* 137(33):10728-10734.
8. Angiolini M (U. S. Patent 20150299192.
9. Laemmli UK (1970) Cleavage of structural proteins during the assembly of the

head of bacteriophage T4. *Nature* 227(5259):680-685.

10. Rosenfeld J, Capdevielle J, Guillemot JC, & Ferrara P (1992) In-gel digestion of proteins for internal sequence analysis after one- or two-dimensional gel electrophoresis. *Anal Biochem* 203(1):173-179.
11. Kinoshita T*, et al.* (2011) FLOWERING LOCUS T regulates stomatal opening. *Curr Biol* 21(14):1232-1238.
12. Saitou N & Nei M (1987) The neighbor-joining method: a new method for reconstructing phylogenetic trees. *Mol Biol Evol* 4(4):406-425.
13. Felsenstein J (1985) Confidence Limits on Phylogenies: An Approach Using the Bootstrap. *Evolution* 39(4):783-791.
14. Zuckerkandl E & Pauling L (1965) Evolutionary divergence and convergence in proteins. Edited in Evolving Genes and Proteins by V. Bryson and H.J. Vogel. *Academic Press, New York*:97-166.
15. Kumar S, Stecher G, & Tamura K (2016) MEGA7: Molecular Evolutionary Genetics Analysis Version 7.0 for Bigger Datasets. *Mol Biol Evol* 33(7):1870-1874.
16. Mockler TC*, et al.* (2007) The DIURNAL project: DIURNAL and circadian expression profiling, model-based pattern matching, and promoter analysis. *Cold Spring Harb Symp Quant Biol* 72:353-363.
17. Winter D*, et al.* (2007) An "Electronic Fluorescent Pictograph" browser for exploring and analyzing large-scale biological data sets. *PLoS ONE* 2(8):e718.
18. Ueno Y*, et al.* (2007) Histone deacetylases and ASYMMETRIC LEAVES2 are involved in the establishment of polarity in leaves of Arabidopsis. *Plant Cell* 19(2):445-457.
19. Kim J & Somers DE (2010) Rapid assessment of gene function in the circadian clock using artificial microRNA in Arabidopsis mesophyll protoplasts. *Plant Physiol* 154(2):611-621.
20. Yoshida T, Murayama Y, Ito H, Kageyama H, & Kondo T (2009) Nonparametric entrainment of the in vitro circadian phosphorylation rhythm of cyanobacterial KaiC by temperature cycle. *Proc Natl Acad Sci U S A* 106(5):1648-1653.
21. Nakamichi N*, et al.* (2012) Transcriptional repressor PRR5 directly regulates clock-output pathways. *Proc Natl Acad Sci U S A* 109(42):17123-17128.
22. Robinson MD, McCarthy DJ, & Smyth GK (2010) edgeR: a Bioconductor

package for differential expression analysis of digital gene expression data. *Bioinformatics* 26(1):139-140.

23. Nakamichi N, *et al.* (2016) Improvement of Arabidopsis Biomass and Cold, Drought and Salinity Stress Tolerance by Modified Circadian Clock-Associated PSEUDO-RESPONSE REGULATORs. *Plant Cell Physiol* 57(5):1085-1097.
24. Mizoi J, *et al.* (2019) Heat-induced inhibition of phosphorylation of the stress-protective transcription factor DREB2A promotes thermotolerance of Arabidopsis thaliana. *J Biol Chem* 294(3):902-917.
25. Nakamichi N, *et al.* (2010) PSEUDO-RESPONSE REGULATORS 9, 7, and 5 are transcriptional repressors in the Arabidopsis circadian clock. *Plant Cell* 22(3):594-605.
26. Legnaioli T, Cuevas J, & Mas P (2009) TOC1 functions as a molecular switch connecting the circadian clock with plant responses to drought. *EMBO J* 28(23):3745-3757.
27. Ito S, *et al.* (2008) Insight into missing genetic links between two evening-expressed pseudo-response regulator genes TOC1 and PRR5 in the circadian clock-controlled circuitry in Arabidopsis thaliana. *Plant Cell Physiol* 49(2):201-213.
28. Mas P, Kim WY, Somers DE, & Kay SA (2003) Targeted degradation of TOC1 by ZTL modulates circadian function in Arabidopsis thaliana. *Nature* 426(6966):567-570.
29. Bechtold N, Ellis J, & Pelletier G (1993) In planta Agrobacterium mediated gene transfer by infiltration of adult Arabidopsis thaliana plants. *C. R. Acad. Sci. Paris, Life Sci.* 316:1194-1199.
30. Hirota T, *et al.* (2010) High-throughput chemical screen identifies a novel potent modulator of cellular circadian rhythms and reveals CKIalpha as a clock regulatory kinase. *PLoS Biol* 8(12):e1000559.